

APPLICATION OF STABLE ISOTOPE PROBING TO IDENTIFY
RDX-DEGRADING BACTERIA IN GROUNDWATER

A Dissertation

by

KUN-CHING CHO

Submitted to the Office of Graduate and Professional Studies of
Texas A&M University
in partial fulfillment of the requirements for the degree of

DOCTOR OF PHILOSOPHY

Chair of Committee,
Committee Members,

Kung-Hui Chu
Bill Batchelor
Robin L. Autenrieth
Thomas J. McDonald
Robin L. Autenrieth

Interim Head of Department,

December 2013

Major Subject: Civil Engineering

Copyright 2013 Kun-Ching Cho

ABSTRACT

Hexahydro-1,3,5-trinitro-1,3,5-triazine (RDX) is soluble, nonvolatile cyclic nitramine explosive. Long-term manufacturing and various applications of RDX have resulted in RDX contamination in soil and groundwater. RDX is a possible human carcinogen; therefore, occurrence of RDX in groundwater has raised a public health concern. As RDX is biodegradable; bioremediation of RDX-contaminated groundwater has been recognized as a feasible cleanup technology. Several RDX-degrading isolates are known to have ability to utilize RDX as carbon and/or nitrogen source. However, little is known about these isolates and their roles in the natural or engineered systems during RDX degradation, or about RDX-degrading microbial communities in responding to engineered interventions. Stable isotope probing (SIP) is a powerful culture independent method that can identify functional active bacteria in various environmental samples. In this study, we applied SIP with ^{13}C -labeled or one of the ring-, nitro- and fully-labeled ^{15}N -RDX to identify microorganisms capable of utilizing RDX and its metabolites as carbon and/or nitrogen sources in groundwater microcosms, and to associate active RDX-degrading microbial communities in responding to engineered interventions.

Derived sequences from ^{13}C -DNA were clustered in *Bacteroidia*, *Clostridia*, α -, β - and δ -*Proteobacteria*, and *Spirochaetes*, which were different from previously described RDX degraders. Cheese whey amendment stimulated RDX biotransformation, altered the types of RDX-degrading bacteria, and decreased microbial community

diversity. Derived sequences from ^{15}N -DNA were grouped in *Clostridia*, β -*Proteobacteria* and *Spirochaetes*. In comparison to the results among ^{13}C -SIP and ^{15}N -SIP studies with presence of cheese whey, derived sequences were clustered in γ -*Proteobacteria* and *Bacilli*. The combination of these findings suggested that RDX-degrading microorganisms in groundwater are more phylogenetically diverse than what has been inferred from studies with RDX-degrading isolates. RDX biodegradation was observed when amended microcosms with different electron acceptors: Mn(IV), Fe(III), sulfate and CO_2 (from added succinate). Derived clones from different electron-accepting conditions were identified, which were grouped in α -, γ -*Proteobacteria*, and *Clostridia*. A real-time PCR assay targeted catabolic *xenB* gene was validated and tested with soil and groundwater samples. The presence of *xenB* gene would indicate that indigenous of microbial population with *xenB* gene are present, which can be used to estimate the potential of natural attenuation of RDX.

DEDICATION

Dedicated to

my beloved parents, my wife, my son, and my brother.

ACKNOWLEDGEMENTS

My deepest gratitude goes to my advisor, Dr. Kung-Hui Chu, for giving me the opportunity to pursue this degree, along with her supervision, patience, and continuous encouragement. I am thankful for the excellent example she has provided as a successful scientist and mentor that help me grow as a researcher. My deep gratitude also goes to each of my committee members, Dr. Robin Autenrieth, Dr. Bill Batchelor, and Dr. Thomas McDonald, for their thoughtful guidance, generous help and support of this research.

I must express my deep gratitude to Dr. Mark Fuller and Dr. Paul Hatzinger of CB&I Federal Services for their technical supports in the experiments and excellent suggestions in my research work. I thank Dr. Hyung Keun Roh, Dr. Do Gyun Lee, Mr. Baixin Wang, Dr. Myung Hee Kim, Mr. Steven Hand and all the research members of our lab for their support, advice, and friendship.

I also owe my sincere gratitude to Dr. Ya-Jen Yu, Dr. Chia-Lan Liu, Dr. Gisela Lin, Dr. Yu-Wen Huang, and Dr. Xu Liu for their help, support and friendship. I would also in particular thank Mr. David Wohlers, Mrs. Elizabeth Wohlers, Mr. Glenn Payne, Mrs. Peggy Payne and all brothers and sisters in my Church life.

Last but not least, my deepest appreciation goes to my parents, my beloved wife Yu-Shan, and my son KuanYing, for their love, support and encouragement during my study. Finally, I thank to my parents in-laws, brothers and friends for their love, support and encouragement.

TABLE OF CONTENTS

	Page
ABSTRACT	ii
DEDICATION	iv
ACKNOWLEDGEMENTS	v
TABLE OF CONTENTS	vi
LIST OF TABLES	ix
LIST OF FIGURES.....	x
CHAPTER I INTRODUCTION AND OBJECTIVES	1
1.1. Introduction	1
1.2. Goal, objectives and hypotheses	3
1.3. Dissertation overview.....	5
CHAPTER II LITERATURE REVIEW.....	6
2.1. RDX: Property, toxicity, fate and transport of RDX in the environment	6
2.2. Treatment technologies for RDX	8
2.2.1. Abiotic degradation of RDX	9
2.2.2. Aerobic biodegradation of RDX	9
2.2.3. Anaerobic biodegradation of RDX.....	12
2.3. Culture independent methods.....	16
CHAPTER III MATERIALS AND METHODS	18
3.1. Materials and methods used in Chapter IV to Chapter VI.....	18
3.1.1. Chemicals	18
3.1.2. Bacterial cultures.....	19
3.1.3. Sample sites and microcosms setup	19
3.1.4. Separation of ¹³ C- and ¹² C-DNA.....	26
3.1.5. Separation of ¹⁴ N- and ¹⁵ N-DNA	27
3.1.6. Analysis of microbial community structure analysis	28
3.1.7. Cloning and sequencing	29
3.1.8. Chemical analysis.....	31
3.2. Materials and methods used in Chapter VII.....	31
3.2.1. Chemicals	31
3.2.2. Organisms and culture conditions	32

3.2.3. Development of real-time PCR assay for <i>xenB</i> genes.....	32
3.2.4. Validation of developed real-time PCR assay.....	33
3.2.5. Column studies.....	33
CHAPTER IV APPLICATION OF ¹³C-STABLE ISOTOPE PROBING TO IDENTIFY RDX-DEGRADING MICROORGANISMS IN GROUNDWATER.....	36
4.1. Introduction.....	36
4.2. Results and discussion.....	38
4.2.1. Biodegradation of RDX in groundwater microcosms in the presence and absence of cheese whey.....	38
4.2.2. Changes of RDX-degrading microbial community structure in groundwater microcosms.....	45
4.2.3. Microorganisms capable of using RDX or RDX intermediates as a carbon source.....	46
4.2.4. Active RDX-degrading microorganisms in groundwater microcosms receiving cheese whey.....	51
CHAPTER V PROBING ACTIVE MICROORGANISMS CAPABLE OF USING DIFFERENT NITROGEN IN RDX STRUCTURE AS A NITROGEN SOURCE.....	57
5.1. Introduction.....	57
5.2 Results and discussion.....	59
5.2.1. Effect of cheese whey on RDX biodegradation in groundwater microcosms.....	59
5.2.2. RDX-degrading microbial communities in groundwater microcosms.....	63
5.2.3. Microorganisms capable of using RDX or RDX intermediates as a nitrogen source.....	63
5.2.4. Effects of cheese whey addition on the active RDX utilizers.....	68
CHAPTER VI IDENTIFICATION OF RDX DEGRADING BACTERIA UNDER VARIOUS ELECTRON-ACCEPTING CONDITIONS.....	72
6.1. Introduction.....	72
6.2. Results and discussion.....	74
6.2.1. RDX biodegradation under four different reducing conditions.....	74
6.2.2. Analysis of buoyant densities of DNAs extracted from all microcosms.....	78
6.2.3. Identification of active RDX-degrading microorganisms under different electron accepting conditions.....	82
6.2.4. Active RDX-degrading microbial communities under different reducing.....	87
CHAPTER VII IDENTIFICATION OF SUITABLE BIOMARKERS FOR ASSESSING RDX BIODEGRADATION IN NATURAL AND ENGINEERED SYSTEMS.....	91

7.1. Introduction	91
7.2. Results and discussion.....	93
7.2.1. Validation of developed real-time PCR for <i>xenB</i> gene: specificity and sensitivity	93
7.2.2. Application of developed real-time PCR assay for detecting <i>xenB</i> genes in groundwater and soil column samples.....	95
7.2.3. Potential use of <i>xenB</i> gene as a biomarker for assessing RDX degradation in engineered systems and/or microbial natural attenuation.....	98
 CHAPTER VIII CONCLUSIONS AND RECOMMENDATIONS FOR FUTURE RESEARCH.....	 99
8.1. Conclusions	99
8.2. Recommendations for future research	102
 REFERENCES.....	 104
 APPENDIX A APPLICATION OF ¹³ C-STABLE ISOTOPE PROBING TO IDENTIFY RDX-DEGRADING MICROORGANISMS IN GROUNDWATER.....	 121
 APPENDIX B PROBING ACTIVE MICROORGANISMS CAPABLE OF USING DIFFERENT NITROGEN IN RDX STRUCTURE AS A NITROGEN SOURCE.....	 130

LIST OF TABLES

	Page
Table II.1. Physical and chemical properties of RDX.....	8
Table II.2. Aerobic RDX-degrading isolates	11
Table II.3. Anaerobic RDX-degrading isolates.....	15
Table III.1. Microcosm setup conditions in Chapter IV	22
Table III.2. Microcosm setup conditions in Chapter V.....	23
Table III.3. Setup of microcosms under reducing conditions in Chapter VI	25
Table III.4. Groundwater and column study construction in Chapter VII	35
Table IV.1. Diversity indices of RDX-degrading microbial community structures of groundwater microcosms receiving unlabeled RDX	46
Table VII.1. Screening the presence of <i>xenB</i> genes in groundwater samples.....	97
Table VII.2. Detection of <i>xenB</i> genes in soil column samples	97
Table A.1. Comparison of 16S rRNA gene sequences derived from the microcosms to the 16S rRNA gene sequences derived from background groundwater..	127
Table A.2. Diversity and predicted T-RFs of clones derived from groundwater microcosms receiving ¹³ C-labeled RDX.....	129

LIST OF FIGURES

	Page
Figure II.1. Chemical structure of RDX.....	8
Figure II.2. Biotic and abiotic degradation routes of RDX with <i>Rhodococcus</i> sp. DN22 under aerobic conditions (adapted from Annamaria et.2010 (50))	12
Figure II.3. Two known pathways of RDX microbial degradation under anaerobic conditions (adapted from Halasz and Hawari., 2011) (74).....	14
Figure IV.1. RDX microbial degradation pathways under anaerobic conditions (adapted from Halasz and Hawari., 2011) (74).....	39
Figure IV.2. RDX degradation over time in microcosms receiving either unlabeled or ¹³ C-labeled RDX.....	41
Figure IV.3. RDX degradation over time in microcosms receiving cheese whey and RDX (unlabeled or ¹³ C-labeled RDX)	44
Figure IV.4. Phylogenetic tree representing 16S rRNA gene sequences derived from ¹³ C-DNA fractions of groundwater microcosms receiving only ¹³ C-labeled RDX (i.e. Sample IDs = 5-0-La and 7-0-La).....	48
Figure IV.5. Phylogenetic tree representing 16S rRNA gene sequences derived from ¹³ C-DNA fractions of groundwater microcosms receiving MW5 groundwater, cheese whey, and ¹³ C-labeled RDX (i.e. sample IDs = 5-C-La and 5-C-Lb).....	53
Figure IV.6. Phylogenetic tree representing 16S rRNA gene sequences derived from ¹³ C-DNA fractions of groundwater microcosms receiving MW-7D groundwater, cheese whey, and ¹³ C-labeled RDX (i.e. sample IDs = 7-C-La and 7-C-Lb).....	54
Figure V.1. RDX degradation over time in microcosms receiving one of ring-, nitro-, fully-labeled ¹⁵ N-RDX.....	60
Figure V.2. RDX degradation over time in microcosms receiving cheese whey and one of ring-, nitro-, fully-labeled ¹⁵ N-RDX.	62
Figure V.3. Phylogenetic tree representing 16S rRNA gene sequences derived from ¹⁵ N-DNA fractions of groundwater microcosms from MW-5 and MW-7D receiving ring-, nitro-, fully- ¹⁵ N-labeled RDX.....	65

Figure V.4. Phylogenetic tree representing 16S rRNA gene sequences derived from ¹⁵ N-DNA fractions of groundwater microcosms receiving either MW-5 or MW-7D groundwater, cheese whey, and receiving ring, nitro, fully ¹⁵ N-labeled RDX.....	69
Figure VI.1. RDX biodegradation and the formation nitroso metabolites (MNX, DNX, and TNX) in microcosms under (A) manganese-reducing, (B) iron-reducing, (C) sulfate-reducing , and (D) methanogenic conditions.	76
Figure VI.2. Difference between relative abundance of 16S rRNA gene copies and gradient fractions under (A) manganese-reducing, (B) sulfate-reducing, and (C) methanogenic conditions. No data available on the iron-reducing condition.	80
Figure VI.3. Difference between of relative abundance of 16S rRNA gene copies in gradient fractions in (A) manganese-reducing, (B) iron-reducing, (C) sulfate-reducing, and (D) methanogenic conditions. No data on unlabeled iron-reducing condition.....	81
Figure VI.4. Phylogenetic tree representing 16S rRNA gene sequences derived from ¹³ C-DNA fractions of microcosms receiving ¹³ C-labeled RDX and one of electron acceptors (manganese, iron, sulfate and CO ₂).....	84
Figure VI.5. Phylogenetic tree representing 16S rRNA gene sequences derived from ¹⁵ N-DNA fractions of groundwater microcosms receiving one of ¹⁵ N-labeled RDX (ring-, nitro-, and fully-labeled ¹⁵ N-RDX) and one of electron acceptors (manganese, iron, sulfate and CO ₂).....	85
Figure VI.6. Microbial community structure within the ¹³ C-gradient fraction of the microcosms incubated under (A) manganese-reducing, (B) iron-reducing, (C) sulfate-reducing, and (D) methanogenic conditions.	89
Figure VI.7. Microbial community structure within the ¹⁵ N-gradient fraction of the microcosms receiving ring, nitro and fully ¹⁵ N-labeled RDX incubated under (A) manganese-reducing, (B) iron-reducing, (C) sulfate-reducing, (D) methanogenic conditions.	90
Figure VII.1. Validation the assay with genomic DNA of <i>P. fluorescens</i> I-C. Error bar represented the standard deviation of triplication samples	94
Figure VII.2. Standard curves showing the threshold cycle (Ct) value plotted versus the log number of <i>xenB</i> gene copies. Error bar represented the standard deviation of triplication samples.....	95

Figure A.1. Real-time T-RFLP profile data for sample 5-0-Ua.....	121
Figure A.2. Real-time T-RFLP profile data for sample 5-0-Ub.....	121
Figure A.3. Real-time T-RFLP profile data for sample 5-0-La	122
Figure A.4. Real-time T-RFLP profile data for sample 5-C-Ua	122
Figure A.5. Real-time T-RFLP profile data for sample 5-C-Ub	122
Figure A.6. Real-time T-RFLP profile data for sample 5-C-La.....	123
Figure A.7. Real-time T-RFLP profile data for sample 5-C-Lb	123
Figure A.8. Real-time T-RFLP profile data for sample 7-0-Ua.....	123
Figure A.9. Real-time T-RFLP profile data for sample 7-0-Ub.....	124
Figure A.10. Real-time T-RFLP profile data for sample 7-0-La	124
Figure A.11. Real-time T-RFLP profile data for sample 7-0-Lb	124
Figure A.12. Real-time T-RFLP profile data for sample 7-C-Ua	125
Figure A.13. Real-time T-RFLP profile data for sample 7-C-Ub	125
Figure A.14. Real-time T-RFLP profile data for sample 7-C-La.....	125
Figure A.15. Real-time T-RFLP profile data for sample 7-C-Lb	126
Figure A.16. Predicted relationship between genomic G+C content (ranging from 30-75%) and buoyant density of unlabeled and labeled DNA with ¹³ C or ¹⁵ N (Buckley et al., 2007.) (143).....	126
Figure B.1. Real-time T-RFLP profile data for sample 50-Na	130
Figure B.2. Real-time T-RFLP profile data for sample 50-Fa.....	130
Figure B.3. Real-time T-RFLP profile data for sample 5C-Ra.....	131
Figure B.4. Real-time T-RFLP profile data for sample 5C-Rb.....	131
Figure B.5. Real-time T-RFLP profile data for sample 5C-Na.....	131
Figure B.6. Real-time T-RFLP profile data for sample 5C-Nb	132

Figure B.7. Real- time T-RFLP profile data for sample 5C-Fa	132
Figure B.8. Real- time T-RFLP profile data for sample 5C-Fb	132
Figure B.9. Real- time T-RFLP profile data for sample 70-Ra.....	133
Figure B.10. Real- time T-RFLP profile data for sample 70-Rb	133
Figure B.11. Real- time T-RFLP profile data for sample 70-Na	133
Figure B.12. Real- time T-RFLP profile data for sample 70-Nb	134
Figure B.13. Real- time T-RFLP profile data for sample 70-Fa.....	134
Figure B.14. Real- time T-RFLP profile data for sample 70-Fb.....	134
Figure B.15. Real- time T-RFLP profile data for sample 7C-Ra.....	135
Figure B.16. Real- time T-RFLP profile data for sample 7C-Rb.....	135
Figure B.17. Real- time T-RFLP profile data for sample 7C-Na.....	135
Figure B.18. Real- time T-RFLP profile data for sample 7C-Nb	136
Figure B.19. Real- time T-RFLP profile data for sample 7C-Fa	136
Figure B.20. Real- time T-RFLP profile data for sample 7C-Fb	136

CHAPTER I

INTRODUCTION AND OBJECTIVES

1.1. Introduction

Hexahydro-1,3,5-trinitro-1,3,5-triazine is known as cyclonite, hexogen, or royal demolition explosive (RDX). RDX is a common nitramine explosive used in various commercial and military activities after World War II. Due to its wide applications, RDX is detected in the soils and groundwater of sites (1) with a historical record of military testing and training activities, or near RDX manufacturing plants, and/or some waste disposal areas (2, 3). Because RDX is soluble (up to 42 mg/L at 20° C) and sorbs poorly to soils, RDX become highly mobile once entering the groundwater. As RDX is a potential human carcinogen, the U.S. Environmental Protection Agency (EPA) has established lifetime exposure drinking water health advisory limits for RDX at 2.0 µg/L (3).

RDX can be removed by physical, chemical, or biological processes. Advanced oxidation processes and nanotechnologies are physical/chemical methods that can remove RDX effectively (4-14). However, these methods are costly. RDX is biodegradable under aerobic and anaerobic conditions (15-27). *In situ* bioremediation for RDX-contaminated groundwater is a promising technology, but the success is often unpredictable, and sometime relies on the type of co-substrate addition.

Despite previous intensive research on RDX biodegradation, our understanding of the roles of specific organisms within RDX-degrading microbial communities is still developing. A better understanding of microbial ecology of RDX could potentially guide the isolation of novel RDX degraders (28) and the development of suitable biomarkers for monitoring intrinsic or engineered RDX bioremediation.

Our understanding of the microorganisms involved in RDX biodegradation is limited by a small fraction of RDX isolates, because approximately 99% of microorganisms are uncultivable under laboratory conditions (29). Using a cultivation-independent molecular technique is necessary to probe the insight into RDX-degrading microorganisms in groundwater. Stable isotope probing (SIP) has been recognized as a powerful culture-independent tool to study microbial community function, as this method can identify a set of active microorganisms capable of utilizing a labeled compound.

1.2. Goal, objectives and hypotheses

The goal of this research is to decipher active RDX-degrading microorganisms in RDX-contaminated groundwater, and to use the obtained information to identify suitable biomarkers for assessing intrinsic and/or engineered biodegradation of RDX. To achieve this goal, three specific objectives are identified, and a description of these objectives, hypotheses and associated tasks is outlined below.

Objective 1. Identify active groundwater microorganisms capable of using RDX and its metabolites as a carbon source.

Hypothesis 1. Uncultivable RDX-degrading bacteria, defined as those capable of using RDX and its metabolites as a carbon source, are present in RDX bioremediation sites under different electron-accepting conditions. Addition of co-substrate will affect the types and quantity of RDX-degrading bacteria.

Task 1a: Identify active RDX-degrading bacteria in groundwater microcosms receiving ^{13}C -labeled RDX in the presence and absence of cheese whey.

Task 1b: Identify active RDX-degrading bacteria in microcosms receiving different electron acceptors.

Objective 2. Identify active groundwater microorganisms capable of using RDX and its metabolites as a nitrogen source.

Hypothesis 2. Uncultivable RDX-degrading bacteria, defined as those capable of using RDX and its metabolites as a nitrogen source, are present in RDX bioremediation sites under different electron-accepting conditions.

Addition of co-substrate will affect the types and quantity of RDX-degrading bacteria.

Task 2a: Identify active RDX-degrading bacteria in groundwater microcosms receiving one of ^{15}N -ring-, nitro-, or fully-labeled ^{15}N -RDX in the presence and absence of cheese whey.

Task 2b: Identify active RDX-degrading bacteria in microcosms when receiving different electron acceptors.

Objective 3. Identify suitable biomarkers for assessing anaerobic biodegradation of RDX in natural and engineered systems.

Hypothesis 3. Unique 16S rRNA gene sequences of active RDX-degrading bacteria identified by SIP method, and/or known RDX catabolic genes present in the heavy fractions of DNA are ideal biomarkers for assessing RDX biodegradation potential in RDX-contaminated sites.

Task 3a: Develop real-time PCR assays for unique 16S rRNA gene sequences or known RDX catabolic genes.

Task 3b: Validate developed real-time PCR assays with environmental samples.

1.3. Dissertation overview

This dissertation is organized into eight chapters. The research hypothesis and specific objectives of this study are outlined in Chapter I. The literature review and material and methods for this research are described in Chapter II, and Chapter III, respectively. In Chapter IV, the application of [¹³C]-stable isotope probing to identify RDX-degrading microorganisms in groundwater is addressed. The research described in Chapter IV has been published (30). In Chapter V, Identify RDX-degrading microorganisms in groundwater via different level of [¹⁵N]-labeled RDX. The application of [¹³C]- and [¹⁵N]-stable isotope probing identify active RDX-degrading bacteria in microcosms receiving different electron acceptors is present in Chapter VI. The identification of suitable biomarkers for assessing biodegradation of RDX in natural and engineered systems is addressed in Chapter VII. Finally, Chapter VIII summarizes conclusions of recommendations for future research.

CHAPTER II

LITERATURE REVIEW

2.1. RDX: Property, toxicity, fate and transport of RDX in the environment

RDX, a synthetic and energetic chemical, is the main ingredient in common military energetic materials such as C4, Composition A, Composition B and cyclotol (31, 32). RDX is water soluble, and has a low vapor pressure and octanol-water partition coefficient (K_{ow}). The physical and chemical properties of RDX suggest that RDX would sorb soil poorly and tend to leach into the groundwater from contaminated soil and terrestrial and aquatic plants (3, 33). As RDX is not very lipid soluble, it has a low potential for bioaccumulation in aquatic species. The chemical structure of RDX is shown in Figure II.1. Detailed physical and chemical properties of RDX are listed in Table II.1.

The production of RDX from 1969 to 1971 was estimated to be 15 million pounds per month. However, the annual production of RDX decreased to 16 million pounds after 1984 (3). Ammunition plants and military activities are the major contributors to RDX contamination in the environment. During RDX manufacturing, incidents of explosion, casting, and curing, as well as improper storage practices and disposal of contaminated wastewater can all contribute to RDX release into the environment. Through burning, RDX can be also released into the atmosphere as particulates.

RDX has been detected in indoor air, soil, sediment, groundwater, and plants. RDX concentrations detected in indoor air at ammunition plants ranged from 0.032 to 60 mg/m³. RDX concentrations detected in groundwater near ammunition plants vary from 20 to 13,200 µg/L. RDX has also been detected in sediment samples from Army depots (<0.1 to 3,574 mg/kg) and in composts (>2.9 to 896 mg/kg). Additionally, RDX was detected in plant species when irrigated with or grown in RDX-contaminated water (<20 to 3,196 µg/L) (3).

Toxicity experiments conducted on animal specimens have shown RDX to be toxic. Exposure to RDX through digestion can cause seizures, convulsions, and tremors in rats, deer mice, dogs, and monkeys. Exposure to RDX through dermal contact can cause dermatitis in humans and animals. Furthermore, RDX can cause cancers in rats when exposed a low dose of RDX (at 35 mg/kg/day). The results of animal data suggests that RDX that might cause adverse effect on neurological, gastrointestinal and hematological system in humans (3). The EPA classified RDX as a group C carcinogen, potential human carcinogen, and established lifetime exposure drinking water health advisory limits for RDX at 2.0 µg/L (3, 34).

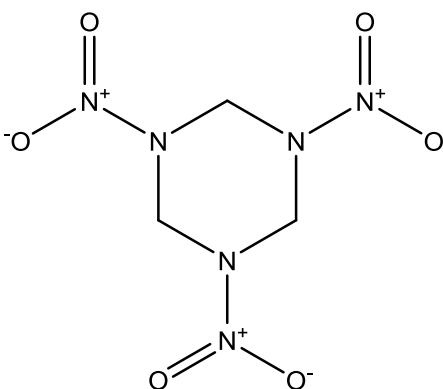


Figure II.1. Chemical structure of RDX.

Table II.1. Physical and chemical properties of RDX

CAS Number	Chemical formula	MW	Melting point (°C)	Boiling point (°C)	Solubility in water (mg/L)	Specific gravity	Vapor pressure (1 bar, 20°C)	Henry's Law constant (bar m ³ /mole)	Partitioning coefficient, log K _{ow}
00121-82-4	C ₃ H ₆ N ₆ O ₆	222.26	204	decomposes	42.3	1.89	5.30E-12	6.3E-8 to 1.96E-11	0.86

2.2. Treatment technologies for RDX

Numerous advanced physical/chemical technologies can treat RDX-contaminated soil and groundwater. However, most of these methods are costly and not practical for treating large groundwater plumes with low concentrations of RDX. As RDX is biodegradable, bioremediation of RDX appears to be a better alternative for treating RDX in large plumes. An understanding of the catabolic pathways of RDX biodegradation, their generic deviations, and the active RDX-degrading microbial communities on contaminated sites is essential to developing an effective *in situ*

bioremediation strategy (35). Previous studies have reported biotransformation of RDX under both aerobic and anaerobic conditions in soils, aquifers, sewage sludge, and marine sediments (28). The following section will summarize our current knowledge of RDX degradation via abiotic and biotic processes.

2.2.1. Abiotic degradation of RDX

The physical/chemical remediation technologies of RDX degradation in soil and groundwater with abiotic processes had been reported. These physical treatment technologies include granular activated carbon adsorption (4) and black carbon adsorption (5). RDX can be degraded through chemical oxidation with strong oxidants, for example, hydrogen peroxide or Fenton's reagent (36, 37), permanganate (38), and ozone (39). Additional treatment technologies of RDX through reduction processes and alkaline hydrolysis include, iron minerals (40), zero-valent iron reduction (9-11, 41, 42), electrochemical reduction (12-14), and alkaline hydrolysis (6-8, 43, 44).

2.2.2. Aerobic biodegradation of RDX

Our understanding of RDX biodegradation is mainly derived from studies of RDX-degrading isolates. Several microorganisms are known to utilize RDX as a nitrogen source under aerobic conditions. These strains are *Stenotrophomonas maltophilia* PB1 (45), *Rhodococcus rhodochrous* DN22 (16), *Rhodococcus rhodochrous* 11Y (15), and *Methylobacterium* spp. (46). Only two strains, *Gordonia* sp. KTR9 and *Williamsia* sp. KTR4 (17), can utilize RDX as both carbon and nitrogen sources. A

summary of the known aerobic RDX degraders showed in Table II.2. One known RDX catabolic gene, *xplA* gene, has been characterized from strain *Rhodococcus rhodochrous* DN22 and the gene has been recently proposed as a biomarker for assessing the potential for RDX biodegradation under aerobic condition. The *xplA* gene identified from the *Rhodococcus rhodochrous* 11Y and DN22 is similar as the functional of cytochrome p-450 system (15, 47). It has been also reported that various *Rhodococcus* sp. carry a plasmid with the *xplA* gene and can use RDX as a sole nitrogen source (48). Recently studies attempted to use the *xplA* gene and engineered the gene into plant species for phytoremediation of RDX (49). The aerobic biodegradation pathways of RDX by *Rhodococcus rhodochrous* DN22 have been proposed (50) (Figure II.2). The initial denitration pathway, a step involving the N-NO₂ bond cleavage, is the key step in RDX biodegradation under aerobic conditions. Following ring cleavage, 4-nitro-diazabutanal (NDAB) is formed as a main end-product (51). Fournier *et. al* reported that NDAB and carbon dioxide account for appropriately 90% of the carbon content in RDX aerobic biodegradation pathway. NDAB and carbon dioxide represents 60% and 30%, respectively, of carbon content from RDX. Recently, Annamaria and coworkers reported that the missing 10% carbon content was due to the formation of an intermediate product, methylenedinitramine (MEDINA) (50, 51).

Table II.2. Aerobic RDX-degrading isolates

Species	Use RDX as C or N source*	Reference
<i>Serratia marcescens</i>	N	(52)
<i>Stenotrophomonas maltophila</i> PB1	N	(45)
<i>Rhodococcus</i> sp. DN22	N	(16, 51, 53)
<i>Rhodococcus</i> sp. YH11	N	(54)
<i>Rhodococcus rhodochrous</i> sp. 11Y	N	(15, 53)
<i>Rhodococcus</i> sp. T7	N	(55)
<i>Rhodococcus</i> sp. T9N	N	(55)
<i>Williamsia</i> sp. KTR4	N, C	(17)
<i>Gordonia</i> sp. KTR9	N, C	(17)
<i>Methylobacterium</i> sp. BJ001	n/a	(46)
<i>Methylobacterium extorquens</i>	n/a	(46)
<i>Methylobacterium organophilum</i>	n/a	(46)
<i>Methylobacterium rhodesianum</i>	n/a	(46)

* N= nitrogen source; C= carbon source; n/a is lack of information.

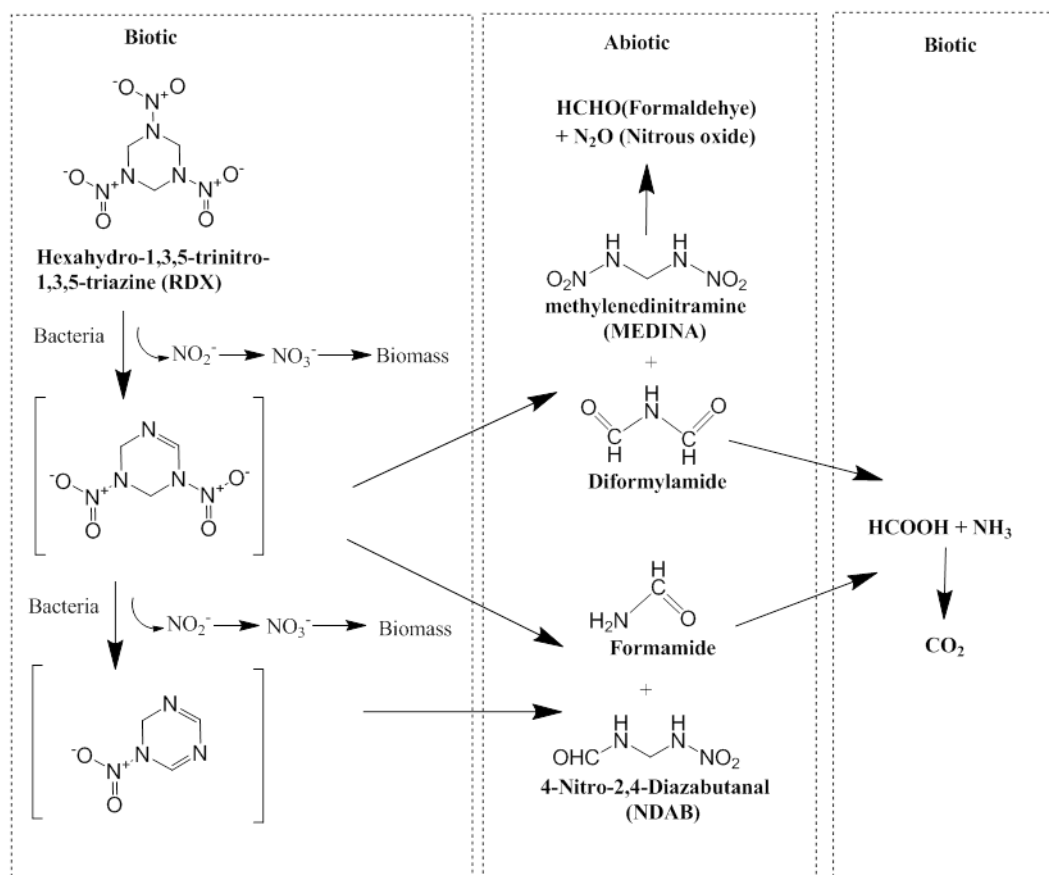


Figure II.2. Biotic and abiotic degradation routes of RDX with *Rhodococcus* sp. DN22 under aerobic conditions (adapted from Annamaria et.2010 (50))

2.2.3. Anaerobic biodegradation of RDX

RDX biodegradation by mixed cultures has been reported under various anaerobic condition, including in municipal anaerobic sludge (56), nitrate-reducing (21), sulfate reducing (22), manganese-reducing (57), acetogenic (58, 59), and methanogenic conditions (60). Anaerobic stains known to degrade RDX include *Acetobacterium* sp. (23, 59), *Clostridium* sp. (61-63), *Citrobacter freundii* NS2 (64), *Desulfovibrio desulfuricans* (65), *Enterobacter cloacae* (66), *Klebsiella pneumonia* SCZ-1 (18),

Morganella morganii B2 (64), *Providencia rettgeri* B1 (64), *Serratia marcescens* (52) and *Shewanella halifaxensis* HAW-EB4 (67). Table II.3. lists known anaerobic RDX isolates.

Several enzymes, including Type I nitroreductases (68), xenobiotic reductases (XenA and XenB) (69), diaphorase (62), nitrate reductase (70), and nitroreductases (NitA and NitB) (71), are known to be involved in RDX biotransformation. Under anaerobic conditions, RDX is sequentially reduced and denitrated. Through sequential reduction, RDX is converted to the following nitroso metabolites: hexahydro-1-nitroso-3,5-dinitro-1,3,5-triazine (MNX), hexahydro-1,3-dinitroso-5-nitro-1,3,5-triazine (DNX) and hexahydro-1,3,5-trinitroso-1,3,5-triazine (TNX). Type I nitroreductase is the key enzyme responsible for the sequential reductions of RDX to form MNX, DNX, and TNX (64, 68). An early study successfully determined the *nsfI* gene that codes for a type I nitroreductase of *Enterobacter cloacae* (72), and the *nsfI* gene was later expressed in *E. coli* for RDX degradation (68).

RDX can also be degraded through a denitration pathway to form intermediates NDAB and MEDINA (18, 63). The denitration process is catalyzed by a diaphorase in *Clostridium kluyveri* when using NADH as an electron donor (62). The diaphorase is an oxygen-sensitive enzyme. Two xenobiotic reductases XenA and XenB can also transform RDX through a denitration pathway (69). The unique character of the xenobiotic reductases XenA and XenB is that these reductases can transform RDX under both anaerobic and aerobic conditions. *xenA* and *xenB* are genes coding the xenobiotic reductases; they have been cloned, sequenced, and purified from *Pseudomonas putida* II-

B and *Pseudomonas fluorescens* I-C (73). Anaerobic RDX biodegradation pathways through a combination of sequential reductions and denitration have been recently proposed (74) (see Figure II.3)

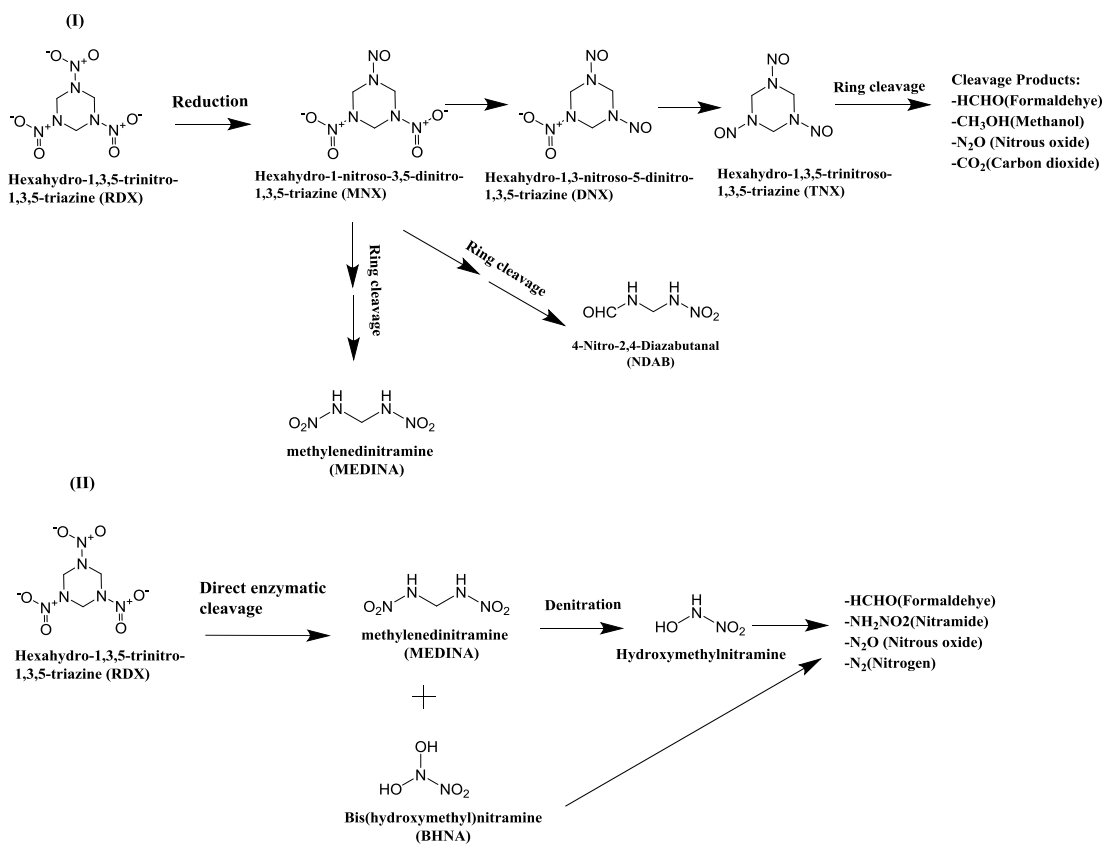


Figure II.3. Two known pathways of RDX microbial degradation under anaerobic conditions (adapted from Halasz and Hawari., 2011) (74).

Table II.3. Anaerobic RDX-degrading isolates

Species	Use RDX as C or N source*	Reference
<i>Geobacter metallireducens</i> GS15	n/a	(24, 25)
<i>Geobacter sulfurreducens</i> PCA	n/a	(25)
<i>Anaeromyxobacter dehatogenans</i> K	n/a	(24)
<i>Desulfitobacterium chloromspirans</i> Co23	n/a	(24)
<i>Desulfovibrio desulfuricans</i> EFX-DES	N, C	(65)
<i>Shewanella oneidensis</i> MR1	n/a	(24)
<i>Enterobacter cloacae</i>	n/a	(68)
<i>Clostridium acetobutylicum</i>	n/a	(61)
<i>Desulfovibrio</i> sp. HAW-ES2	N	(19)
<i>Acetobacterium malicum</i> HAAP-1	n/a	(23)
<i>Acetobacterium wieringae</i>	n/a	(23)
<i>Acetobacterium paludosum</i>	N	(59)
<i>Shewanella sediminis</i> HAW-EB3	n/a	(75)
<i>Shewanella halifaxensis</i> HAW-EB4	n/a	(75)
<i>Shewanella</i> sp. HAW EB1	n/a	(75)
<i>Shewanella</i> sp. HAW EB2	n/a	(75)
<i>Shewanella</i> sp. HAW-EB5	n/a	(75)
<i>Pseudomonas putida</i> II-B	n/a	(69)
<i>Pseudomonas fluorescens</i> I-C	n/a	(69)
<i>Morganella morganii</i> B2	n/a	(64, 68)
<i>Citrobacter freundii</i> NS2	n/a	(64)
<i>Providencia rettgeri</i> B1	n/a	(64)
<i>Klebsiella pneumoniae</i> SCZ1	N	(18, 20)
<i>Clostridium bifermentans</i> HAW-1	N	(20, 63)
<i>Clostridium</i> sp. HAW-G4	N	(20, 63)
<i>Clostridium</i> sp. HAW-E3	N	(20, 63)
<i>Clostridium</i> sp. HAW-HC1	N	(20, 63)
<i>Clostridium</i> sp. HAW-EB17	n/a	(75)
<i>Clostridium</i> sp. EDB2	n/a	(27, 76)
<i>Anaerovibrio lipolyticus</i>	N	(77)
<i>Prevotella ruminicola</i>	N	(77)
<i>Streptococcus bovis</i> IFO	N	(77)

* N= nitrogen source; C= carbon source; n/a is lack of information.

2.3. Culture independent methods

In this study, a quantitative assay for linking microbial community function and structure (Q-FAST) assay will be used to study RDX-degrading microbial community. Q-FAST is a method integrating two techniques, stable isotope probing (SIP) and a real-time terminal restriction fragment polymorphism (real-time-t-RFLP) assay (78). The SIP technique was first introduced to link microbial community function without a need of cultivation (79). SIP relies on the fact that the nucleic acids of active degraders will become heavier due to incorporation of stable isotopes. Nucleic acids in non-degraders of microorganisms will not be changed and will be considered lighter when compared to those of the degradative microorganisms. The labeled DNA (heavier) can be separated from the unlabeled DNA (lighter) through cesium chloride (CsCl) density gradient centrifugation. Applications of DNA-based SIP with ^{13}C -, ^{15}N - or ^{18}O -labeled compounds have provided significant insights into active microbial communities in numerous environmental settings (80-82).

Real-time-t-RFLP, a combination of real-time PCR and T-RFLP, is a quantitative fingerprinting method to simultaneously determine the types and quantity of different microbial groups in a microbial community (78). The real-time PCR assay can provide quantitative information on gene copy numbers, while, the T-RFLP is a fingerprinting method by generating a profile of a given microbial community (83, 84). Real-time PCR assays have been successfully applied to various environmental samples to detect and monitor the presence of specific strains and/or functional genes (85-87). In this study, developed real-time PCR assays target for or unique 16S rRNA sequences and/ or

catabolic genes involved in the biodegradation of RDX in groundwater. The developed assays were used to assess RDX biodegradation potential in natural and engineered systems as described in objective 3.

CHAPTER III

MATERIALS AND METHODS

3.1. Materials and methods used in Chapter IV to Chapter VI

The detail material and methods of the application of [^{13}C]-stable and [^{15}N]-stable isotope probing to identify RDX-degrading microorganisms in groundwater and receiving different electron acceptors from Chapter VI to Chapter VI are described in the follows text.

3.1.1. Chemicals

Fully labeled ^{13}C -RDX (99.9% pure), as well as ring-, nitro-, and fully-labeled ^{15}N -RDX (99.9% pure) were synthesized by Dr. Steve Fallis, US Naval Air Weapons Station China Lake. Hexahydro-1-nitroso-3,5-dinitro-1,3,5-triazine (MNX), hexahydro-1,3-dinitroso-5-nitro-1,3,5-triazine (DNX), hexahydro-1,3,5-trinitroso-1,3,5-triazine (TNX), were obtained from SRI international (Menlo Park, CA). ^{12}C - and ^{13}C -labeled glucoses were purchased from Isotec, Inc. (Miamisburg, OH). ^{14}N - and ^{15}N -labeled ammonia chloride ($^{15}\text{NH}_4\text{Cl}$) were purchased from Sigma-Aldrich, Inc. (St. Louis, MO). Cesium chloride (CsCl , 99.999% pure) and ethidium bromide (EtBr, 10 mg/ml) were purchased from Fisher Scientific (Fair Lawn, NJ) and Promega (Madison, WI), respectively. Cheese whey used in studies was an animal feed product provided by International Ingredient Corporation (St. Louis, MO) which consists of a 50:50 mix of powdered cheese product and spray dried whey.

3.1.2. Bacterial cultures

Genomic ^{13}C -DNA and ^{12}C -DNA of *E. coli* were used as reference standards (78). *E. coli* was grown in ammonia mineral salts medium (88) containing ^{13}C -labeled or ^{12}C -labeled glucose (400 mg/L) as a sole carbon source. Similarly, genomic ^{14}N -DNA and ^{15}N -DNA of *E. coli* were used as reference standards in ^{15}N -SIP experiments. *E. coli* was grown in ammonia mineral salts medium containing either NH_4Cl or $^{15}\text{NH}_4\text{Cl}$ (10mg/L) as a sole nitrogen source and glucose as carbon source (400 mg/L). The cultures were transferred twice in medium, and the inocula were kept small in volume (1/100) to minimize ^{14}N carryover from the starter cultures. The strain was incubated overnight at 30°C at 150 rpm.

The genomic DNA of *E. coli* was extracted using FastDNA spin kit (MP Biomedical, Solon, OH). The DNA concentrations were determined using a Hoefer DQ 300 Fluorometer (Hoefer Inc., San Francisco, CA) with Hoechst 33258 dye, and a NanoDrop ND-1000 Spectrophotometer (Fisher Scientific., Fair Lawn, NJ).

3.1.3. Sample sites and microcosms setup

Site A: (Chapter IV and Chapter V)

Groundwater samples were collected from two monitoring wells (MW-5 and MW-7D) at a U.S. Army facility in northern New Jersey. The site was known to have been contaminated with explosives for several decades. Biodegradation of RDX and other explosives had been stimulated in situ at the site by repeated addition of cheese whey to the aquifer. Cheese whey was observed to support RDX biodegradation in the

site groundwater during prior treatability testing (data not shown) (89). Prior to the addition of cheese whey, groundwater in these wells was aerobic [dissolved oxygen (DO) 2.5 mg/L and oxidation-reduction potential (ORP) +10 mV], and contained RDX, octahydro-1,3,5,7-tetranitro-1,3,5,7-tetrazocine (HMX), and 1,3,5-trinitrotoluene (TNT) at 50-130 µg/L. 2-Amino-4,6-dinitrotoluene and 4-amino-2,6-dinitrotoluene were also present at 40 µg/L each. The groundwater had been amended on four occasions with a cheese whey solution to promote explosives biodegradation, with the final amendment occurring 385 days prior to sample collection. Total organic carbon (TOC) concentrations increased from 3 mg/L to > 80 mg/L in the sample wells immediately after the cheese whey was added. At the time of sampling for this study, RDX and TNT were below detection (< 0.25 µg/L), and HMX was below detection in MW-7D (< 0.1 µg /L) and was present at 6.2 µg/L in MW-5. TOC in the wells was 4.2 mg/L (MW-5) and 14.9 mg/L (MW-7D) and the groundwater was anoxic (DO < 0.25 mg/L) and reducing (ORP < -120 mV). The pH range was 6.2 to 6.5 in both wells.

In Chapter IV, the groundwater microcosms were prepared in 2-L sterile glass bottles containing groundwater (1.6 L) from one of the two wells (MW-5 and MW-7D). RDX (unlabeled or ¹³C-labeled RDX, final concentration 10 mg/L) and cheese whey (100 mg/L). Cheese whey was added as dry powder. A parallel set of groundwater microcosms without addition of cheese whey were used. The microcosms were sealed and maintained under anoxic conditions. All sampling was performed in an anaerobic glove bag. The dissolved oxygen (DO) was checked periodically using a colorimetric assay (CHEMetrics, Inc, Midland, VA) (detection limit was 0.2 mg/L), and was

consistently less than 0.2 mg/L for all microcosms. No difference in DO concentration was observed between the microcosms with or without cheese whey amendment, indicating that the residual TOC in the groundwater was sufficient to keep the microcosms anaerobic even if no cheese whey was added. See Table III.1 for microcosm setup conditions. Bottles were incubated in the dark at the in situ groundwater temperature (~15°C), and were manually shaken a few times per week. Samples were removed to monitor the RDX concentration using high performance liquid chromatography (HPLC) use the standard method as described in below. When the initial spike of RDX was completely degraded, a portion of the enrichment (at least 1 L) was removed and the biomass was collected by filtration using Sterivex filter units (SVG 010 RS, Millipore Corp., Billerica, MA). The filters were frozen at -80°C until analysis. The remaining volume received a second spike of RDX (final concentration of 10 mg/L), and the biomass was collected when RDX degradation was complete.

In Chapter V, the groundwater microcosms were prepared similarly as described by Cho and collaborator (30), except that ring-, nitro-, and fully-labeled ¹⁵N-RDX were used. See Table III.2 for setup conditions for each microcosm.

Site B: (Chapter VI and Chapter VII)

Groundwater samples and saturated sediments were collected from monitoring wells at a testing facility belong to Department of Defense in the eastern United States. Sediment was collected using a GeoProbe, returned to the laboratory, and thoroughly

homogenized. Groundwater was pumped directly into bleached and sterilized 20 L soda kegs.

Table III.1. Microcosm setup conditions in Chapter IV

Microcosm setup condition and coding				
Groundwater source	Cheese whey addition	RDX addition	Microcosm ID	Sample ID*
MW-5	No	Unlabeled	5-0-U	5-0-Ua
				5-0-Ub
MW-5	No	¹³ C-labeled	5-0-L	5-0-La
				Not available
MW-5	Yes	Unlabeled	5-C-U	5-C-Ua
				5-C-Ub
MW-5	Yes	¹³ C-labeled	5-C-L	5-C-La
				5-C-Lb
MW-7D	No	Unlabeled	7-0-U	7-0-Ua
				7-0-Ub
MW-7D	No	¹³ C-labeled	7-0-L	7-0-La
				7-0-Lb
MW-7D	Yes	Unlabeled	7-C-U	7-C-Ua
				7-C-Ub
MW-7D	Yes	¹³ C-labeled	7-C-L	7-C-La
				7-C-Lb

In Chapter VI, microcosms were prepared with sediment (0.5 kg wet wt) and groundwater (8 L) were placed into five 10 L mini-kegs (also bleached and sterilized) and the kegs were purged with nitrogen for 3 hours to remove most of the oxygen. The groundwater plus sediment contained RDX at 0.05 mg/L RDX, 0.6 mg/L perchlorate, 150 mg/L sulfate, and about 1 mg/L nitrate. All kegs were amended with sodium succinate and RDX to achieve initial concentrations of 40 mg/L and 0.15 mg/L, respectively. Each keg was assigned a different electron acceptor condition which amended with one of electron acceptor (1 mM), MnO_2 , $\text{FeCl}_3 \cdot 6\text{H}_2\text{O}$ and K_2SO_4

Table III.2. Microcosm setup conditions in Chapter V

Microcosm setup condition and coding				
Groundwater source	Cheese whey addition	RDX addition	Microcosm ID	Sample ID*
MW-5	No	^{15}N -ring labeled	50-R	Not available (no degradation)
		^{15}N -nitro labeled	50-N	50-Na
		^{15}N -fully labeled	50-F	50-Fa
MW-5	Yes	^{15}N -ring labeled	5C-R	5C-Ra & 5C-Rb
		^{15}N -nitro labeled	5C-N	5C-Na & 5C-Nb
		^{15}N -fully labeled	5C-F	5C-Fa & 5C-Fb
MW-7D	No	^{15}N -ring labeled	70-R	70-Ra & 70-Rb
		^{15}N -nitro labeled	70-N	70-Na & 70-Nb
		^{15}N -fully labeled	70-F	70-Fa & 70-Fb
MW-7D	Yes	^{15}N -ring labeled	7C-R	7C-Ra & 7C-Rb
		^{15}N -nitro labeled	7C-N	7C-Na & 7C-Nb
		^{15}N -fully labeled	7C-F	7C-Fa & 7C-Fb

Samples were removed from the kegs periodically as described below: 2 ml passed through a 0.45 μm glass microfiber (GMF) filter for RDX and breakdown products (via HPLC); 25 ml passed through a 0.22 μm nylon filter into a vial acidified with nitric acid for soluble iron (HACH kit, 0.5 mg/L detection limit); 5 ml passed through a 0.22 μm nylon filter into a vial acidified with nitric acid for soluble manganese (HACH kit, 0.5 mg/L detection limit); 10-15 ml passed through a 0.22 μm nylon filter into a sterile polypropylene tube for perchlorate (IC, 0.01 mg/L detection limit), succinate (IC, 0.5 mg/L detection limit), nitrate (IC, 0.5 mg/L detection limit), and sulfate (IC, 0.5 mg/L detection limit). Samples were also collected to measure the dissolved oxygen concentration (ChemMet kits) and solution pH.

After reducing condition was developed and RDX was depleted in the enrichment kegs, a series of new microcosms were prepared from the enrichment kegs to identify the active RDX-degrading microorganisms under different electron-accepting conditions in microcosms. All microcosms were mixed with N_2 -purged site groundwater (~1.5L), saturated site sediments (100 g wet weight) from the enrichment kegs, and amended with sodium succinate and ^{13}C -labeled RDX, or one of three ^{15}N -labeled RDX (ring-, nitro-, or fully-labeled) to achieve initial concentrations of 160 mg/L and 10 mg/L, respectively. Each microcosm was assigned a different electron-accepting condition and amended with 2.3 mM of electron acceptors: MnO_2 , $\text{FeCl}_3 \cdot 6\text{H}_2\text{O}$, or K_2SO_4 . The microcosms were sacrificed after RDX and RDX metabolites were depleted. The biomass was collected by filtration using Sterivex filter units (SVG 010 RS, Millipore Corp., Billerica, MA). The biomass were extracted

DNA as using the FastDNA spin kit as described in section 3.1.2. See Table III.3 for setup of microcosms under reducing conditions in Chapter VI.

Table III.3. Setup of microcosms under reducing conditions in Chapter VI

Microcosms ID	Electron acceptor	RDX addition
A1	CO ₂	unlabeled
A2	CO ₂	¹³ C-labeled
C1	FeCl ₃ -6H ₂ O	unlabeled
C2	FeCl ₃ -6H ₂ O	¹³ C-labeled
D1	MnO ₂	unlabeled
D2	MnO ₂	¹³ C-labeled
E1	K ₂ SO ₄	unlabeled
E2	K ₂ SO ₄	¹³ C-labeled
A3	CO ₂	¹⁵ N ring-labeled
A4	CO ₂	¹⁵ N nitro-labeled
A5	CO ₂	¹⁵ N fully-labeled
C3	FeCl ₃ -6H ₂ O	¹⁵ N ring-labeled
C4	FeCl ₃ -6H ₂ O	¹⁵ N nitro-labeled
C5	FeCl ₃ -6H ₂ O	¹⁵ N fully-labeled
D2	MnO ₂	¹⁵ N ring-labeled
D3	MnO ₂	¹⁵ N nitro-labeled
D4	MnO ₂	¹⁵ N fully-labeled
E3	K ₂ SO ₄	¹⁵ N ring-labeled
E4	K ₂ SO ₄	¹⁵ N nitro-labeled
E5	K ₂ SO ₄	¹⁵ N fully-labeled

3.1.4. Separation of ^{13}C - and ^{12}C -DNA

In Chapter IV, the DNA in the frozen Sterivex filters were extracted using FastDNA spin kit for soil samples (MP Biomedical, Solon, OH). The extracted DNA was separated into ^{13}C -DNA and ^{12}C -DNA fractions using equilibrium centrifugation in CsCl-EtBr density gradients as described by Yu and Chu (78) with minor modifications. Briefly, the extracted DNA (10 μg) was loaded into 3.5-mL Beckman centrifuge tubes containing 2,000 μg of EtBr and 1.0 g/mL CsCl in TE buffer solution. Both ^{13}C - and ^{12}C -DNA of *E. coli* were loaded into a parallel tube as a reference. All tubes were sealed and centrifuged using a desk-top Beckman Coulter TLX-120 Optima Ultracentrifuge in a TLA 100.3 rotor at 70,000 rpm at 20°C for 24 h. Following centrifugation, the bands of ^{12}C - and ^{13}C -DNA fractions were visualized under UV light at a wavelength of 365 nm. The DNA in each of the ^{12}C - and ^{13}C -DNA fractions was extracted and recovered as described previously by Yu and Chu (78). The recovered DNA were stored at -20 °C before use.

In Chapter VI, the ^{13}C -DNA in microcosms were separated used the method similarly as described in Chapter V with a slightly modification. Briefly, the extracted DNA (10 μg) was loaded into 3.5-mL Beckman centrifuge tubes without adding EtBr. A fraction recovery system (Beckman Coulter, CA) was used to collect ^{13}C - and ^{12}C -DNA fractions. The syringe pump (Model 7801001, Fisher Scientific, Fair Lawn, NJ) at a flow rate 250 $\mu\text{L}/\text{min}$ was used to dispense mineral oil into the top of the tube and collected the 20 fractions of 100 μL from the bottom of the tube. The buoyant density of each DNA fraction was determined based on the refractive index that was measured by a

Reichert AR200 digital refractometer (Depew, NY). The DNA fractions were extracted and recovered via ethanol precipitation. The DNA in fractionated solution was extracted and purified as described previously (78). Purified DNA was stored at -20 °C.

3.1.5. Separation of ^{14}N - and ^{15}N -DNA

In Chapter V, the DNA in the frozen Sterivex filters were extracted using FastDNA spin kit for soil samples (MP Biomedical, Solon, OH). The extracted DNA was separated into ^{14}N -DNA and ^{15}N -DNA using equilibrium centrifugation in CsCl-EtBr density gradients described by Roh and collaborator with following minor modification. Ten μg of DNA was loaded into 3.5-mL Beckman centrifuge tubes containing 2,000 μg of EtBr and 1.1 g/mL CsCl in TE buffer solution. All tubes were sealed and centrifuged using a desk-top Beckman Coulter TLX-120 Optima Ultracentrifuge in a TLA 100.3 rotor at 65,000 rpm at 20°C for 24 h. Following centrifugation, the bands of ^{14}N -DNA and ^{15}N -DNA fractions were visualized under UV light wavelength at 365 nm. A fraction recovery system (Beckman Coulter, CA) was used to collect DNA fractions. The syringe pump (Model 7801001, Fisher Scientific, Fair Lawn, NJ) at a flow rate 250 $\mu\text{L}/\text{min}$ was used to dispense mineral oil into the top of the tube and collected the 20 fractions of 100 μL from the bottom of the tube. The buoyant density of each DNA fraction was determined based on the refractive index that was measured by a Reichert AR200 digital refractometer (Depew, NY). The DNA fractions were extracted and recovered via ethanol precipitation. The DNA in

fractionated solution was extracted and purified as described previously (78). Purified DNA was stored at -20 °C.

In Chapter VI, the ¹⁵N-DNA in microcosms method was similarly as described in Chapter VI with a slightly modification. Briefly, the extracted DNA (10 µg) was loaded into 3.5-mL Beckman centrifuge tubes without adding EtBr. A fraction recovery system (Beckman Coulter, CA) was used to collect ¹⁴N- and ¹⁵N-DNA fractions.

3.1.6. Analysis of microbial community structure analysis

To characterize overall and active RDX-degrading microbial community structure in each microcosm, real-time terminal restriction fragment length polymorphism (real-time-t-RFLP) assays were performed (78, 90). Genomic DNA extracted from microcosms receiving unlabeled RDX were used as templates for determining overall microbial community structures. The ¹³C-DNA fractions from ¹³C-RDX-amended microcosms were used as templates to determine the active RDX-degrading microbial community structure. Similarly, the ¹⁵N-DNA fractions from ring, nitro, and fully labeled ¹⁵N-RDX-amended microcosms were used as templates to determine the active RDX-degrading microbial community structure. The real-time PCR reactions were performed using Bio-Rad iQ5 multicolor Real-Time PCR detection System (Hercules, CA). The results of real-time-t-RFLP were used to calculate four structural diversity indices as described by Roh and Chu (91). These four indices are (i) richness (*S*), (ii) the Shannon-Weaver diversity (*H'*), (iii) evenness (*E*), and (iv) the reciprocal of Simon's index (*I/D*). The richness (*S*) of the microbial community was

obtained from the total numbers of unique T-RFs in the real-time-t-RFLP community profile. The Shannon-Weaver diversity index (H') was calculated using the equation, $H' = -\sum(P_i \cdot \log_2 P_i)$, where P_i is the relative abundance value of i number of fragments. Evenness (E) was derived from the equation, $E = H' / (\log_2 [S])$. The reciprocal of Simon's index ($1/D$) was determined by the equation, $1/D = 1 / (\sum P_i^2)$.

3.1.7. Cloning and sequencing

The identities of active RDX-degrading microorganisms were determined based on the 16S rRNA gene sequences derived from the ^{13}C -DNA fractions of the microcosms receiving ^{13}C -RDX or ^{15}N -DNA fractions of the microcosms receiving ring, nitro and fully labeled ^{15}N -RDX. The PCR reactions for 16S rRNA gene amplification were performed as described by Roh et al (89). Briefly, the amplified fragments of the 16S rRNA genes were cloned into the vector pCR4-TOPO using a TA Cloning Kit (One Shot TOP10 Competent cells) (Invitrogen, Carlsbad, CA). Colonies with inserts were verified by PCR with primers M13F (5'-GTAAAACGACGGCCAG-3') and M13R (5'-CAGGAAACAGCTATGAC-3'), and screened on 1.5% agarose gels (Fisher Scientific, Fair Lawn, NJ). For each ^{13}C -DNA fraction sample, seventy clones were randomly selected from the plates (i.e., a total of 280 clones from the microcosms receiving ^{13}C -labeled RDX). The amplified 16S rRNA were purified using a PurLink PCR purification kit (Invitrogen, Carlsbad, CA), followed by digestion with enzymes, *Hha*I and *Hae*III (Promega Corp., Madison, WI). The clones with unique restriction fragment length polymorphism (RFLP) patterns on 4% metaphor agarose gels (Lonza, Rockland,

ME) (78) were then selected for sequencing. The selected clones were grown overnight in 10 mL of Luria-Bertani (LB) broth with 50 mg/L kanamycin before use for plasmid extraction. The plasmids were extracted using a plasmid purification Kit (QIAGEN, Valencia, CA). The inserted sequences were determined using an Applied Biosystems 3100 DNA sequencer (Perkin-Elmer, Foster City, CA) at the Gene Technologies Lab (GTL) at Texas A&M University. The assembled sequences with chimera were discarded without further analysis (92, 93). The assembled sequences were compared to the sequences of known RDX-degraders in GenBank using Basic Local Alignment Search Tool program (BLAST) and also used for *in-silico* analysis as described previously (90). The Classifier of Ribosomal Database Project (RDP) version 10 (94) was used to assign taxonomic identity to each sequence. Phylogenetic analyses of aligned sequences were created using neighbor-joining approaching MEGA version 5.0 (95). *In-silico* analysis were performed using program TRiFLE (96) to predict the theoretical terminal restriction fragments (T-RF) of the 16S rRNA gene sequences obtained from this study. The predicted T-RFs corresponded to the measured T-RFs in the microbial community profile and used to link to the most possible ribotypes (90). The 16S rRNA gene sequences were deposited in GenBank under accession numbers JX066666 to JX066697, and JX073128 to JX073134 in Chapter IV. The 16S rRNA gene sequences were deposited in GenBank under accession numbers JX470441-JX470483 in Chapter V. The 16S rRNA gene sequences were deposited in GenBank under accession numbers KF737868-KF737909 in Chapter VI.

3.1.8. Chemical analysis

The concentrations of RDX and their breakdown products were determined according to a modified EPA Method 8330 using a Dionex 3000 Ultimate HPLC with an Agilent E1 column. The mobile phase was methanol: water (50:50), and the flow rate was 1 mL/min. The column temperature was maintained at 33 °C. The detection limit for RDX was 10 µg/L and for the RDX metabolites (MNX, DNX, and TNX) was around 50 µg/L. No analyses for 4-nitro-2,4-diazabutanal (NDAB) or methylenedinitramine (MEDINA) were performed, as NADB and MENDINA can be formed from MNX under specific anaerobic conditions (97). In addition, MEDINA is a short-lived metabolite that quickly decomposes in water (98).

3.2. Materials and methods used in Chapter VII

The detail material and methods of the application of identification of suitable biomarkers for assessing biodegradation of RDX in natural an engineered system in u VII are described in the follows text.

3.2.1. Chemicals

Primers for real-time-PCR assays were purchased from Integrated DNA Technologies, Inc (Coralville, CA). Quanti-Tect SYBR Green supermix were purchased from Qiagen (Valencia,CA).). FastDNA SPIN kit was purchased from MP Biomedicals (Solon,OH).

3.2.2. Organisms and culture conditions

Bacterial strain *P. fluorescens* I-C possessing the *xenB* gene was grown aerobically in Reasoner's 2A (R2A) medium. Incubation was at 30°C with rotary shaking at 160 rpm. The cells in the late exponential phase (OD₆₀₀ ~ 0.8-1.0) were harvested by centrifugation at 10,000×g for 5 min and extracted the genomic DNA as manufactory instruction.

3.2.3. Development of real-time PCR assay for *xenB* genes

Primers sequences were initially designed with the Primer-Blast tool (<http://www.ncbi.nlm.nih.gov/tools/primer-blast/>) using the *Pseudomonas fluorescens* xenobiotic reductase B (*xenB*) gene fragment, accession numbers AF154062. The primers used were as follows: *xenB* forward 750F (5'-GTTCTTGCAAAGCAGCACCA-3'); *xenB* reverse 1074R, (5'-CTTGGTGAAACGCTCGTTGG-3'). All primers were custom ordered from Integrated DNA Technologies, Inc. (Coralville, CA). The genomic DNA from all samples in this study were extracted using FastDNA spin kit (MP Biomedical, Solon, OH). The DNA concentrations were determined using a NanoDrop ND-1000 Spectrophotometer (Fisher Scientific., Fair Lawn, NJ). The PCR amplification was conducted in an automated thermal cycler (PCR Sprint system, Thermo Electron Corp.m Waltham, MA). Each 25 µL PCR mixture contained 400 nM forward/reverse primers set and 12.5 µL of Taq DNA polymerase PCR mix buffer (Qiagen, Valencia, CA). The thermal cycling protocol as follows: 95 °C for 15 min; 35 cycles of 95 °C for 30 sec, 55 °C for 1 min, and 72 °C for 2 min and a final extension at 72°C for 10 min.

The presence of PCR amplicons was determined using gel electrophoresis. The amplicons of *xenB* gene was cloned into the vector pCR4-TOPO using a TA Cloning Kit (One Shot TOP10 Competent cells) (Invitrogen, Carlsbad, CA). Colonies with inserts were verified by PCR with primers M13F (5'-GTAAAACGACGGCCAG-3') and M13R (5'-CAGGAAACAGCTATGAC-3'), and screened on 1.5% agarose gels (Fisher Scientific, Fair Lawn, NJ). The cloned plasmid DNA of *xenB* gene fragment was extracted using a plasmid purification Kit (QIAGEN, Valencia, CA).

3.2.4. Validation of developed real-time PCR assay

All real-time PCR amplification reactions were performed using a Bio-Rad iQ5 Multicolor Real-Time PCR Detection System (Bio-Rad Laboratories, Inc., Hercules, CA). PCR was carried out in 25 μ L volumes in 96 well reaction plates. Each 25 μ L PCR mixture contained 400 nM forward/reverse primers set and 12.5 μ L SYBR Green PCR kit (Qiagen, Valencia, CA). Amplification condition for this reaction consisted of a single step as follows: 95 °C for 15 min; 40 cycles of 95 °C for 30 sec, 55 °C for 1 min, and 72 °C for 2 min and final at 4°C. Cloned plasmid DNA of *xenB* gene concentration (ranging from 1.0×10^3 to 1.0×10^8 copies, $R^2 > 0.99$) was constructed as a standard for quantification.

3.2.5. Column studies

Several groundwater samples were collected and used for detect the presenting of *xenB* gene with real-time PCR assays. DNA collected from groundwater microcosms as

used in Chapter IV to VI were selected and test the assay. In addition, aquifer materials and groundwater collected from a testing facility site in the eastern of United States were used to construct the column study (Table III.4). The site was contaminated with explosive for several decades. Groundwater in these monitoring wells was aerobic and contained RDX. The pH range was 4 to 5. Nitrate and sulfate in groundwater concentration was 1 to 5 mg/L. No significant soluble iron were detected (<1 mg/L).

Three columns treatment were prepared with emulsified oil substrate amendment for biostimulation of RDX degradation. Each column was made from 7 cm ID aluminum tubing cut to a length of 30 cm. Site sediment was homogenized and packed into the columns. Groundwater was collected at the field site and used as the column mobile phase. An emulsified vegetable oil substrate, which includes lactate and trace nutrients (EOS, EOS Remediation, Inc, Raleigh, NC), was added to the columns to promote biological reduction of nitramine explosives. A buffer solution (AquaBupH) was amended. After RDX degradation, three sections (0-10, 10-20, and 20-30 cm) of sediments samples were collected for DNA extraction, respectively. Groundwater was collected from the sites and effluent from column studies were collected and filtered the biomass for DNA extraction.

Table III.4. Groundwater and column study construction in Chapter VII

Sample ID	Source Description	Treatment	
Background groundwater	A	C-02	-
	B	D-04	-
	C	IW-8	-
	D	MW-8	-
	E	Influent Groundwater	-
Column 1	K-1	Col 1 sediment (0-10cm)	EOS-Low Salt
	K-2	Col 1 sediment (10-20cm)	
	K-3	Col 1 sediment (20-30cm)	
Column 2	L-1	Col 2 sediment (0-10cm)	Control
	L-2	Col 2 sediment (10-20cm)	
	L-3	Col 2 sediment (20-30cm)	
Column 3	M-1	Col 3 sediment (0-10cm)	EOS-Low Salt and AquaBupH buffer
	M-2	Col 3 sediment (10-20cm)	
	M-3	Col 3 sediment (20-30cm)	

CHAPTER IV
APPLICATION OF ¹³C-STABLE ISOTOPE PROBING TO IDENTIFY
RDX-DEGRADING MICROORGANISMS IN GROUNDWATER

4.1. Introduction

Hexahydro-1,3,5-trinitro-1,3,5-triazine (RDX) is a soluble, nonvolatile cyclic nitramine explosive that has been widely used in military and civilian applications (99). RDX is also a common groundwater contaminant (100-104) and a possible human carcinogen. Although there is no federal drinking water standard for RDX, this nitramine has been placed on the U.S. Environmental Protection Agency (EPA) Contaminant Candidate List, and the EPA has issued a health advisory level of 2 µg/L for RDX in drinking water (3).

RDX is biodegradable under both aerobic and anaerobic conditions, and numerous RDX-degrading isolates have been reported (15-27, 55). Yet, our understanding of the roles of these known RDX degraders in the environment, the prevalence of RDX degraders in natural or engineered systems, as well as their associated RDX-degrading microbial communities in response to engineered interventions is still developing.

* Reprinted from Environmental Pollution, Vol 178, Cho, K.-C., Lee, D.G., Roh, H., Fuller, M.E., Hatzinger, P.B., Chu, K.-H., Application of ¹³C-stable isotope probing to identify RDX-degrading microorganisms in groundwater, Pages 350-360., Copyright (2013), with permission from Elsevier.

A better knowledge of in situ RDX degradation could potentially guide the isolation of novel RDX degraders (28) and the development of suitable biomarkers for monitoring intrinsic or engineered RDX bioremediation.

Our current understanding of RDX biodegradation is mainly derived from studies using RDX-degrading isolates. To date, only a few such isolates have been characterized under laboratory conditions. For example, some of these isolates can use the nitramine as a sole nitrogen or energy source (15, 18, 19, 47, 54, 55, 62, 63, 69, 105-112), or as a sole carbon source (65). Only two strains can use RDX for both carbon and nitrogen sources (17).

Our understanding of the microorganisms involved in RDX biodegradation is also limited by the fact that only a small fraction of environmental organisms can be isolated and cultivated in the laboratory. Therefore, using a cultivation-independent molecular technique is necessary to identify the active microorganisms responsible for RDX degradation in the environment. Stable isotope probing (SIP) has been recognized as a powerful culture-independent tool to study microbial community function, as this method can identify active microorganisms capable of utilizing a labeled compound (80, 81, 89, 113-118). When a labeled compound is readily biodegradable and structurally simple with one or two carbons, the uncultivable microorganisms identified from the SIP method can be easily recognized as “utilizers.” For a compound like RDX, the application of SIP can provide insight into an active RDX-degrading microbial community consisting of microorganisms that can derive and/or utilize carbon or nitrogen from RDX and/or RDX metabolites. This aspect can be easily illustrated using

two known anaerobic degradation pathways as shown in Figure IV.1 (74). Organisms involved in direct attack on the parent RDX molecules and capable of using RDX for growth can be defined as RDX utilizers. Those capable of utilizing RDX metabolites can be referred as RDX scavengers.

In a previous study, we successfully applied ^{15}N -RDX SIP to identify fifteen phylogenetically diverse RDX- degrading microorganisms in groundwater microcosms receiving cheese whey (89). Our previous results also suggested that the addition of a carbon and nutrient source like cheese whey (i.e., to enhance the anaerobic biodegradation of explosives) may stimulate different RDX-degrading microorganisms. In this study, we applied ^{13}C -RDX SIP to identify active microorganisms capable of using RDX as a carbon source in groundwater microcosms with and without cheese whey. The effects of an additional carbon amendment (in the form of cheese whey) on the active RDX-degrading microbial community structure were also examined.

4.2. Results and discussion

4.2.1. Biodegradation of RDX in groundwater microcosms in the presence and absence of cheese whey

RDX biodegradation was observed in the microcosms that did not receive additional cheese whey (Figure IV.2(A)-(B)). In microcosms from MW-5 (which only had a small amount of residual TOC remaining from *in-situ* whey addition), the rates of RDX biodegradation were much more variable (Figure IV.2(A)).

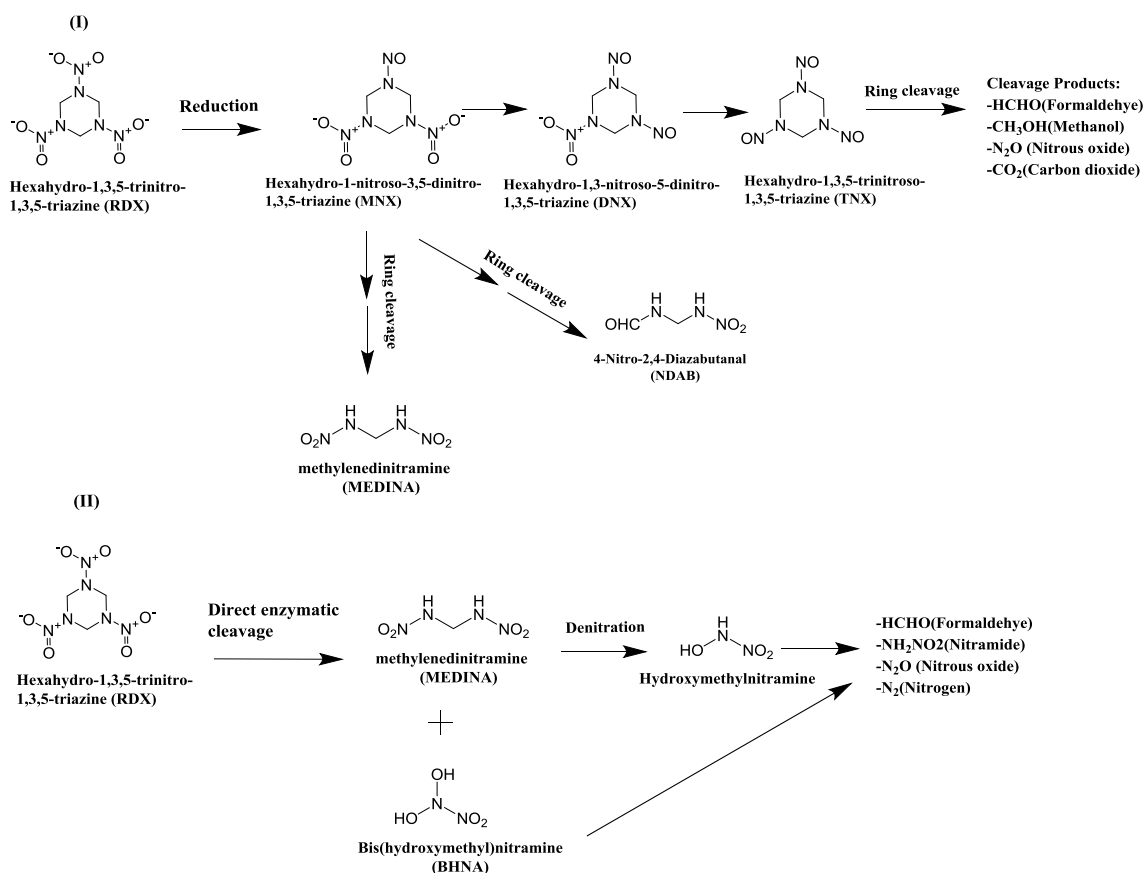


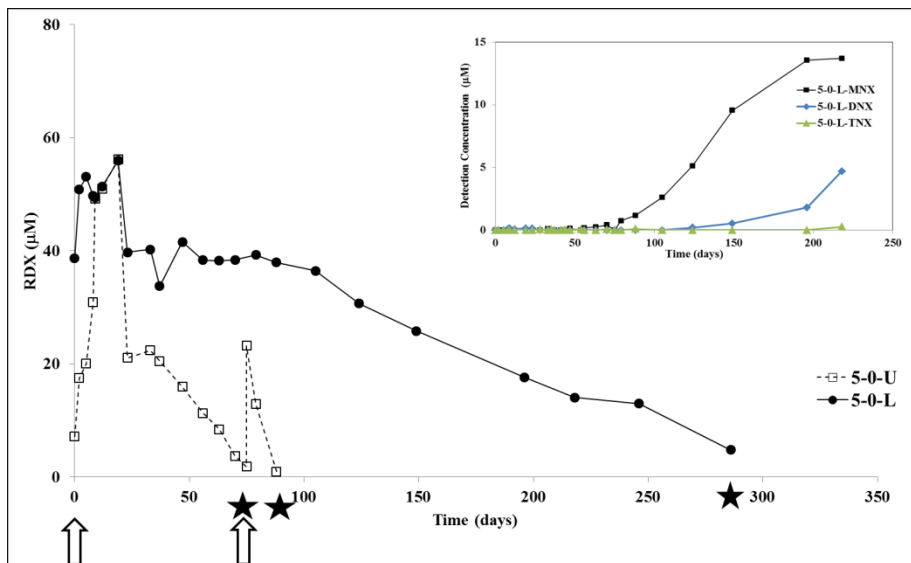
Figure IV.1. RDX microbial degradation pathways under anaerobic conditions (adapted from Halasz and Hawari., 2011) (74).

In one microcosm, which received unlabeled RDX (5-0-U), complete biodegradation occurred over approximately 75 days after the first spike, and then < 20 days after the second RDX addition. By comparison, in a second microcosm that received ¹³C-RDX (5-0-L), slow biodegradation occurred over 200 days after an initial lag phase of nearly 100 days. The degradation was confirmed by the detection and accumulation of nitroso metabolites (MNX, DNX, and TNX) after day 75 (insert of Figure IV.2(A)). The total amount of nitroso metabolites (i.e. summation of moles of detected metabolites) detected

accounted for approximately 10% of RDX degraded (molar basis). The appearance of the nitroso metabolites was consistent with the slow RDX degradation pattern observed in microcosm 5-0-L. As shown in Figure IV.1, RDX can be degraded via two potential degradation routes— sequential nitroreduction and direct ring cleavage under anaerobic conditions. Through sequential reduction of the nitro groups, MNX, DNX and TNX are formed. Ring cleavage of MNX is also possible, forming MEDINA (a short-live metabolite in water) and NDAB. Alternatively, the ring of RDX can be cleavage directly to produce MENDINA and bis(hydroxymethyl) nitramine (BHNA). Other abiotic or chemical reactions might have occurred to produce unknown RDX metabolites that were not investigated in this study. Overall, these might explain that only 10 % of nitroso metabolites had been recovered due to different degradation routes involved in both well. However, the reason for the inconsistency between these two microcosms is unclear.

In microcosm (7-0-L) prepared from MW-7D (which had > 10 mg/L of residual TOC remaining from *in-situ* treatment), RDX biodegradation was rapid, and rates increased after additional spike of the nitramine were added to each bottle (Figure IV.2(B)). A noticeable decrease of RDX was observed after day 12. Also, MNX, DNX, and TNX were detected on day 7, day 18, and day 24, respectively (see insert in Figure IV.2(B)). The total amount of MNX accounted for 20-30% of RDX degraded in microcosm 7-0-L.

(A)



(B)

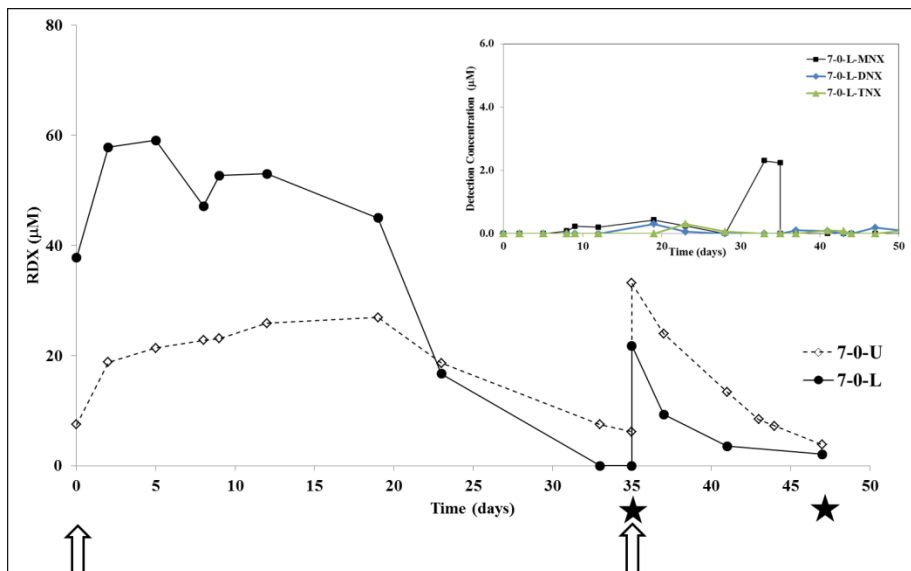


Figure IV.2. RDX degradation over time in microcosms receiving either unlabeled or ^{13}C -labeled RDX. Microcosms constructed from MW-5 groundwater (A) with unlabeled RDX (5-0-U) or ^{13}C -labeled RDX (5-0-L). Microcosms constructed from MW-7D groundwater (B) with unlabeled RDX (7-0-U) or ^{13}C -labeled RDX (7-0-L). Arrows indicate the addition of RDX. Stars (*) indicate time of sampling for SIP and other molecular analyses. Initial concentration of RDX in microcosms was 10 mg/L (45 μM). The inserts represent nitroso metabolites (MNX, DNX, and TNX) production over time in Microcosms 5-0-L and 7-0-L.

Unlike the slow RDX degradation observed in the absence of cheese whey, more rapid RDX degradation was observed in microcosms from MW-5 and MW-7D to which additional cheese whey was added (Microcosms 5-C-U, 5-C-L, 7-C-U, and 7-C-L). The initial RDX was degraded over a period of 30 days (Figure IV.3(A)-(B)), and additional spikes of RDX in these microcosms were degraded even more rapidly, suggesting conditions within the microcosms were ideal for RDX biotransformation/degradation likely via an increase in microbial biomass/activity or both. The RDX breakdown products MNX, DNX and TNX were detected sporadically in these microcosms. These nitroso metabolites (MNX, DNX, TNX) were observed over the period of 35 days in Microcosms 5-C-L and 7-C-L (see inserts of Figure IV.3(A) and Figure IV.3(B)). The concentrations of these metabolites in the microcosms were very low, ranging from 0.2 to 0.6 mg/L (e.g., less than 10% of the added RDX).

In Microcosm 7-0-L prepared from MW-7D (which had > 10 mg/L of residual TOC remaining from *in-situ* treatment), RDX biodegradation was rapid, and rates increased after an additional spike of the nitramine was added to each bottle (Figure IV.2 (B)). A noticeable decrease of RDX was observed after day 12. Also, MNX, DNX, and TNX were detected on day 7, day 18, and day 24, respectively (see insert in Figure IV.2 (B)). The total amount of MNX accounted for 20–30% of RDX degraded in microcosm 7-0-L.

Unlike the slow RDX degradation observed in the absence of cheese whey, more rapid RDX degradation was observed in microcosms from MW-5 and MW-7D to which additional cheese whey was added (microcosms 5-C-U, 5-C-L, 7-C-U, and 7-C-L). The initial RDX was degraded over a period of 30 days (Figure IV.3 (A) and (B)), and an additional spike of RDX in these microcosms was degraded even more rapidly, suggesting conditions within the microcosms were ideal for RDX biotransformation/degradation likely via an increase in microbial biomass/activity or both. The RDX breakdown products MNX, DNX and TNX were detected sporadically in these microcosms. These nitroso metabolites (MNX, DNX, and TNX) were observed over the period of 35 days in Microcosms 5-C-L and 7-C-L (see inserts of Figure IV.3 (A) and (B)). The concentrations of these metabolites in the microcosms were very low, ranging from 0.2 to 0.6 mg/L (e.g., less than 10 % of the added RDX).

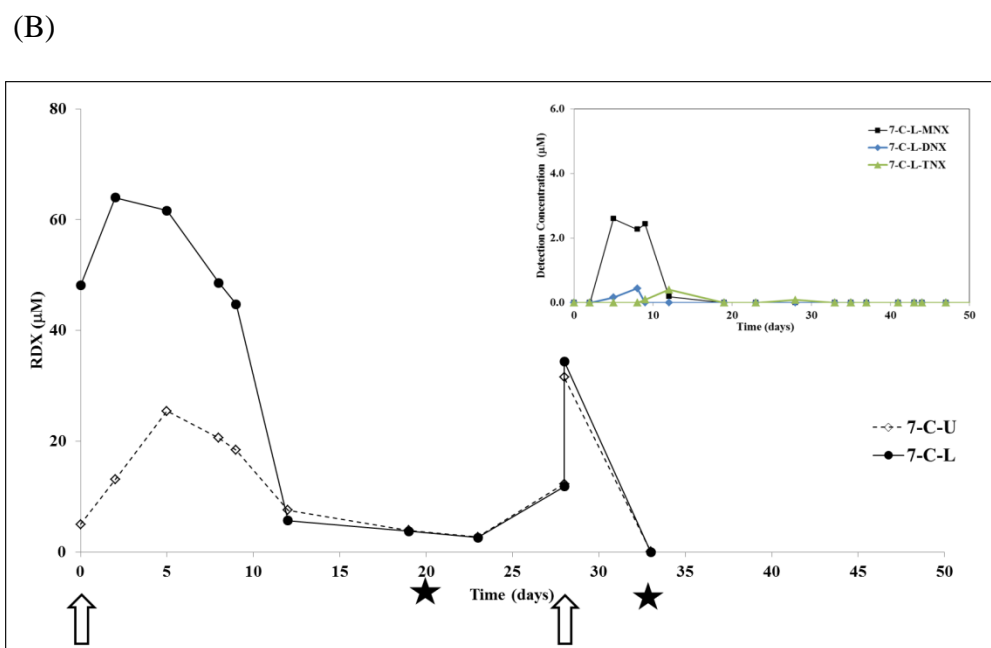
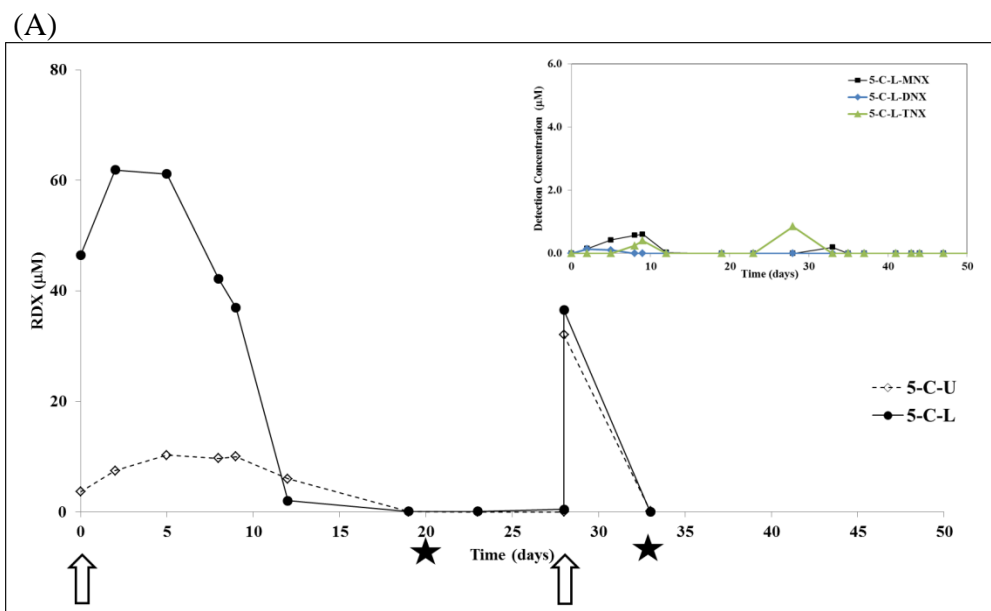


Figure IV.3. RDX degradation over time in microcosms receiving cheese whey and RDX (unlabeled or ¹³C-labeled RDX). Microcosms constructed from MW-5 groundwater (A) with unlabeled RDX (5-C-U) or ¹³C-labeled RDX (5-C-L). Microcosms constructed from MW-7D groundwater (B) with unlabeled RDX (7-C-U) or ¹³C-labeled RDX (7-C-L). Arrows indicate the addition of RDX. Stars (*) indicate time of sampling for SIP and other molecular analyses. Initial concentrations of RDX and cheese whey in microcosms were 10 mg/L (45 µM), and 100 mg/L, respectively. The inserts represent nitroso metabolites (MNX, DNX, and TNX) production over time in Microcosms 5-C-L and 7-C-L.

4.2.2. Changes of RDX-degrading microbial community structure in groundwater microcosms

By using real-time-t-RFLP analysis, the effects of RDX and cheese whey additions on RDX-degrading microbial community structure of groundwater microcosms were examined. The results of real-time-t-RFLP analyses (Figure A.1-A.15 in Appendix A) were used to calculate four diversity indices: S , H' , E , and $1/D$ (Table IV.1). Note that different microorganisms in environmental samples might contribute to a single fragment. As such, the diversity indices based on the number of terminal fragments might also inherit the same uncertainties. By comparing the diversity indices for microcosm 7-0-U with those for microcosm 5-0-U, the groundwater from MW-7D appeared to have a more diverse and richer microbial community structure than that from MW-5. This may reflect the fact that MW-7D still had more than 10 mg/L of TOC from *in-situ* cheese whey addition, whereas MW-5, which was upgradient of MW-7D, had very little residual TOC (4 mg/L compared to typical background values of 3 mg/L). These results seem to indicate that the presence of higher residual TOC in MW-7 contributed to a more diverse microbial community. Nevertheless, the impacts of residual TOC on microbial community post treatment remained. In contrast, the addition of cheese whey was likely to cause a dramatic and quick increase of labile TOC content, which would in turn be favorable for rapid growth of a small subset of bacterial species, and lead to less a diverse microbial community.

In general, the second addition of RDX caused a decrease in microbial diversity compared to the microbial community structure after the initial RDX concentration was

depleted. The addition of cheese whey significantly affected the microbial community structure, causing the community to become less diverse (compared the Shannon-Weaver and Simon's indices of Microcosms 5-0-U vs. 5-C-U, and 7-0-U vs. 7-C-U).

Table IV.1. Diversity indices of RDX-degrading microbial community structures of groundwater microcosms receiving unlabeled RDX

Microcosms ID	Diversity Indices* of Microbial Community Structure after the initial RDX spike was depleted				Diversity Indices of Microbial Community Structure after the second RDX spike was depleted			
	<i>S</i>	<i>H'</i>	<i>E</i>	<i>1/D</i>	<i>S</i>	<i>H'</i>	<i>E</i>	<i>1/D</i>
5-0-U	7	2.5	0.9	5.0	7	2.5	0.9	4.8
5-C-U	9	1.9	0.6	2.2	7	2.0	0.7	3.2
7-0-U	10	2.8	0.8	5.9	9	2.6	0.8	5.1
7-C-U	6	1.8	0.7	2.8	7	1.7	0.6	3.0

*S = richness; H' = Shannon-Weaver diversity; E = evenness; 1/D = the reciprocal of Simon's

4.2.3. Microorganisms capable of using RDX or RDX intermediates as a carbon source

Active microorganisms capable of using RDX and/or RDX intermediates (NMX, DNX, TNX, MEDINA, and NDAB) as a carbon source (see Figure IV.1) were identified from the ¹³C-DNA fractions of groundwater microcosms receiving the first spike of ¹³C-RDX without cheese whey (i.e. sample IDs 5-0-La and 7-0-La). Ten different 16S rRNA gene sequences were derived from sample 5-0-La, and six different 16S rRNA gene sequences were derived from sample 7-0-La (Figure IV.4). The ten sequences

derived from sample 5-0-La were widespread among four different classes: α -*Proteobacteria* (2 sequences), β -*Proteobacteria* (5 sequences), δ -*Proteobacteria* (2 sequences), and *Spirochaetes* (1 sequences). The six sequences derived from sample 7-0-La clustered among four different classes: *Bacteroidia* (1 sequence), *Clostridia* (1 sequence), β -*Proteobacteria* (2 sequences), and *Spirochaetes* (2 sequences). The differences between derived sequences indicate that RDX-degrading bacteria were present and phylogenetically diverse. Some, but not all, of these 16 clones have > 85% homology to the 25 clones derived from the background groundwater (outside the plume) (89) (see Table A.1 in Appendix A). Table A.2 (in Appendix A) summarizes the theoretical T-RFs of the derived clones from all ^{13}C -DNA fractions and linked to the profiles of microbial ribotypes obtained from real-time-t-RFLP analyses (Figures A1-A15 in Appendix A). However, the theoretical T-RFs corresponded only to a few measured T-RFs. The discrepancy might be due to a bias against low abundance sequences in PCR-based sequencing and cloning (119, 120).

The difference in residual TOC from in situ cheese whey injection between wells MW-5 and MW-7D at the time of sampling may also have contributed to the differences in microbial community structure. A significant finding of this study was that all the 16 sequences from both wells were different from any known RDX-degraders (< 95% homology) (16, 17, 23, 59, 61, 63), which are clustered in *Actinobacteria*, *Clostridia*, and γ -*Proteobacteria*. Nine different 16S rRNA genes sequences were derived from sample 7-0-Lb, a sample taken after the depletion of the second RDX addition in the microcosms (data not shown). The nine clones were different from the 16 clones

recovered after the first RDX spike had been depleted. The nine clones might represent true rapid RDX utilizers (i.e., utilize C in parent RDX) due to enrichment, or RDX scavengers organisms that were labeled due to cross-feeding on labeled organisms that degraded the first spike of RDX. To be conservative in our analysis, these nine clones were excluded from the phylogenetic analysis.

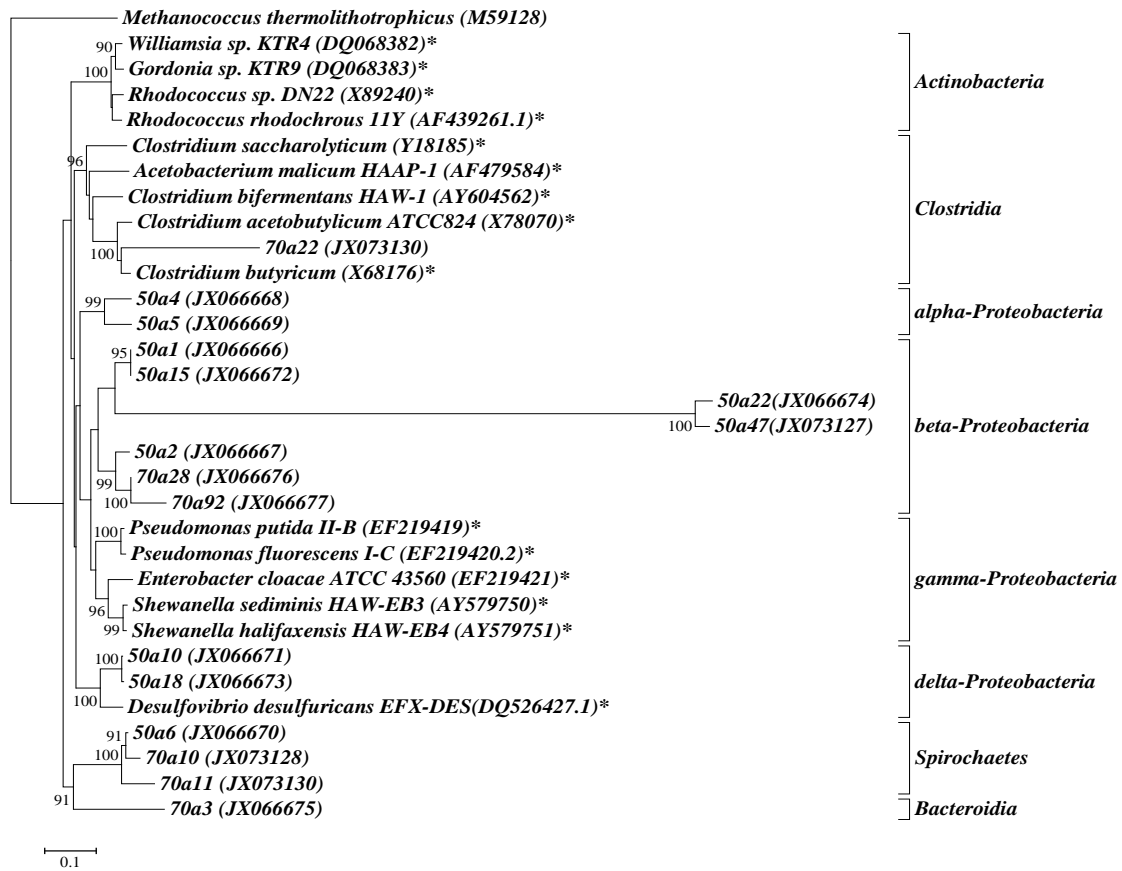


Figure IV.4. Phylogenetic tree representing 16S rRNA gene sequences derived from ^{13}C -DNA fractions of groundwater microcosms receiving only ^{13}C -labeled RDX (i.e. Sample IDs = 5-0-La and 7-0-La). The tree was rooted with *Methanococcus thermolithotrophicus* and was constructed using the neighbor-joining algorithm. The number of clone sequences and the GenBank accession numbers are in parentheses. Only bootstrap values above 85% are shown (1,000 replications). Bar, 10% estimated sequence divergence. An asterisk (*) indicates a known RDX degrader.

All the derived clones are different from known RDX degraders, except one sequence (70a22) resides in *Clostridia*, a phylum with several known RDX degraders (19, 61). Fuller et al. reported that *Clostridia* were the major 16S rRNA gene sequences recovered from groundwater samples and groundwater microcosms derived from the same contaminated aquifer (121). Zhang and Hughes reported that *Clostridium acetobutylicum* ATCC 824 was able to reductively transform RDX into several polar intermediates when hydrogen was supplied as the electron donor (61). The other two sequences, 50a10 and 50a18, were identified as *Desulfovibrio* sp.; they showed 97 % similarity to *Desulfovibrio mexicanus* strain Lup1 (accession number: NR028776). Several studies have reported that *Desulfovibrio* sp. were capable of mineralizing RDX and using RDX as a carbon source under anoxic conditions (19, 65, 75). As RDX biodegradation has been reported under sulfate-reducing conditions (22), the detection of these two sequences 50a10 and 50a18 suggested that some *Desulfovibrio* sp. might be able to utilize RDX or RDX metabolites as a carbon source.

Sequences 50a4 and 50a5 fell within the cluster of Order *Rhizobiales*, which are nitrogen-fixing bacteria. Using ^{15}N -RDX SIP, our previous study (89) identified three ^{15}N clones (RDX clones 15N-2, 8, 13) that were very close to *Azospirillum* sp. (a nitrogen-fixing bacterium). It is interesting to note that the same groups of nitrogen-fixing organisms were detected via both ^{15}N -RDX and ^{13}C -RDX SIP. Overall, these results implicated the presence of nitrogen-fixing strains that are also capable of using RDX as a nitrogen source and/or a carbon source.

With the aid of ^{13}C -RDX SIP, we observed 11 out of 16 clones in the *Bacteroidia* (70a3), the β -*Proteobacteria* (50a1, 50a2, 50a15, 50a22, 50a47, 70a28, 70a92) and the *Spirochaetes* (50a6, 70a10, 70a11). To our knowledge, this is the first report of RDX degradation attributed to these taxonomic groups. Sequences 50a1 and 50a15 showed 97% similarity to an iron-reducing bacterium, *Rhodoferrax fermentans* strain FR2 (accession number: NR025840). Increasing numbers of *Rhodoferrax* sp. were reported during RDX degradation in aquifer materials amended with acetate or lactate (26). Since iron-reducing bacteria are ubiquitous in groundwater, future studies are needed to investigate the role of *Rhodoferrax* sp. in RDX biodegradation (122-125).

The sequences 50a2, 70a28, and 70a92 fell with the cluster *Rhodocyclaceae*, a family of denitrifying bacteria. These findings suggest that many unknown RDX-degrading bacteria play an important role during in situ RDX biodegradation. Future research is needed to explore the significance of these strains, such as *Desulfovibrio* sp., *Azospirillum* sp., and *Rhodoferrax* sp., during intrinsic biodegradation of RDX. These strains might be important biomarkers for assessing in situ RDX biodegradation when monitored natural attenuation is selected as a remediation option. Research efforts focusing on isolating these strains from sites for detailed biochemical studies are also warranted.

In this study, application of ^{13}C -SIP to RDX-degrading microcosms has yielded an interesting insight into microbial ecology of RDX degradation. This is the first time that we realized the diversity and variation of RDX utilizers and RDX scavengers in the environmental samples. Our results are considered conservative since the ^{13}C -labeled

DNA were obtained from the same position of the 100% ^{13}C -labeled DNA of *E. coli*. with a 51% genome G+C content, which was used as a reference in the control tubes. Due to difference in genomic G+C content, the buoyant density of 100% ^{13}C -labeled DNA from an organism with a 51% genome G+C content (such as *E. coli*) will have the same as the buoyant density of 50% ^{13}C -labeled DNA from an organism with a 67% genome G+C content (such as *Rhodococcus jostii* RHA1), and the same as the buoyant density of 27% ^{13}C -labeled DNA from an organism with a 75% genome G+C content (such as *Micrococcus luteus*) (see Figure A.16 in Appendix A). While our approach did not capture those fallen beyond the buoyant density of the 100% ^{13}C -labeled DNA of *E. coli*, it is expected that our approach will capture partially ^{13}C -labeled microorganisms with various genomic G+C content (ranging approximately from 50 to 75%). Another limitation of using SIP in this study was to differentiate the true RDX utilizers from the RDX scavengers (defined previously as those capable of utilizing RDX metabolites). Nevertheless, both RDX utilizers and scavengers are important and contribute to complete mineralization of RDX in natural and engineered systems.

4.2.4. Active RDX-degrading microorganisms in groundwater microcosms receiving cheese whey

Addition of cheese whey changed the types and distribution of microorganisms capable of using RDX and/or RDX metabolites as a carbon source. Fourteen different ^{13}C -clones were derived from samples 5-C-La and 5-C-Lb. Unlike the wide distribution of ^{13}C -clones obtained from microcosms receiving only ^{13}C -labeled RDX, these 14

clones clustered in γ -*Proteobacteria* and *Bacilli* (Figure IV.5). The seven sequences (5Ca2, 5Ca12, 5Ca25, 5Ca31, 5Cb2, 5Cb5, and 5Cb10) were identified as *Pseudomonas* sp. and clustered in γ -*Proteobacteria* with two known RDX degraders, *Pseudomonas fluorescens* I-C and *Pseudomonas putida* II-B (69, 73, 126). This observation is consistent with the findings of Fuller et al (121), in which many *Pseudomonas* sp. sequences were recovered from groundwater and laboratory enrichments when biostimulation was performed to promote RDX degradation. Our results also suggest that *Pseudomonas* sp. play a key role in the transformation of RDX and other nitramine explosives in the environment, as some strains have been shown to transform RDX under anoxic conditions (69). The rest of clones were clustered in the *Bacilli* (discussed below).

From sample 7-C-La and 7-C-Lb, another 10 distinct ¹³C-clones were recovered, distributed among three phyla β -*Proteobacteria*, *Actinobacteria*, and *Bacilli* (Figure IV.6). Among the 10 clones, four sequences (7Ca15, 7Ca21, 7Cb6 and 7Cb11) resided in *Actinobacteria*, a phylum with four known RDX degraders: *Rhodococcus* sp. DN22, *Rhodococcus rhodocrous* 11Y, *Gordonia* sp. KTR9, and *Williamsia* KTR4 (15-17, 47, 69). However, only sequence 7Cb11 in the present study was identified as a *Rhodococcus* sp. Although some *Rhodococcus* strains have recently been shown to degrade RDX slowly under microaerophilic conditions (112), the anoxic conditions maintained in the microcosms during this study may have limited their activity.

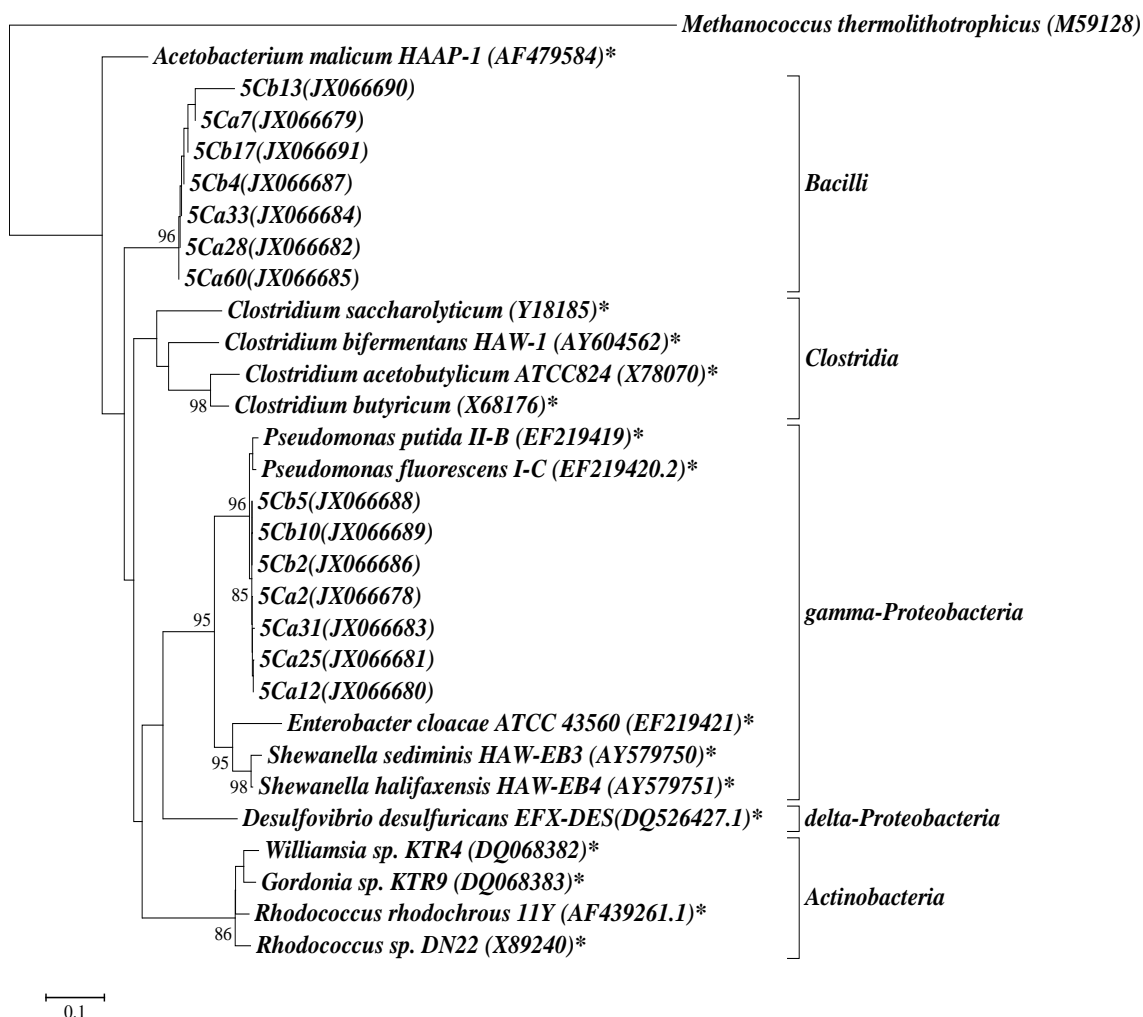


Figure IV.5. Phylogenetic tree representing 16S rRNA gene sequences derived from ^{13}C -DNA fractions of groundwater microcosms receiving MW5 groundwater, cheese whey, and ^{13}C -labeled RDX (i.e. sample IDs = 5-C-La and 5-C-Lb). The tree was rooted with *Methanococcus thermolithotrophicus* and was constructed using the neighbor-joining algorithm. The number of clone sequences and the GenBank accession numbers are in parentheses. Only bootstrap values above 85% are shown (1,000 replications). Bar, 10% estimated sequence divergence. An asterisk (*) indicates a known RDX degrader.

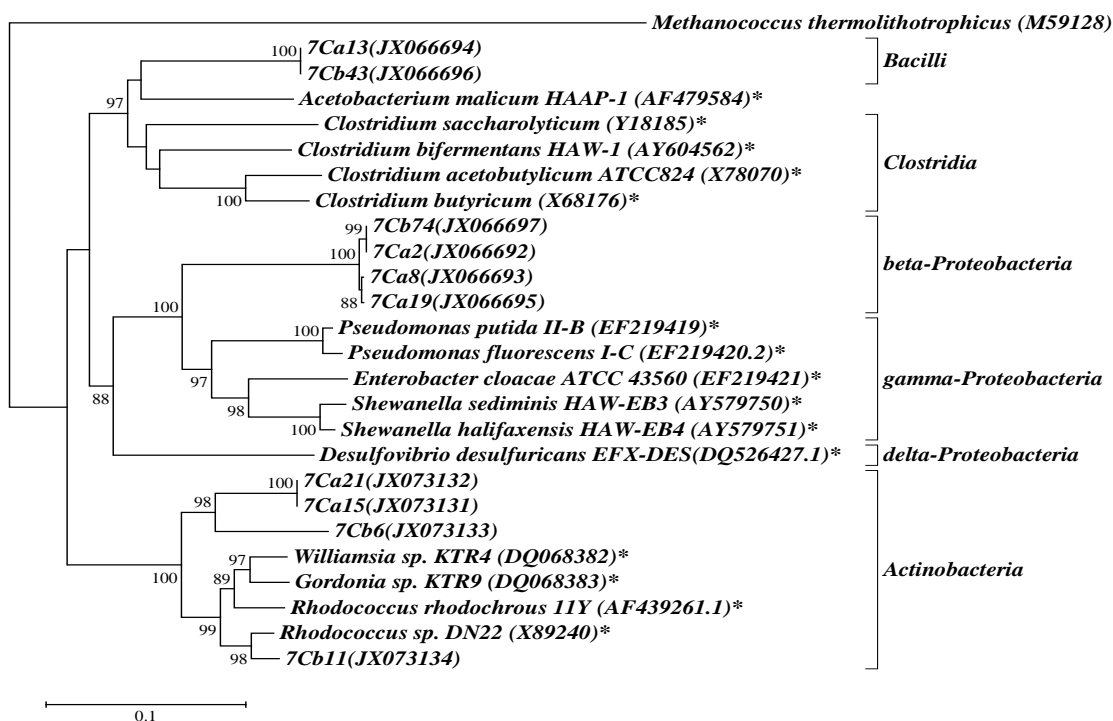


Figure IV.6. Phylogenetic tree representing 16S rRNA gene sequences derived from ^{13}C -DNA fractions of groundwater microcosms receiving MW-7D groundwater, cheese whey, and ^{13}C -labeled RDX (i.e. sample IDs = 7-C-La and 7-C-Lb). The tree was rooted with *Methanococcus thermolithotrophicus* and was constructed using the neighbor-joining algorithm. The number of clone sequences and the GenBank accession numbers are in parentheses. Only bootstrap values above 85% are shown (1,000 replications). Bar, 10% estimated sequence divergence. An asterisk (*) indicates a known RDX degrader.

A significant number of clones derived from cheese whey-amended microcosms were found clustered in *Bacilli*. For example, seven sequences recovered from microcosm 5-C-L (5Ca7, 5Ca28, 5Ca33, 5Ca60, 5Cb4, 5Cb13, and 5Cb17) and two sequences from microcosm 7-C-L (7Ca13, and 7Cb43) cluster in *Bacilli*. The reason that a high number of clones in the cheese whey-amended microcosms are *Bacilli* is unknown. However, the addition of nutrients (particularly the high amounts of the sugar lactose (typically 70-75% (w:w) of cheese whey) (127, 128) is known to promote reactivation of spores (129), which may have been present in both the groundwater and the cheese whey itself. Nevertheless, our SIP results clearly indicated that the *Bacilli* were stimulated by the cheese whey addition and that they assimilated ^{13}C initially derived from ^{13}C -labeled RDX in our microcosms.

Using the ^{13}C -clones obtained from this study, the distribution of RDX-utilizing/degrading microorganisms was analyzed. As shown in Table IV.1 and Table A.2. (in Appendix A), among the 16 clones obtained from the samples without cheese whey addition (e.g., with only residual TOC in the groundwater from previous in situ whey addition more than one year previous), the diversity of RDX-utilizing bacteria was high, being distributed among six different classes. However, when cheese whey was added, the distribution shifted dramatically from four to two classes for microcosm 5-C-L (based on a total number of 14 clones), and from four to three classes for microcosm 7-C-L (based on a total number of 10 clones).

Interestingly, in the absence of cheese whey addition, none of previously reported RDX-degraders were detected. In the absence of whey, we identified three classes (*Spirochaetes*, *Bacteroidia*, and α -*Proteobacteria*) that have not been previously associated with RDX biodegradation. This finding suggests a new direction of research to better understand RDX-utilizing bacteria that may be important during in situ RDX bioremediation or natural RDX attenuation under anoxic conditions (e.g., with natural TOC in groundwater). A majority of the clones identified in this study are not closely related to any known RDX degraders. As such, the use of known RDX degraders (like *Rhodococcus* DN 22) or a catabolic gene (like *xplA*)— which are associated with aerobic RDX degradation—as biomarkers might not be appropriate to assess RDX biodegradation potential or to monitor the progress of RDX biodegradation in situ, particularly for those under anoxic conditions. Future research efforts should be placed on the development better biomarkers for assessing RDX biodegradation potential under various geochemical conditions, perhaps based on sequences that have been directly linked to RDX degradation via ^{13}C - or ^{15}N -SIP, or both.

CHAPTER V
PROBING ACTIVE MICROORGANISMS CAPABLE OF
USING DIFFERENT NITROGEN IN RDX STRUCTURE AS A NITROGEN
SOURCE

5.1. Introduction

Hexahydro-1,3,5-trinitro-1,3,5-triazine (RDX) is a common military explosive and a common soil and groundwater contaminant; it is particularly detected in many historical munitions sites. As RDX is moderately soluble and sorbs weakly to soil, RDX-contaminated groundwater is potentially to impact local drinking water supplies (100-104). RDX is a possible human carcinogen and has been listed on the Contaminant Candidate List 3 by the U.S. Environmental Protection Agency (EPA). The U.S. EPA has issued a health advisory level of 2 µg/L for RDX in drinking water (3).

Aerobic and anaerobic biodegradation of RDX have been documented in both engineered systems and natural environments (28), and various RDX-degrading isolates are known to have an ability to utilize RDX as a nitrogen and/or carbon source (15, 17-19, 47, 54, 55, 62, 63, 65, 105-111). Previous efforts on studying these RDX isolates have provided valuable knowledge of RDX microbiology; however, little is known about their roles in the natural or engineered systems during RDX degradation, or about their RDX-degrading microbial communities in responding to engineered interventions.

Stable isotope probing (SIP) is a powerful culture independent method that can identify functionally active bacteria in various environmental samples (80, 81, 89, 113-

118). Recent applications of SIP with ^{13}C -labeled RDX or ^{15}N -labeled RDX have provided a new insight into RDX-degrading microbial community and a better understanding of their identities in the field samples (30, 89, 130). Yet, our current knowledge about RDX biodegradation is just the tip of iceberg.

Roh et al. (2009) conducted the first SIP study with ring-labeled ^{15}N -RDX to identify fifteen phylogenetically diverse RDX degraders in anaerobic groundwater microcosms (89). As RDX has a six-membered ring with alternate CH_2 and $\text{N}(\text{NO}_2)$, both the nitrogen (N) in the nitro (NO_2) group and in the ring structure can serve as a nitrogen source for bacterial growth. Thus, we hypothesized that bacteria capable of using nitro-N in RDX are different from those capable of using ring-N in RDX.

The goal of this study was to better understand the RDX degradative microbial population, particularly focusing on their ability to use different N in the RDX structure. In this study, we used ring-, nitro-, and fully-labeled ^{15}N -RDX to conduct SIP experiments in groundwater microcosms. The identities of bacteria capable of using different nitrogen in the RDX were determined. Additionally, a parallel set of microcosms was amended with cheese whey, an effective nutrient to promote RDX degradation (89). The effects of cheese whey on the RDX-degrading microbial communities of the groundwater microcosms were also examined.

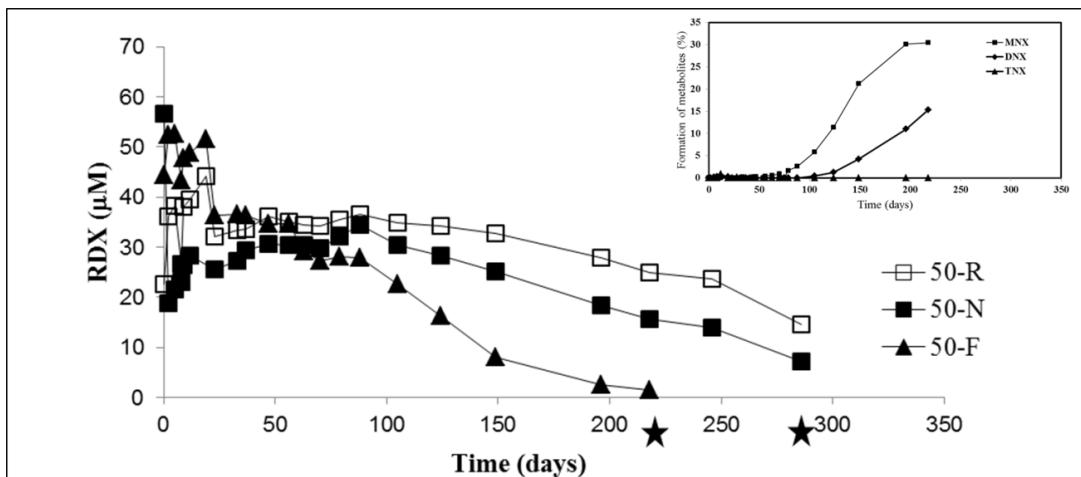
5.2 Results and discussion

5.2.1. Effect of cheese whey on RDX biodegradation in groundwater microcosms

Biodegradation of RDX was observed in the microcosms without cheese whey addition (Microcosms 50-R, 50-N, 50-F, 70-R, 70-N, and 70-F) (Figure V.1 (A)-(B)). A 5-fold longer accumulation period was observed in Microcosms 50-R, 50-N, and 50-F than those in Microcosms 70-R, 70-N, and 70-F), i.e, 100 days vs. 20 days. Additionally, slower RDX biodegradation occurred in Microcosms 50-R, 50-N, and 50-F than those in Microcosms 70-R, 70-N, and 70-F.

In Microcosm 50-N (which received nitro-labeled ^{15}N -RDX), RDX started to degrade approximately after 100 days of accumulation and then reached 80% degradation of added RDX on day 250. In Microcosm 50-F, which received fully-labeled ^{15}N -RDX, a similar slow degradation pattern was observed and nitroso metabolites (MNX, DNX, and TNX) were observed after 75 days of incubation (see insert in Figure V.1(A)). In Microcosm 50-R (received ring-labeled ^{15}N -RDX), less than 30% of initial RDX was degraded after 250 days of incubation. Thus, no sample was collected from this microcosm for further analysis. RDX was degraded much rapidly in Microcosms (70-R, 70-N, and 70-F) than observed in Microcosms 50-N and 50-F (Figure V.1 (B)). Approximately 50% of RDX was degraded within 20 days. Also, rapid RDX degradation was observed after the second RDX addition (RDX degradation was completed in 5-10 days).

(A)



(B)

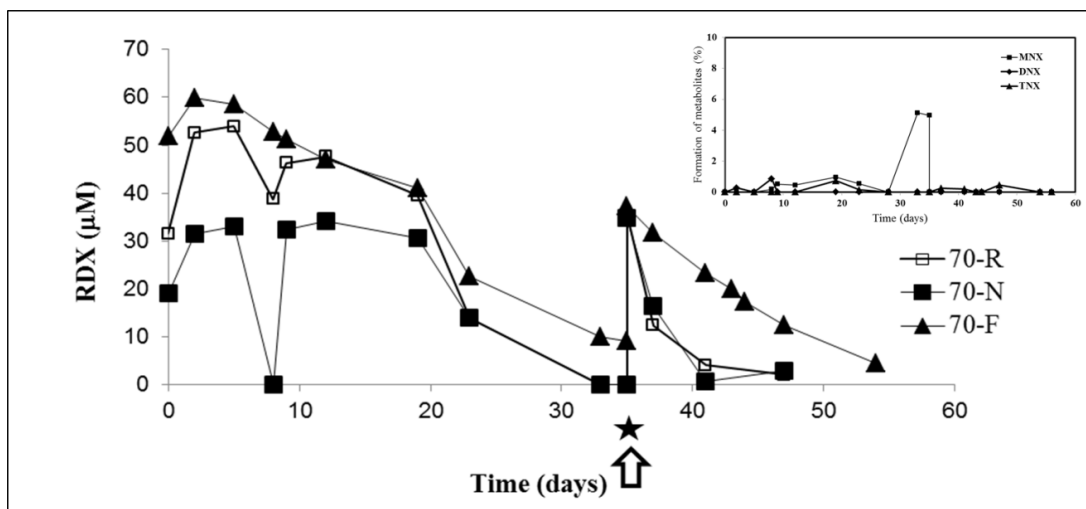


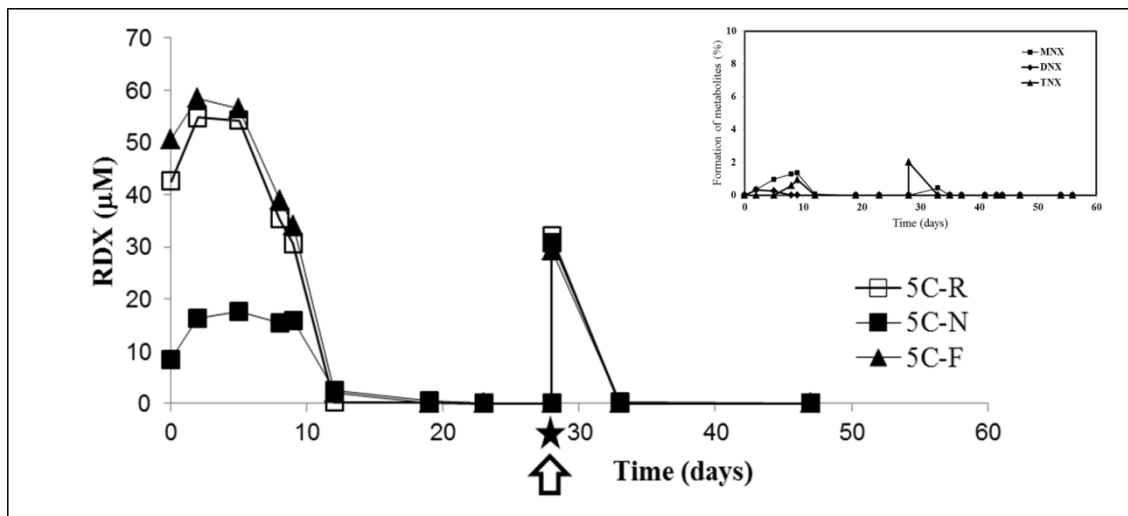
Figure V.1. RDX degradation over time in microcosms receiving one of ring-, nitro-, fully-labeled ^{15}N -RDX. Microcosms constructed from MW-5 groundwater (A) with ring-labeled ^{15}N -RDX (50-R), nitro-labeled ^{15}N -RDX (50-N) or fully-labeled ^{15}N RDX (50-F). Microcosms constructed from MW-7D groundwater (B) with ring-labeled ^{15}N -RDX (70-R) or nitro-labeled ^{15}N -RDX (70-N) or fully-labeled ^{15}N -RDX (70-F). Arrows indicate the addition of RDX. Stars (*) indicate time of sampling for SIP and other molecular analyses. Initial concentration of RDX in microcosms was 45 μM . No samples were taken from Microcosms 50-R for further analysis. The inserts represent production of nitroso metabolites (MNX, DNX, and TNX) over time in Microcosms 50-F and 70-F.

Nitroso metabolites in forms of MNX, DNX and TNX were detected in Microcosm 70-F at the concentrations between 0.1 to 0.5 mg/L (see insert of Figure V.1(B)). The concentration of MNX in Microcosm 70-F was 0.5 mg/L that was 5-fold lower than that observed in Microcosm 50-F.

The total organic carbon (TOC) concentrations are 14.9 mg/L and 4.2 mg/L in the groundwater from MW-7D and from MW-5, respectively. Note that no additional carbon/nitrogen sources or electron donor was supplied for RDX degradation in Microcosms 50-R, 50-N, 50-F, 70-R, 70-N, and 70-F. The high TOC can be the extra carbon source in groundwater promote RDX degradation which observed in Microcosms 70-R, 70-N, and 70-F.

Addition of cheese whey resulted in rapid RDX degradation; this was evident in Microcosms 5C-R, 5C-N, 5C-F, 7C-R, 7C-N, and 7C-F. After 5 days of acclimation, almost 80% of initial RDX was degraded within 5 days, and complete degradation of RDX was observed over a period of 30 days (Figure V.2 (A)-(B)). Similarly, the second spikes of RDX in these microcosms resulted in rapid RDX degradation (about 5 days). The RDX breakdown products MNX, DNX and TNX were detected sporadically at low concentration (ranging from 0.2 to 0.6 mg/L) in these microcosms (insert of Figure V.2 (A) and (B)). These observations were similar to the results of our previous SIP study that cheese whey addition enhanced RDX biotransformation/degradation. The enhanced RDX degradation was most likely due to an increase in microbial biomass and/or activity (30).

(A)



(B)

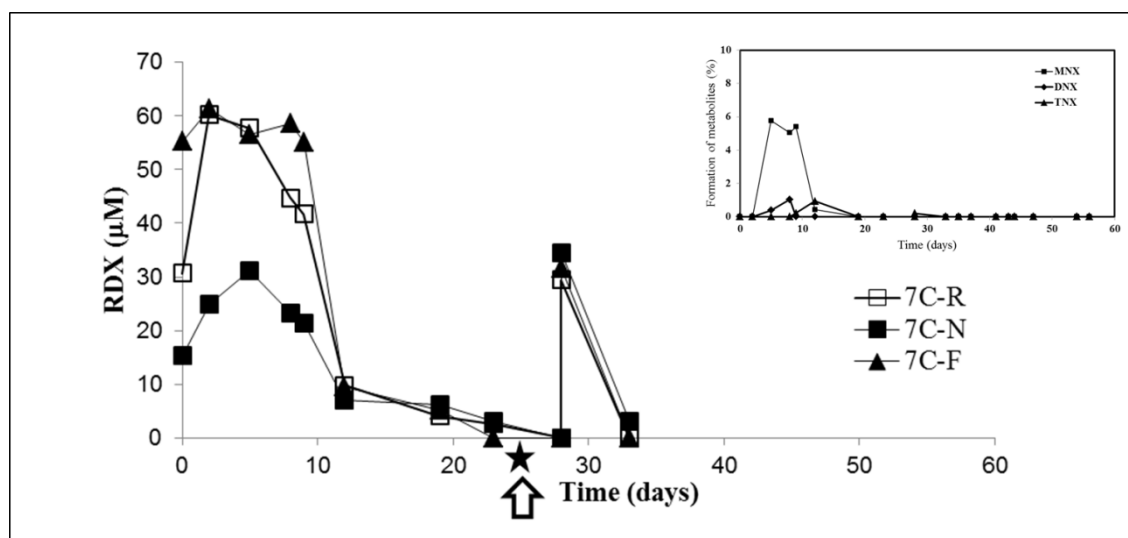


Figure V.2. RDX degradation over time in microcosms receiving cheese whey and one of ring-, nitro-, fully-labeled ^{15}N -RDX. Microcosms constructed from MW-5 groundwater (A) with ring-labeled ^{15}N -RDX (5C-R) or nitro-labeled ^{15}N -RDX (5C-N) or fully-labeled ^{15}N -RDX (5C-F). Microcosms constructed from MW-7D groundwater (B) with ring-labeled ^{15}N -RDX (7C-R) or nitro-labeled ^{15}N -RDX (7C-N) or fully-labeled ^{15}N -RDX (7C-F). Arrows indicate the addition of RDX. Stars (*) indicate time of sampling for SIP and other molecular analyses. Initial concentration of RDX in microcosms was 45 μM . The inserts represent production of nitroso metabolites (MNX, DNX, and TNX) over time in Microcosms 5C-F and 7C-F.

5.2.2. RDX-degrading microbial communities in groundwater microcosms

The active RDX-degrading microbial community structures of microcosms in the presence and absence of cheese whey were examined using real-time-t-RFLP analysis with ^{15}N -DNA fractions as templates. Cheese whey (as powder) contains more than 60~70% of lactose, and approximately to 10 % of protein, 10 % of minerals, 10 % of lactic acid, and 5 % of fats (131). The microbial community profiles derived from real-time-t-RFLP analyses are shown in Figure B.1.-B.16 in supporting materials (see in Appendix B). In Microcosms 50-N, 50-F, 70-R, 70-N, and 70-F (without cheese whey), the average 16S rRNA gene copies was 5×10^4 copies/ml. In contrast, in the presence of cheese whey, about 60-fold higher biomass was observed. The average 16S rRNA gene copies was 3×10^6 copies/ml in cheese-whey-receiving Microcosms (5C-R, 5C-N, 5C-F, 7C-R, 7C-N, and 7C-F). The high biomass in all cheese-whey-receiving microcosms also showed rapid RDX biodegradation, indicating the presence of bacteria that are capable of using cheese whey as a carbon source and RDX as a nitrogen source.

5.2.3. Microorganisms capable of using RDX or RDX intermediates as a nitrogen source

By using the ^{15}N -DNA fractions of 5 microcosms (50-Na, 50-Fa, 70-Na, 70-Ra and 70-Fa) as templates, a total of fifteen 16S rRNA gene sequences were derived. These sequences were contributed from metabolically active bacteria capable of using RDX and/or RDX intermediates as a nitrogen source. These sequences were clustered in three major phyla: *Clostridia* (2 sequences), β -*Proteobacteria* (7 sequences), and

Spirochaetes (6 sequences) (Figure V.3), indicating that RDX-degrading bacteria were present and they are phylogenetically diverse in groundwater. Mostly, all the 15 sequences were different from any known RDX degraders (16, 17, 23, 59, 61, 63).

As the same groundwater was used in our previous ^{13}C -RDX study (30) and this study, the clone libraries in the previous study were compared to those established in this study. Common clones in both libraries of ^{13}C -SIP and ^{15}N -SIP studies would indicate that these common clones might be able to use RDX or its metabolites as both nitrogen and carbon source.

Two sequences (70-Ra22 and 70-Na4) in β -*Proteobacteria* showed high homology (>97%) to one clone derived from background groundwater (GW clone 16, EU907859), and one clone (^{13}C -RDX clone 50-a1, JX066666) identified from the ^{13}C -RDX SIP study(30), suggesting that these two clones can be able to use RDX as both carbon and nitrogen sources. Both clones were corresponding to the 105 bp T-RF in the microbial community profiles (See the Figure B.9 and Figure B.11 in Appendix B).

The sequence 70-Ra22, contributed from the bacterium capable of using ring-nitrogen of RDX as sole nitrogen source. The sequence is high similarity to two iron-reducing strains: *Rhodiferax ferrireducens* strain T118 (accession number: NR074760) and *Rhodiferax fermentans* strain FR2 (accession number: NR025840) (132). Increased numbers of *Rhodiferax* sp. in aquifer materials was reported when acetate or lactate was amended to promote RDX biodegradation (26).

A recent study reported a shift of the dominant Fe(III)-reducers in the RDX-contaminated groundwater, changing from β -*Proteobacteria* to δ - , β -*Proteobacteria* (*Geobacter* sp.) when acetate was amended to enhance RDX biodegradation (133).

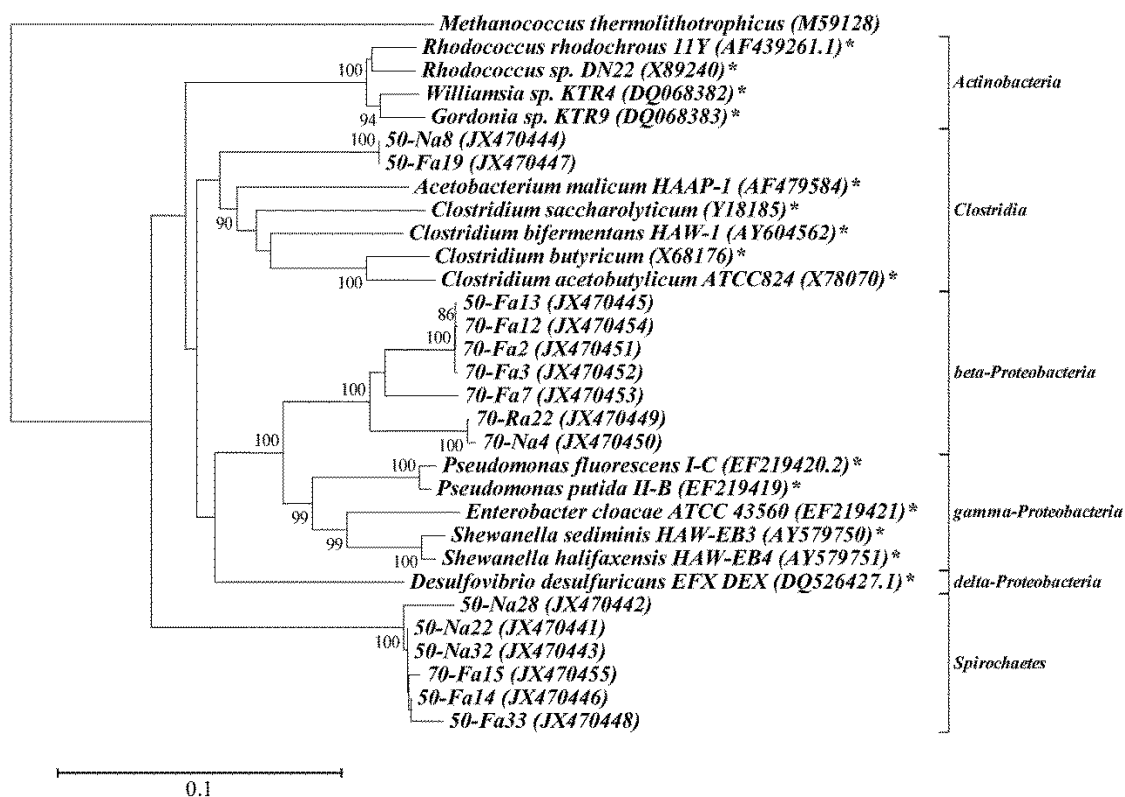


Figure V.3. Phylogenetic tree representing 16S rRNA gene sequences derived from ^{15}N -DNA fractions of groundwater microcosms from MW-5 and MW-7D receiving ring-, nitro-, fully- ^{15}N -labeled RDX. The tree was rooted with *Methanococcus thermolithotrophicus* and was constructed using the neighbor-joining algorithm. The number of clone sequences and the GenBank accession numbers are in parentheses. Only bootstrap values above 85% are shown (1,000 replications). Bar, 10% estimated sequence divergence. An asterisk (*) indicates a known RDX degrader.

Four sequences (50-Fa13, 70-Fa2, 70-Fa3, and 70-Fa12) in *β-Proteobacteria* also showed highly similarity (>95%) to the two clones ¹³C-RDX clones 70-a28 and 70-a92 (30). These four sequences show 92% homology to *Ferribacterium limneticum* (accession number: NR026464.1), a Fe(III)-reducing bacteria, isolated from mining-impacted sediment (134). The high homology of these four sequences to Fe (III)-reducing bacteria (such as *Albidiferax* sp. (basonym *Rhodoferax*) and *Ferribacterium* sp. were presented) also suggests that Fe-reducers might be able to use RDX as a carbon and nitrogen source. These four sequences also corresponded to T-RF =106 bp (predicted of 108 bp) in the microbial community profiles (See the Figure B.2 and Figure B.13 in Appendix B).

No studies have reported bacteria in *Spirochaetes* capable of degrading RDX, except for the previous ¹³C-RDX study (30) and this ¹⁵N-RDX study. Six clones (50-Na22, 50-Na28, 50-Na32, 50-Fa14, 50-Fa33, and 70-Fa15) in *Spirochaetes* are similar (>98%) to the ¹³C-RDX clone 50-a6 (accession number: JX066670), suggesting certain strains in *Spirochaetes* are capable of using RDX as a carbon and nitrogen source. These six sequences also have a theoretical T-RF of 108 bp and potentially corresponded to 106 bp T-RF in the microbial community profiles (See the Figure B.2 and Figure B.13 in Appendix B).

Interestingly, several clones derived from ring-, nitro, and fully-labeled ¹⁵N-RDX were identical. These identical clones were clustered within *Clostridia*, *β-Proteobacteria* and *Spirochaetes*. For instance, two sequences 50-Na8 and 50-Fa19 in *Clostridia* were identical and have the same T-RF=106 bp (predicted of 108 bp) in the

microbial community profile (See the Figure B.1 and Figure B.2. in Appendix B). The nearest relatives for these clones is *Desulfosporosinus meridiei* (accession number: NR074129), belonging to a family of sulfate-reducing bacteria. *D. meridiei* was previously isolated from a gasoline contaminated soil. A number of *Desulfosporosinus* sp. can utilize a wide spectrum of carbon source, ranging from aromatic compounds to short-chained fatty acids. (135). Several sulfate-reducing bacteria are known to utilize RDX as a nitrogen source (19, 22, 65) under anaerobic condition. Thus, these two clones (50-Na8 and 50-Fa19) are very likely to be *Desulfosporosinus* sp., and they are also capable of using the N from the nitro-groups of RDX.

Another interesting sequence is sequence 70-Fa7. This sequence was related to *Herbaspirillum lusitanum* (accession number: NR028859), a nitrogen-fixing bacterium associated with root nodules of *Phaseolus vulgaris* (136). To our knowledge, no studies have reported bacteria genera in this group exhibiting RDX degradation ability.

5.2.4. Effects of cheese whey addition on the active RDX utilizers

Addition of cheese whey altered the types and distributions of RDX-degrading microbial community populations when compared to those observed in Microcosms 50-N, 50-F, 70-R, 70-N, and 70-F. A total of twenty eight sequences were derived from these cheese-whey-receiving microcosms (5C-Na, 5C-Ra, 5C-Fa, 7C-Na, 7C-Ra, and 7C-Fa). These sequences (n=28) were grouped into *Bacteroidia*, *Bacilli*, α -, β -, and γ -*Proteobacteria* (Figure V.4), with the majority in α -, β -, and γ -*Proteobacteria*. Once again, none of the derived sequences were an exact match to any of known RDX degraders.

By comparing the clone libraries of ^{13}C -SIP and ^{15}N -SIP studies, there were three overlapping groups: β -, γ -*Proteobacteria* and *Bacilli*. Two sequences (5C-Ra12 and 5C-Na12), derived from Microcosms 5C-Ra and 5C-Na, showed high similarity (95%) to two known RDX degraders, *Pseudomonas fluorescens* I-C and *Pseudomonas putida* II-B (73, 126). *Pseudomonas* sp. are aerobes and/or facultative anaerobes and they have been identified in many contaminated soil and groundwater. Our results are consistent with previous findings that many *Pseudomonas* sp. sequences were recovered from groundwater or laboratory enrichments when biostimulation was performed to enhance RDX degradation (30, 89, 121). *P. fluorescens* I-C and *P. putida* II-B strains can transform RDX using xenobiotic reductases XenA and XenB under both aerobic and anaerobic conditions (69). The RDX transformation by the reductases was much faster anaerobically than aerobically, since oxygen can inhibit the activity of the enzymes. Along with previous findings, results suggest that *Pseudomonas* sp. play an

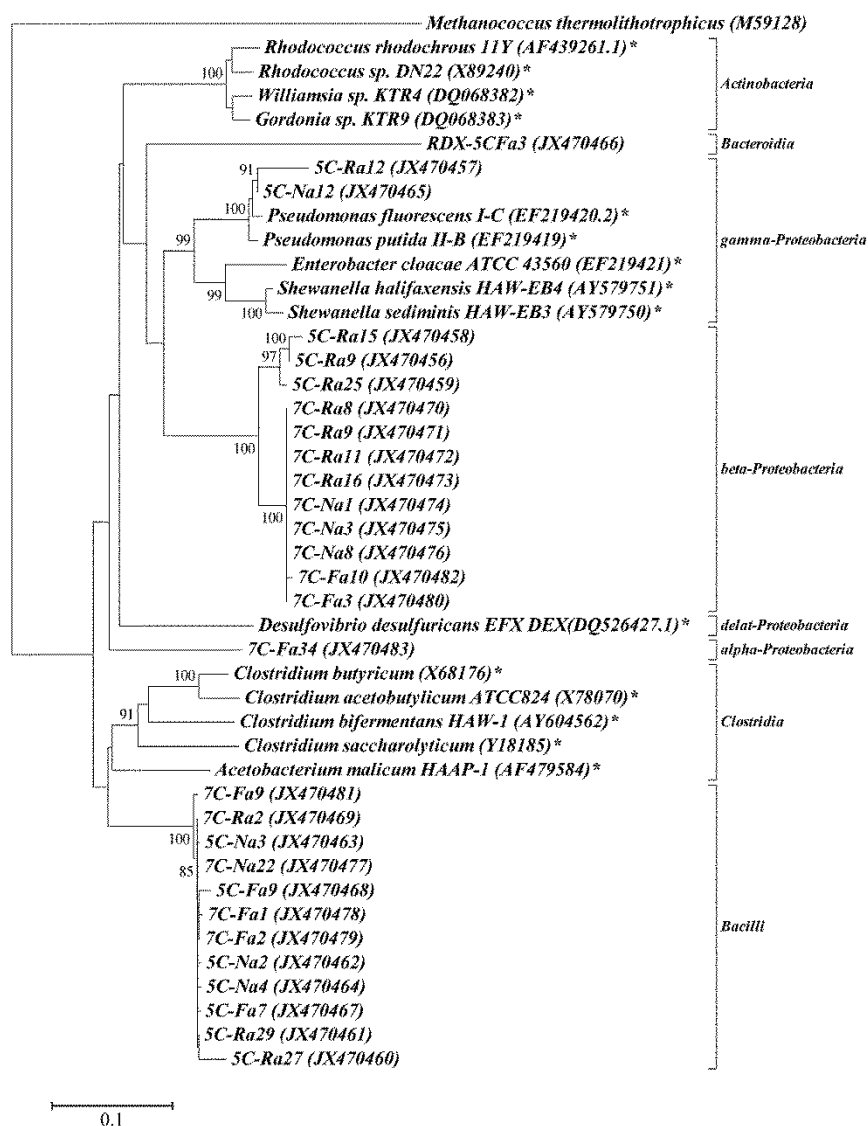


Figure V.4. Phylogenetic tree representing 16S rRNA gene sequences derived from ^{15}N -DNA fractions of groundwater microcosms receiving either MW-5 or MW-7D groundwater, cheese whey, and receiving ring, nitro, fully ^{15}N -labeled RDX. The tree was rooted with *Methanococcus thermolithotrophicus* and was constructed using the neighbor-joining algorithm. The number of clone sequences and the GenBank accession numbers are in parentheses. Only bootstrap values above 85% are shown (1,000 replications). Bar, 10% estimated sequence divergence. An asterisk (*) indicates a known RDX degrader.

important role in transforming RDX and other nitramine explosives in the environment. In addition, the catabolic genes that code the xenobiotic reductases can be a useful biomarker to assess potential and/or progress of RDX biodegradation under anoxic conditions.

A total of 12 sequences were derived from cheese whey-amended microcosms. These sequences were clustered in *Bacilli*. Among the 12 sequences, seven sequences (5C-Ra27, 5C-Ra29, 5C-Na2, 5C-Na3, 5C-Na3, 5C-Na4, and 5C-Fa7) were derived from Microcosms 5C-Na, 5C-Ra and 5C-Fa. The other five sequences (7C-Ra22, 7C-Na22, 7C-Fa1, 7C-Fa2, and 7C-Fa9) were derived from Microcosms 7C-Na, 7C-Ra, and 7C-Fa. Most of these sequences were highly homologous (>97%) and were repetitively observed in microcosms receiving ring-, nitro-, or fully-labeled ^{15}N -RDX. Our results were similar to previous ^{13}C -SIP study (30) that the high numbers of sequences in *Bacilli* (nine sequences in ^{13}C -SIP study, 5Ca7, 5Ca28, 5Ca33, 5Ca60, 5Cb4, 5Cb13, 5Cb17, 7Ca13, and 7Cb43) were associated with the cheese whey-amended microcosms. These 12 sequences were very close to *Trichococcus flocculiformis* (accession number: NR042060), a low G+C content strain capable of utilizing various carbohydrates for acid production (137). Although no studies have reported the RDX degradation ability of *Trichococcus* sp, our results clearly indicated that the *Bacilli* were stimulated by cheese whey addition and that they can assimilate ^{15}N from ^{15}N -labeled RDX.

Through the application of ^{15}N -SIP, a substantial number of sequences were derived. These sequences represent the strains that were capable of utilizing RDX and RDX metabolites as a sole nitrogen. As many of these sequences are clustered in β -

Proteobacteria and *Bacilli*, it is possible to use the information to develop a set of biomarkers for assessing RDX biodegradation.

Based on derived sequences, our results once again indicate the diversity of active microorganisms associated with RDX biodegradation in the environmental samples. When cheese whey was absent, none of known RDX-degraders were detected in this study. Some, but not all, clones identified from this study were highly similar to ¹³C-SIP (30) study that the same groundwater source was used. With cheese whey addition, RDX degradation was significantly enhanced and the active microbial community structure shifted dramatically when compared to those without cheese whey addition. Results of this study also imply the importance of examining RDX microbiology under various geochemical conditions, particularly in the presence of different electron acceptors.

CHAPTER VI
IDENTIFICATION OF RDX DEGRADING BACTERIA UNDER VARIOUS
ELECTRON-ACCEPTING CONDITIONS

6.1. Introduction

Hexahydro-1,3,5-trinitro-1,3,5-triazine (RDX) is a common explosives contaminant which has been often detected in soil and groundwater at military sites (100-104). RDX is moderately soluble and thus can migrate rapidly from soil through groundwater aquifers. Due to the toxicity and human health effects of RDX, the U.S. Environmental Protection Agency (EPA) has listed RDX in Contaminant Candidate List 3. The EPA has established a health advisory level (2 µg/L) for RDX in drinking water (3).

RDX biodegradation can occur in the presence of various reducing conditions, including nitrate-reducing (21), manganese-reducing conditions (57), iron-reducing (25, 138), sulfate-reducing (22), acetogenic (58) as well as methanogenic conditions (60). Freedman et al. (21) reported RDX biotransformation under nitrate-reducing conditions only occurred when the nitrate was depleted and organics and acetate was presence. Bradley et. al (57) reported a significant of mineralization of RDX to carbon dioxide when Mn(IV) was amended into anoxic sediment microcosms. Adding soluble electron shuttles, such as humic substances or anthraquinone-2,6-disulfonate, can also enhance RDX reduction rate. (25). Boopathy et al. (22) reported that RDX transformed by a sulfate-reducing bacterial consortium, *Desulfovibrio* sp., which can use RDX as sole

nitrogen source for growth. Adrian et al. (60) reported complete RDX biotransformation by a methanogenic mixed culture when amended with ethanol, propylene glycol, or hydrogen gas were present as electron donor.

Numerous RDX-degrading microorganisms have been isolated from soil or sludge under anaerobic conditions; however, only a few strains are known to use RDX as nitrogen sources (19, 20, 59, 63, 77). *Desulfovibrio desulfuricans* EFX-DES is the only known anaerobic strain capable of using RDX as carbon and nitrogen sources under anaerobic condition (65). Studies of these isolates have provided the insight of RDX microbiology, however, it remains unclear if these isolates are responsible for RDX degradation observed in the field. Since only a small fraction of environmental organisms can be isolated and cultivated in the laboratory (139), it is possible that many active but uncultivable RDX-degrading microorganisms are present in the field waiting for discovery.

Stable isotope probing (SIP) is a powerful tool to identify active degradative microorganisms in the complex microbial communities without cultivation (80, 81, 114). Recent applications of SIP with labeled RDX have provided interesting insights on anaerobic RDX-degrading bacteria and microbial communities in soil and groundwater (30, 89, 130). However, these studies did not systematically examine the metabolically active RDX utilizer under different reducing conditions.

The goal of this study is to identify RDX-degrading microorganisms capable of using RDX or metabolites as a carbon and/or nitrogen source under different electron-accepting conditions. To achieve this goal, we first developed a series of microcosms

containing groundwater and sediment. These microcosms were first amended with one of four electron acceptors: manganese, iron, sulfate, and CO₂ (succinate was added to produce CO₂), to establish four different electron reducing conditions. Once the reducing conditions were developed, a parallel set of microcosms were constructed by providing one of ¹³C- or ring-, nitro-, fully-labeled ¹⁵N-RDX and one of the four electron acceptors. The identities of RDX utilizers under different reducing conditions were determined and their associated to microbial community structures were also characterized. Results of this study provide ta new understanding of RDX microbiology that would occur under different electron accepting conditions.

6.2. Results and discussion

6.2.1. RDX biodegradation under four different reducing conditions

Biodegradation of RDX was observed in all microcosms amended with different electron acceptors: Mn(IV), Fe(III), sulfate and CO₂ (derived from added succinate). The formation of nitroso metabolites, hexahydro-1-nitroso-3,5-dinitro-1,3,5-triazine (MNX), hexahydro-1,3-dinitroso-5-nitro-1,3,5-triazine (DNX) and hexahydro- 1,3,5,-trinitroso- 1,3,5, triaxine (TNX), were also detected in all microcosms (Figure VI.1).

Under manganese-reducing conditions, RDX degradation was noted after 110 days of incubation (Figure VI.1(A)), followed by complete degradation of RDX on day 128. During the RDX degradation, nitroso metabolites (MNX, DNX, and TNX) were detected. From day 114 to day 128, MNX was first formed, accumulated and then reduced to DNX and TNX. Similarly to MNX, DNX concentrations increased and then

decreased to form TNX. TNX continued to accumulate and the concentration accounted for 95% of added RDX (molar basis) after 140 days of incubation. After day 265, the concentration of TNX declined to 20 % of added RDX, suggesting the cleavage of ring structure of RDX. Enhanced mineralization of RDX, but no nitroso metabolites accumulation was reported when amended with Mn(IV) (57). To our knowledge, this is the first study demonstrated the sequential reduction of RDX to MNX, DNX, and TNX under such condition over 300 days of incubation.

Under iron-reducing conditions, RDX concentration was reduced completely after 14 days of incubation (Figure VI.1(B)), followed by the formation of nitroso metabolites on day 12. The RDX reduction trend was similar to that observed under Mn(IV)-reducing conditions. However, nitroso metabolites accumulated quickly and then transformed completely to TNX on day 16, followed a gradual disappearance to 50 % of added RDX on day 117. The results are consistent to those observed by Kwon et al. (140) that nitroso metabolites accumulated when acetate was amended as an electron donor under iron-reducing conditions. In this study, one notable observation in both Mn(IV)-amended and Fe(III)-amended samples was the significant accumulation of nitroso metabolites during RDX degradation. The accumulation of the nitroso metabolite indicates that nitro group reduction, not denitration, was the initial steps of RDX biodegradation when Mn(IV) or Fe(III) was used as electron acceptor.

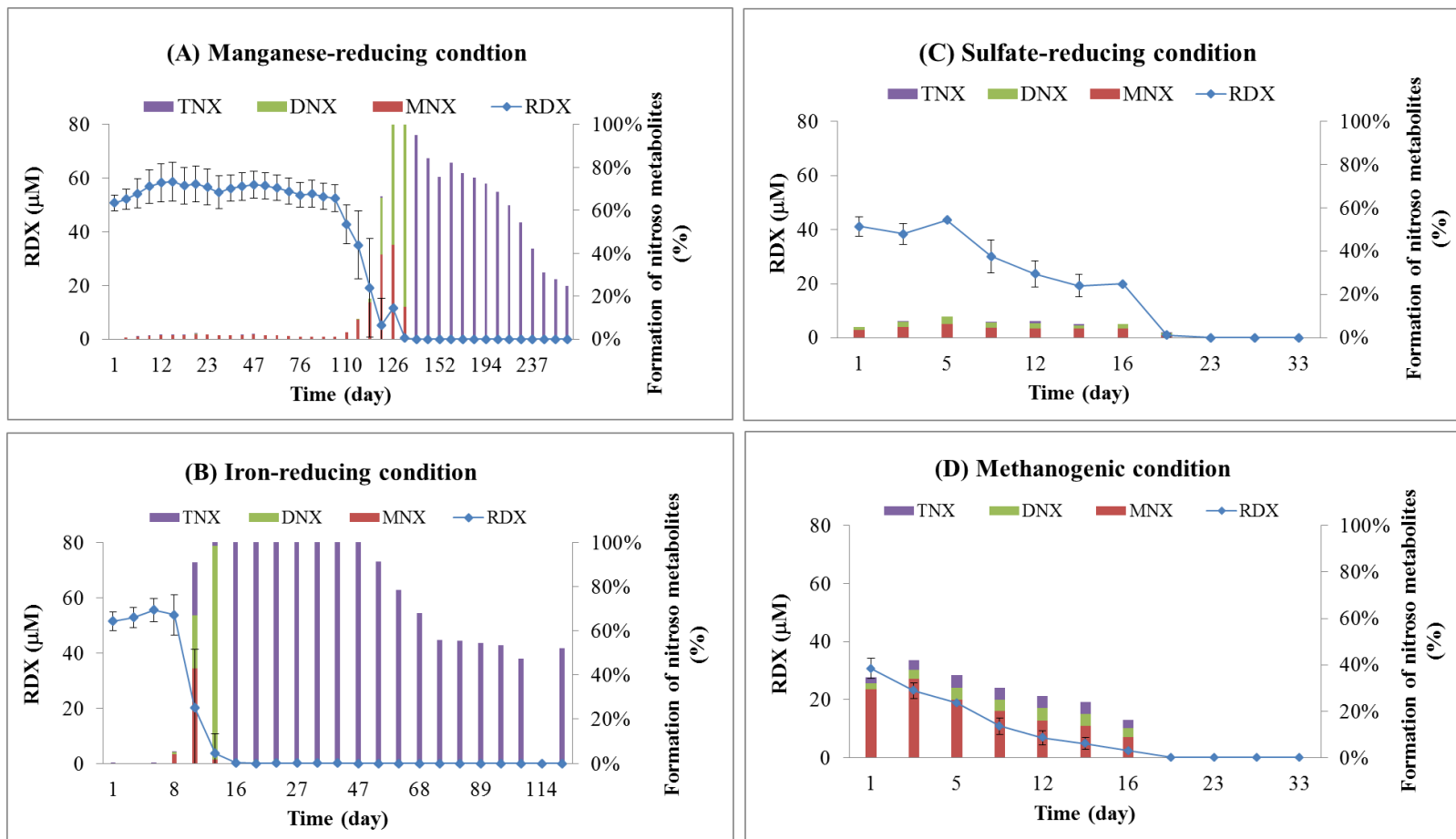


Figure VI.1. RDX biodegradation and the formation nitroso metabolites (MNX, DNX, and TNX) in microcosms under (A) manganese-reducing, (B) iron-reducing, (C) sulfate-reducing, and (D) methanogenic conditions. The initial concentration of RDX was 45 µM in all microcosms. Results are the means of analyses of microcosms receiving ¹³C-labeled RDX or ring-, nitro-, fully-labeled ¹⁵N-RDX and bars indicate standard deviation.

In sulfate-amended microcosms, approximately 60 % of added RDX was degraded within the first 8 days and RDX was completely degraded on day 20 (Figure VI.1 (C)). Unlike the Mn- and Fe-amended samples, low levels of nitroso metabolite concentrations (<0.5 mg/L of either MNX, DNX, and TNX) that accounted for less than 10% of the total RDX added, were detected during the first 16 days of incubation.

Under methanogenic conditions, fast RDX degradation was observed, i.e. approximately 90 % of added RDX was degraded by day 12 (Figure VI.1 (D)). Nitroso metabolites, mainly MNX, were MNX since day 1 and the total amount of three metabolites (MNX, DNX, and TNX) accumulated for 40 % of added RDX. Different from the slow RDX degradation observed in Mn(IV) and Fe(III)- amended samples, much faster RDX degradation was detected microcosms under both sulfate-reducing and methanogenic condition. Under sulfate-reducing and methanogenic condition samples, the total amount of metabolites was less than 10% and 40% of the added RDX, respectively (Figure VI.1 (C)-(D)). The data indicated that nitro group reduction was not the major RDX degradation pathway under sulfate-reducing or under methanogenic conditions, which is opposite to what are observed in Mn(IV)- or Fe(III) –amended microcosms. The abiotic RDX degradation in the Mn(IV)- or Fe(III)-reducing systems might be possible; however, this phenomenon was not determine in this study.

RDX biodegradation has been reported under sulfate-reducing condition (141). Research has shown a sulfate-reducing bacteria microbial consortium, *Desulfovibrio* sp. degraded RDX and the other explosives within 18 days. These sulfate-reducing bacteria can use RDX as a sole nitrogen source but not a carbon source (22). A novel species of

Desulfovibrio, with a 95.1% similarity to *Desulfovibrio desulfuricans*, can grow on RDX as a sole source of carbon and nitrogen (65), indicating its potential role in RDX biodegradation.

6.2.2. Analysis of buoyant densities of DNAs extracted from all microcosms

Following RDX degradation, groundwater and sediment samples were collected for DNA extraction. Manganese-reducing and iron-reducing samples were collected on day 265 and day 117, respectively. Sulfate-reducing and methanogenic samples were collected on day 33. The extracted DNA was fractionated after gradient centrifugation. The 16S rRNA gene copies and buoyant densities (BD) in each fractionation were determined.

The relative abundance of 16S rRNA gene copies in each of the gradient fractions collected from microcosms receiving ^{13}C -labeled and unlabeled were evaluated (Figure VI.2). Compared to the peak of the unlabeled gradient, the peaks of labeled curves shifted significantly toward the right, i.e., buoyant densities of the peaks shifted from 1.697g/ml (for unlabeled) to 1.711 g/ml (for ^{13}C -labeled) (Figure VI.2 (A)-(C)). When 80% to 100% of ^{13}C is incorporated into the DNA molecule, the DNA will become heavier and its BD is expected to increase ~0.04 g/ml, theoretically (142, 143). In this study, BD shift is 0.015 g/ml, indicating approximately 35~50% of ^{13}C incorporation under tested reducing conditions.

Under the manganese-reducing condition, the peak of the ^{13}C -gradient was shifted slightly from the unlabeled peak buoyant density with 10% of relative abundance

of 16S rRNA genes copies were recovered in the microbial population, suggesting the small portion of ^{13}C -labeled assimilation into the DNA (Figure VI.2 (A)). In contrast, the ^{13}C -peak gradient under sulfate-reducing and methanogenic conditions with 30 % to 40 % relative abundance of 16S rRNA genes recovered in the heavy fractions (Figure VI.2 (B)-(C)). The data suggested the possible of ^{13}C -labeled assimilated under sulfate-reducing and methanogenic conditions.

The difference between relative abundance of 16S rRNA gene copies and gradient fractions from samples receiving ring-, nitro-, and fully- labeled ^{15}N -RDX under manganese-reducing, iron-reducing, sulfate-reducing and methanogenic conditions were showed (Figure VI.3). The peaks of the ^{15}N -gradient DNA were shifted right, in the range of 1.716 ~ 1.720 g/ml when in comparison to the unlabeled DNA. Under manganese-reducing condition, no significant BD shift was observed ring-, and nitro- ^{15}N labeled samples. However, the significant BD shift (from 1.701 g/ml to 1.721 g/ml) was observed for fully- ^{15}N -labeled samples (Figure VI.3 (A)). Under iron-reducing and sulfate-reducing conditions, BD shift was observed and the peaks for ring-, nitro, and fully-labeled ^{15}N samples overlapped on each other (Figure VI.3 (B)-(C)). Under methanogenic condition, the BD also shifted among ring-, nitro, and fully-labeled ^{15}N samples, ranging from 1.706 g/ml to 1.722 g/ml (Figure VI.3 (D)). Compared to the peak of unlabeled gradient, the shift of BD in ^{15}N -gradient suggested 70~100 % of ^{15}N -labeled incorporation into DNA (143). Our data implied a higher assimilation of ^{15}N than that of ^{13}C in the reducing microcosms.

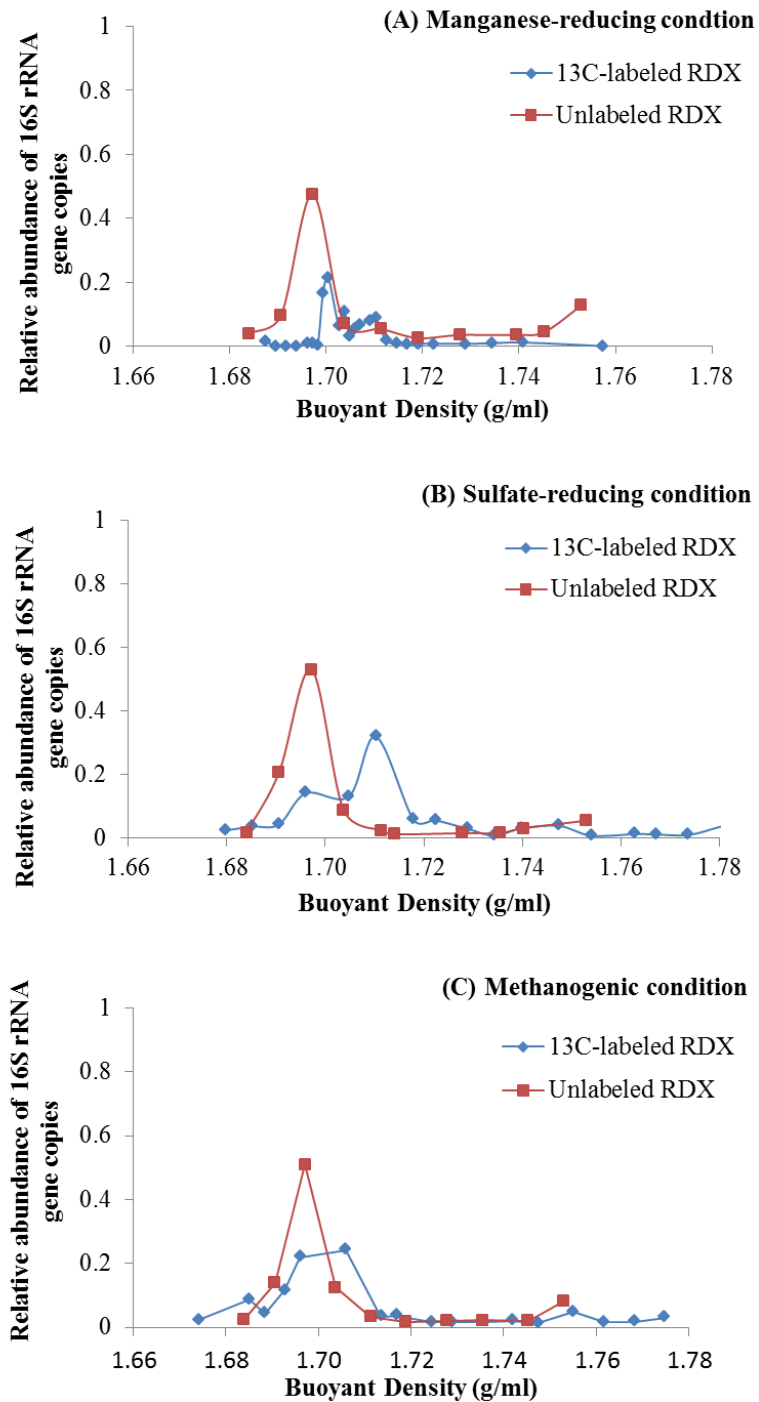


Figure VI.2. Difference between relative abundance of 16S rRNA gene copies and gradient fractions under (A) manganese-reducing, (B) sulfate-reducing, and (C) methanogenic conditions. No data available on the iron-reducing condition.

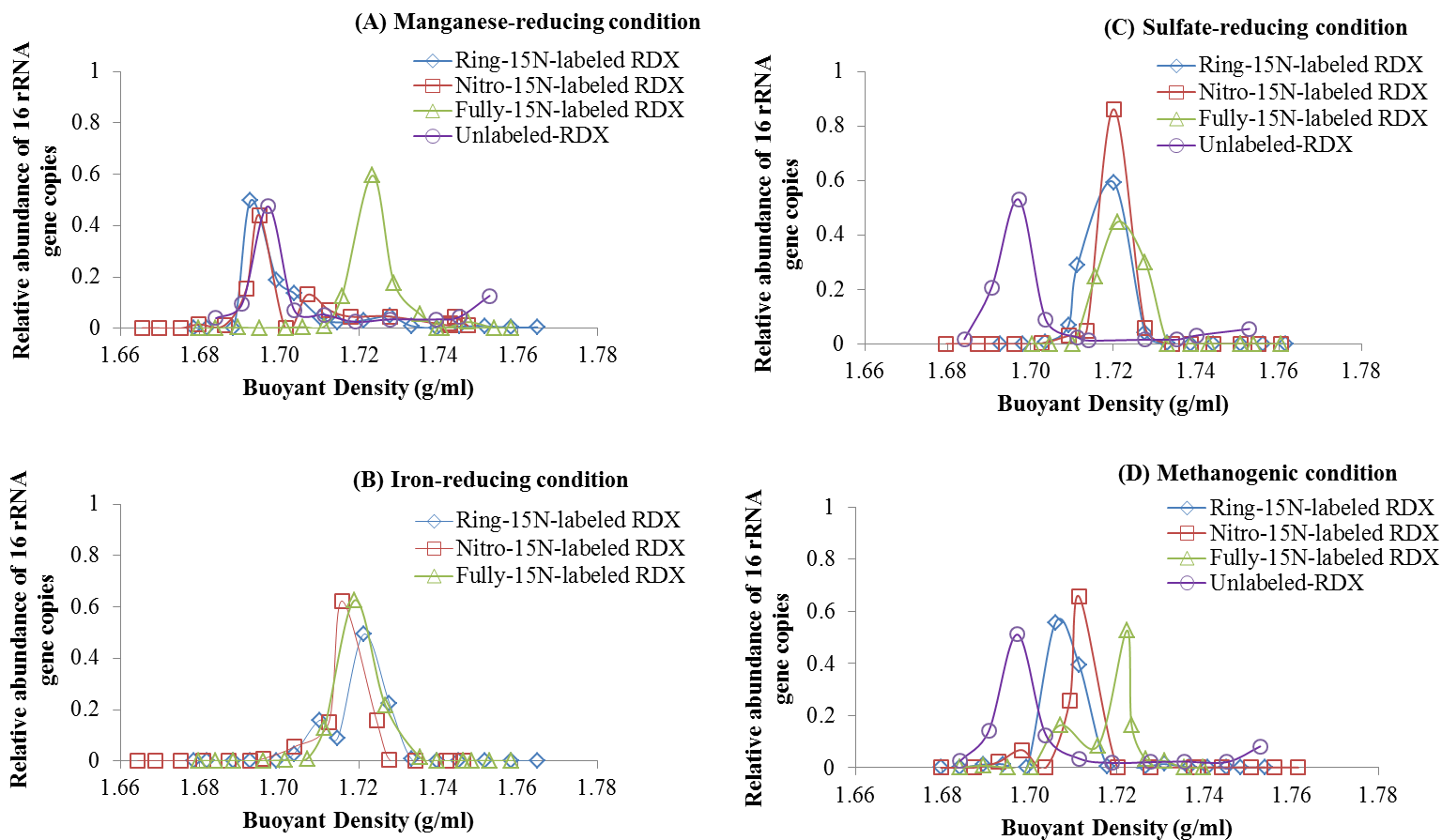


Figure VI.3. Difference between of relative abundance of 16S rRNA gene copies in gradient fractions in (A) manganese-reducing, (B) iron-reducing, (C) sulfate-reducing, and (D) methanogenic conditions. No data on unlabeled iron-reducing condition.

6.2.3. Identification of active RDX-degrading microorganisms under different electron accepting conditions

By using the ^{13}C -DNA fractions from the reducing microcosms receiving ^{13}C -labeled RDX as templates for cloning and sequencing, identities of active bacteria capable of using RDX and/or RDX intermediates as a carbon source were determined. A total of fifteen 16S rRNA sequences were derived. These sequences resided in four major clusters: *Actionbacteria* (*Eggerthella*), α -*Proteobacteria* (unclassified *Rhizobiales*), γ -*Proteobacteria* (*Pseudomonas*), and *Clotridia* (*Desulfosporosinus*) (Figure VI.4).

Similarly, a total of twenty seven sequences were derived from ^{15}N -DNA fractions of the reducing microcosms (D3-D5, C3-C5, E3-E5 and A3-A5) with one of ring-, nitro- and fully-labeled ^{15}N -RDX, respectively (Figure VI.5). Interestingly, the clone library assembly from ^{15}N -DNA fractions was similar to that from the ^{13}C -DNA fractions. These sequences formed the three major groups in α -*Proteobacteria* (unclassified *Rhizobiales*), γ -*Proteobacteria* (*Pseudomonas*), and *Clotridia* (*Desulfosporosinus*).

One sequence (manganese D2H5, derived from the Microcosm D2) in *Actionbacteria* in Figure VI.4 shows a close match to *Eggerthella* sp., whereas, two sequences (manganese D2H2 and D2H6) were grouped in α -*Proteobacteria* (unclassified *Rhizobiales*). In contrast, three sequences (manganese D3H2, manganese D4H6, and sulfate E4H2) in α -*Proteobacteria* were derived from Microcosm D3, D4, and E4 receiving ring- and nitro-labeled ^{15}N -RDX, respectively. No previous studies have reported these genera bacteria associated to RDX degradation. Additionally, the

derived sequences data from ^{13}C - and ^{15}N -SIP implied these unknown bacteria in α -*Proteobacteria* can use RDX or metabolites as a carbon and/or a nitrogen source.

Three sequences (manganese D2H4, sulfate E2H6 and methanogenic A2H3,) in γ -*Proteobacteria* were derived from Microcosms (D2, E2, and A2) receiving ^{13}C -labeled RDX under manganese-reducing, sulfate-reducing and methanogenic conditions, respectively. These three sequences were identified as the closest matches (95% homology) to the known RDX degraders, *Pseudomonas fluorescens* I-C and *Pseudomonas putida* II-B (73, 126). Both *P. fluorescens* I-C and *P. putida* II-B strains transform RDX with xenobiotic reductases XenA/ XenB (69). Interestingly, the *Pseudomonas* sp. were also found in the ^{15}N -fractions clone library. Three sequences (manganese_D3H1, sulfate_E3H5 and methanogenic_A3H2) in γ -*Proteobacteria* were derived from Microcosms (D3, E3 and A3) receiving ring-labeled ^{15}N -RDX, while one sequences (manganese_D4H6) in γ -*Proteobacteria* was derived from Microcosm (D4) receiving nitro-labeled ^{15}N -RDX. The common sequences identified the *Pseudomonas* sp. from both clone libraries in ^{13}C - and ^{15}N -SIP studies suggested that *Pseudomonas* sp. are likely to use RDX or its metabolites as a carbon and/or a nitrogen source. However, Fuller et al reported that *Pseudomonas* sp. with xenobiotic reductases capable of degraded RDX, but these strains not utilized RDX as sole carbon or nitrogen source (69). Therefore, these *Pseudomonas* sp. involved on RDX degradation with nutrient supplies and utilized RDX metabolites as a carbon and/or a nitrogen source.

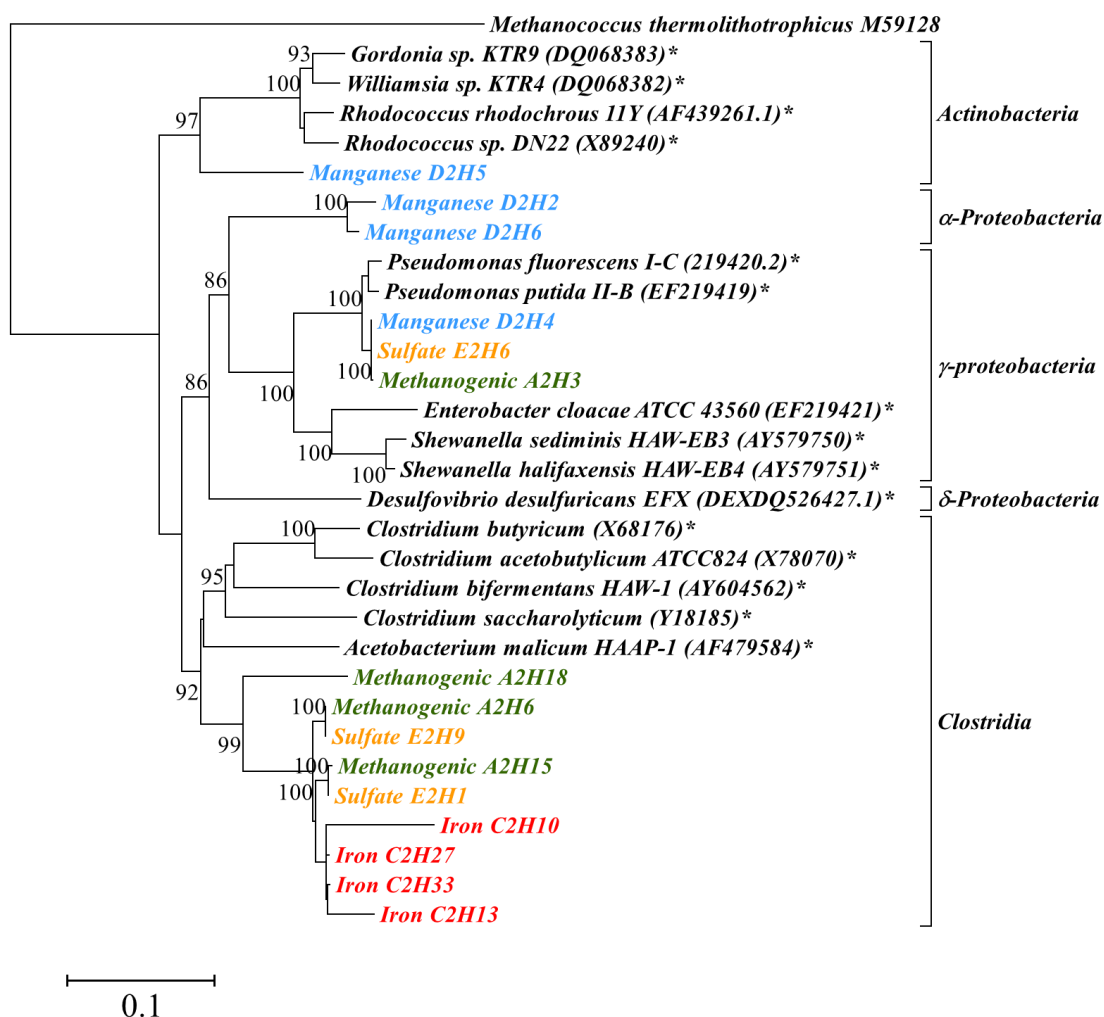


Figure VI.4. Phylogenetic tree representing 16S rRNA gene sequences derived from ^{13}C -DNA fractions of microcosms receiving ^{13}C -labeled RDX and one of electron acceptors (manganese, iron, sulfate and CO_2). The tree was rooted with *Methanococcus thermolithotrophicus* and was constructed using the neighbor-joining algorithm. Only bootstrap values above 85% are shown (1,000 replications). Bar, 10% estimated sequence divergence. An asterisk (*) indicates a known RDX degrader.

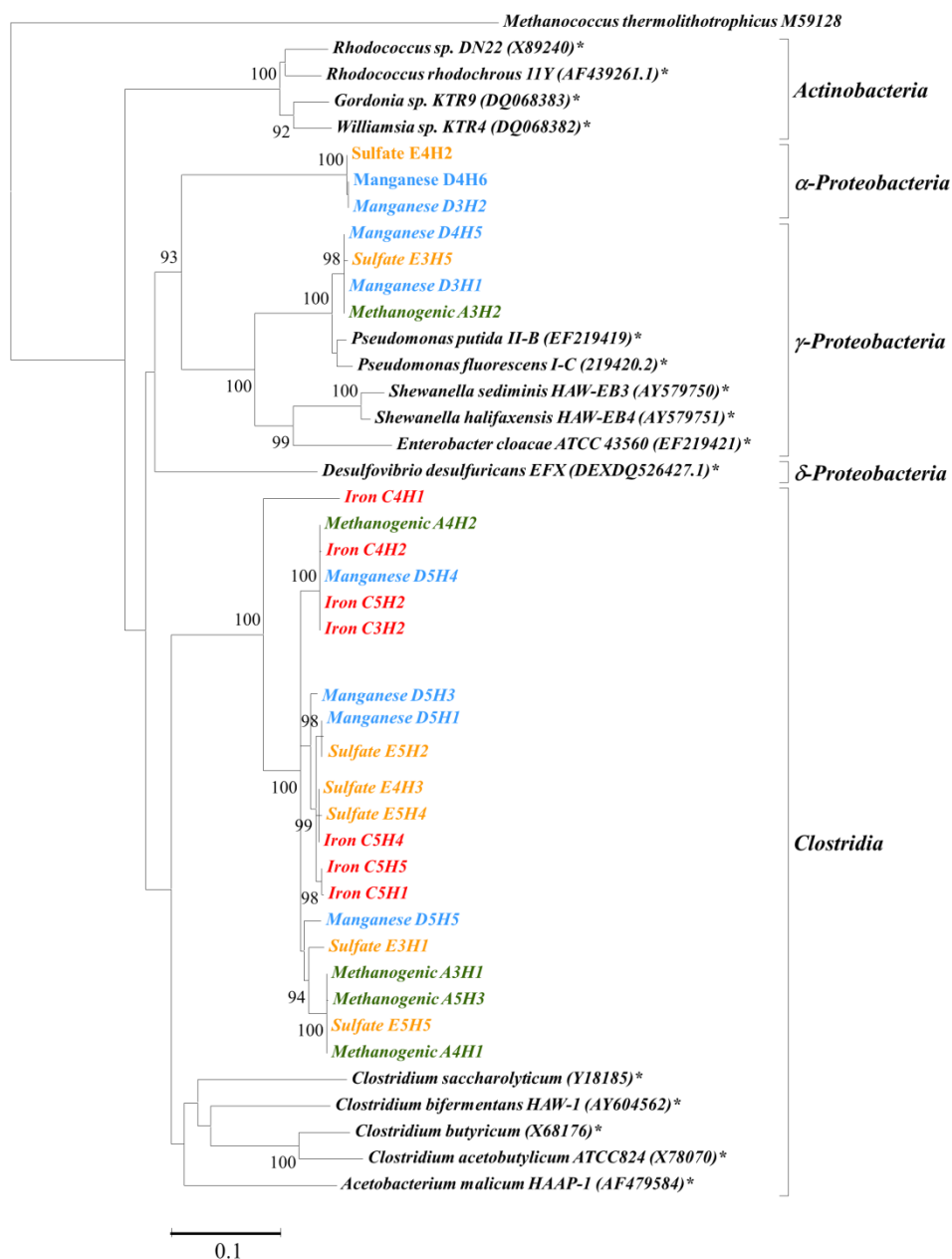


Figure VI.5. Phylogenetic tree representing 16S rRNA gene sequences derived from ^{15}N -DNA fractions of groundwater microcosms receiving one of ^{15}N -labeled RDX (ring-, nitro-, and fully-labeled ^{15}N -RDX) and one of electron acceptors (manganese, iron, sulfate and CO_2). The tree was rooted with *Methanococcus thermolithotrophicus* and was constructed using the neighbor-joining algorithm. Only bootstrap values above 85% are shown (1,000 replications). Bar, 10% estimated sequence divergence. An asterisk (*) indicates a known RDX degrader.

Our findings indicate this genus *Desulfosporosinus* can use RDX and its metabolites as a carbon and/or a nitrogen source, suggesting that they are potentially important in RDX biodegradation at contaminated sites with high sulfate level in aquifer material (groundwater and sediment). In this study, a major group of *Desulfosporosinus*, a family of sulfate-reducing bacteria, was identified from both ^{13}C -SIP and ^{15}N -SIP clone libraries. A total of nine sequences (iron C2H10, iron C2H13, iron C2H27, iron C2H33, sulfate E2H1, sulfate E2H9, methanogenic A2H6, and methanogenic A2H18) were derived from microcosms (C2, E2, and A2) under iron-reducing, sulfate-reducing and methanogenic conditions receiving ^{13}C -RDX, respectively. In addition, a total of twenty two sequences were derived from microcosms (D5, C3-C5, E3-E5, A3-A5) under manganese-reducing, iron-reducing, sulfate-reducing and methanogenic conditions receiving ring-, nitro, and fully-labeled ^{15}N -RDX, respectively. These sequences were found highly similar in both ^{13}C -SIP and ^{15}N -SIP clone libraries and the closest match (95~99% homology) to the species *Desulfosporosinus lacus* (accession number: NR042202) and *Desulfosporosinus meridiei* (accession number: NR074129). *Desulfosporosinus* spp. can reduce sulfate for energy conservation, and some species can also grow by using nitrate, Fe(III), or As(V) as terminal electron acceptors or by fermentative processes (135). No previous studies have shown the *Desulfosporosinus* sp. related to RDX biodegradation. However, several studies revealed that sulfate-reducing bacteria, such as *Desulfovibrio* sp., are known to utilize RDX as a nitrogen source (19, 22, 65) under anaerobic condition.

6.2.4. Active RDX-degrading microbial communities under different reducing

Active RDX-degrading microbial community structures of reducing microcosms were examined by using the real-time-t-RFLP analysis. Based on the DNA gradient fractions shown in Figure VI.2 and Figure VI.3, the heavy labeled with ^{13}C - or ^{15}N -gradient fractions were used as templates for characterized the active RDX-degrading microbial community structures under different electron accepting condition.

As shown in Figure VI.6, four ribotypes (t-RFs = 101, 106, 109 and 329 bp) were observed in all microbial community profiles in microcosms under all four different reducing conditions (Figure VI.6). Several other three peaks t-RFs (107, 108 and 118 bp) showed in the iron-reducing microbial communities. The 16S rRNA genes copies were higher in 106 and 109 bp T-RFs higher than those in other T-RFs.

Different patterns of microbial community profiles were observed in the reducing microcosms receiving one of ring-, nitro-, and fully-labeled ^{15}N -RDX (Figure VI.7). The common T-RFs (106, 109, and 116 bp) were dominated in all peak 116 bp T-RFs in microcosms receiving ring-labeled ^{15}N -RDX. However, the patterns were shifted to the common peaks 135, 138, 140, and 150 bp T-RFs in microcosms when receiving the nitro-, and fully-labeled ^{15}N -RDX.

In summary, a wide variety of organisms have been identified to with the ^{13}C - and ^{15}N -labeled RDX SIP approaches in this SIP study. Three major groups in α -*Proteobacteria* (unclassified *Rhizobiales*), γ -*Proteobactreia* (*Pseudomonas*), *Clotridia* (*Desulfosporosinus*) are likely to be present and responsible for RDX degradation under reducing conditions. These sequences analysis data indicate the diversity of active

organisms in the field, and these findings are valuable to the future researches on the development of molecular tools or identified suitable biomarkers for assessing the occurrence and potential of RDX biodegradation at contaminated sites.

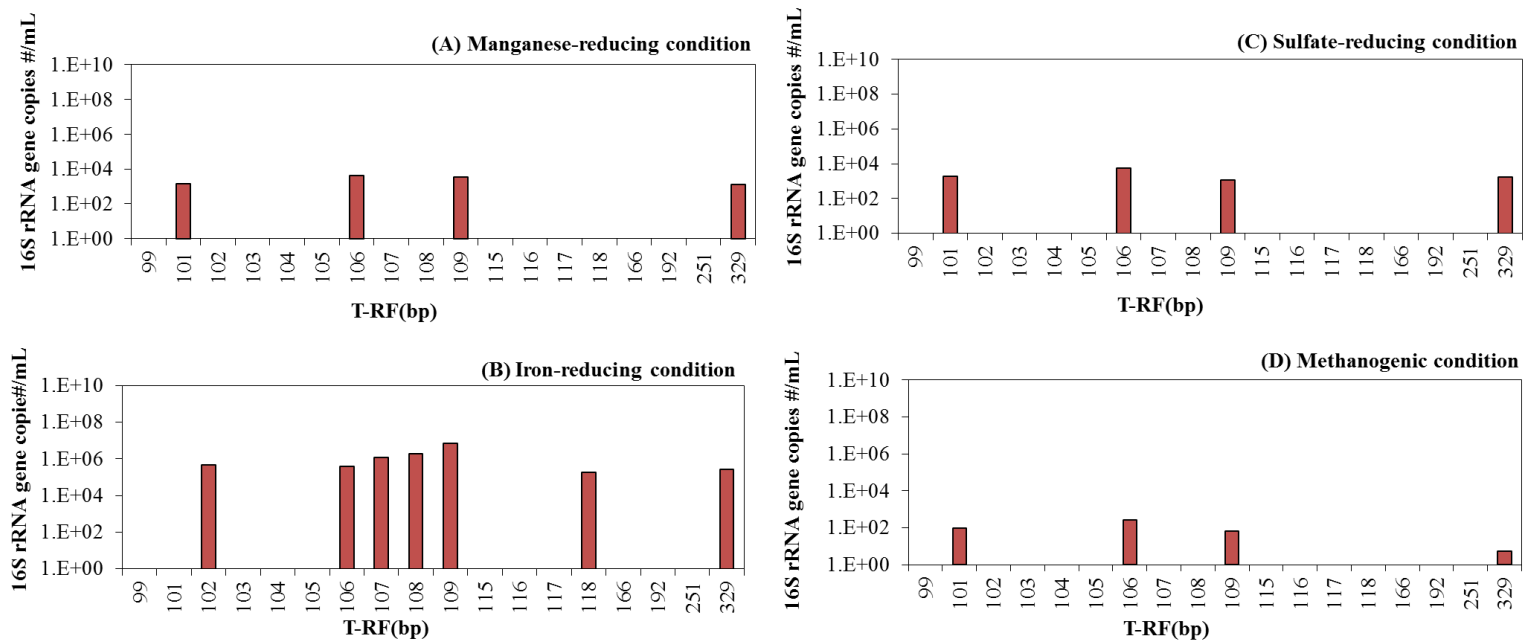


Figure VI.6. Microbial community structure within the ^{13}C -gradient fraction of the microcosms incubated under (A) manganese-reducing, (B) iron-reducing, (C) sulfate-reducing, and (D) methanogenic conditions.

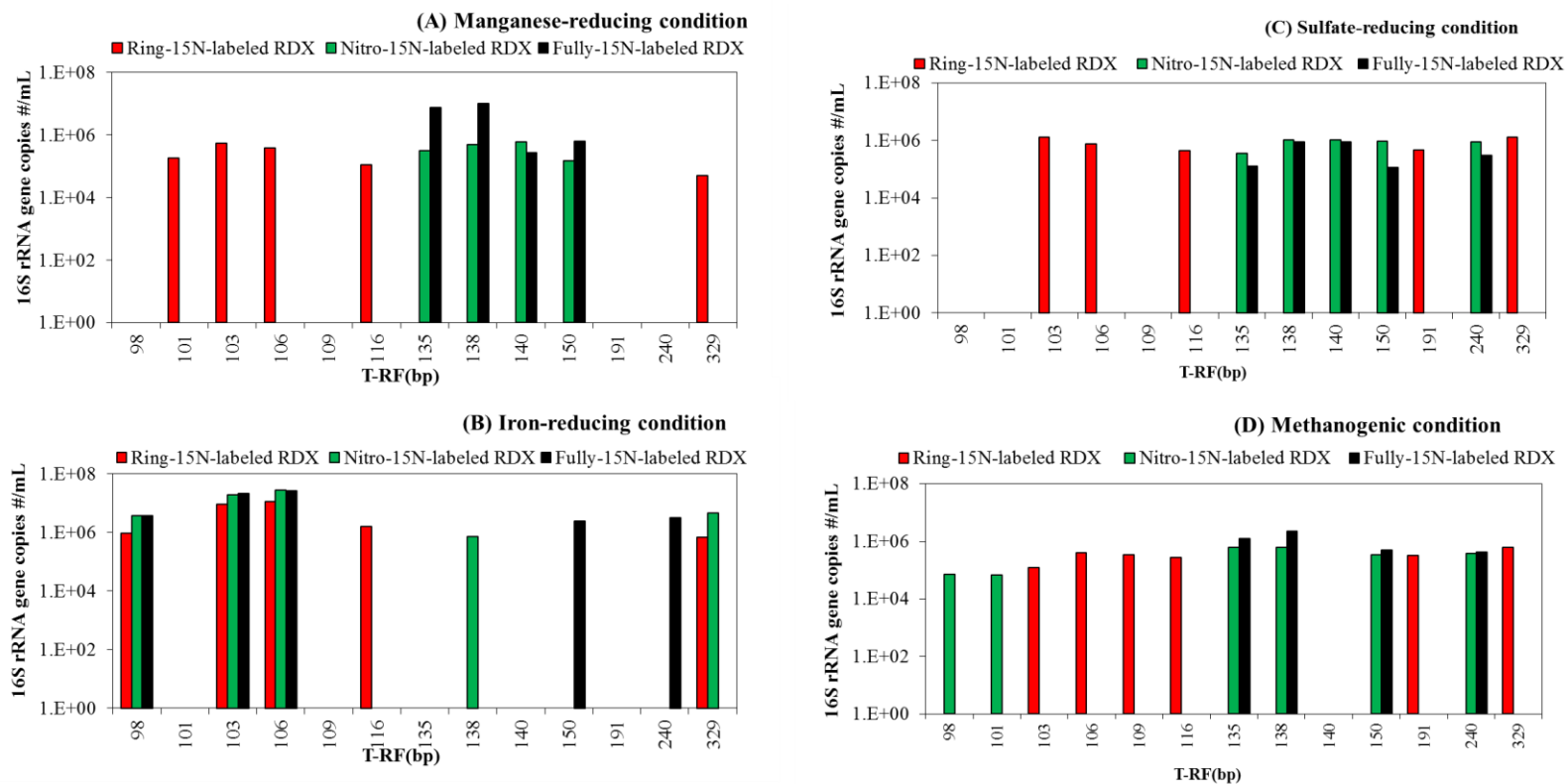


Figure VI.7. Microbial community structure within the ¹⁵N-gradient fraction of the microcosms receiving ring, nitro and fully ¹⁵N-labeled RDX incubated under (A) manganese-reducing, (B) iron-reducing, (C) sulfate-reducing, (D) methanogenic conditions.

CHAPTER VII
IDENTIFICATION OF SUITABLE BIOMARKERS FOR
ASSESSING RDX BIODEGRADATION IN NATURAL
AND ENGINEERED SYSTEMS

7.1. Introduction

Past and current of munitions productions and a variety of applications have resulted in the release of explosive-contaminated soil and groundwater. There is a great concern of these explosives in soil and groundwater because of their mobility, persistence, and toxicity (104). Hexahydro-1,3,5-trinitro-1,3,5-triazine (RDX), a common energetic compound, is often detected in groundwater (100-104) at historical munitions site. RDX is a possible human carcinogen and it has been placed on the U.S. Environmental Protection Agency (EPA) Contaminant Candidate List 3, and the EPA has issued a health advisory level of 2 µg/L for RDX in drinking water (3).

Numerous RDX-degrading isolates have examined the biological transformation of RDX and identified these strains can utilize RDX as sole nitrogen source or energy source (15, 18, 19, 47, 54, 55, 62, 63, 69, 105-112), or as a sole carbon source (65), or as both carbon and nitrogen sources (17). However, knowledge is limited on the microbial genes and enzyme systems that facilitate the RDX biodegradation process.

Few studies have reported on the identification of bacterial enzyme systems in RDX biodegradation/transformation. The diaphorase isolated from an anaerobic bacterium *Clostridia kluyveri* was reported to transform RDX by using NADH as the

electron donor under anaerobic conditions (62). Three catabolic genes involved in RDX transformation are *xplA/B* genes, *xenA/B* genes and *nsfI* genes. The *xplA/B* genes, isolated from *Rhodococcus* sp. and *Gordonia* sp., relate to a flavodoxin-cytochrome P450 enzyme (48, 49, 144, 145). The *xenA/B* genes, isolated from two *Pseudomonas* sp. (73), encode two xenobiotic reductases, XenA/XenB, known for their ability to transform RDX under both aerobic and anaerobic conditions (69). The *nsfI* gene is a Type I nitroreductase isolated from *Enterobacter cloacae* (72). The *nsfI* gene has been expressed from a plasmid in *Escherichia coli* to confirm the RDX transformation activity of Type I nitroreductase (68). These functional genes are potential biomarkers for monitoring the progress and/or potential of RDX biodegradation.

The real-time quantitative PCR is a powerful molecular tool to provide quantitative information of gene copy numbers for detecting and monitoring the presence of specific target genes. The method has been applied to detect the presence of specific functional genes in various environmental samples. A real-time PCR assay has been successfully used for targeting the *xplA* functional gene which was developed by Indest and collaborators (146). For our knowledge, however, there is no report on developing the real-time PCR assays for targeting *xenA/B* genes in the field for assessing biodegradation of RDX in natural and engineered systems.

The goal of this study is to develop a real-time PCR assay for quantifying functional *xenB* genes in natural and engineered environments. The specificity and sensitivity of this assay was evaluated using *Pseudomonas fluorescens* I-C which contains *xenB* like gene. The developed assay was applied to different groundwater

samples collected from the RDX contaminated sites and samples of RDX-degrading soil columns.

7.2. Results and discussion

7.2.1. Validation of developed real-time PCR for *xenB* gene: specificity and sensitivity

The primers set (xenB750F and xenB1074R) for real-time PR was successfully designed to target the *xenB* gene from *Pseudomonas fluorescens* I-C. The developed assay was tested for its specificity using genomic DNA of *Pseudomonas fluorescens* I-C and those of non *xenB* gene-containing bacteria *E.coli* and *Rhodococcus* DN22. The genomic DNA from *P. fluorescens* I-C was used to test the amplification sensitivity. Specific amplification was observed from 0.1 ng genomic DNA of strain *P. fluorescens* I-C. Good linear regression ($R^2 > 0.9$) was observed when 0.6 ng genomic DNA was used in the amplification reaction (Figure VII.1). The 325-bp PCR amplicons were observed in the agarose gel and the aplicoms were then purified from the gel for cloning and sequencing. The obtained sequence was blasted to confirm the detection of *xenB* gene of *P. fluorescens* I-C. No specific amplification was observed in *E.coli* and *Rhodococcus* DN22 strain with the primers sets.

The detection limit of the assay was determined using a series dilution of cloned *xenB* gene from extracted plasmid DNA. Specific amplification was observed from 2 fg plasmid DNA of cloned *xenB* gene, which was equivalent to 450 gene copies. No good linear relationship was observed ($R^2 < 0.9$) in the region where less than 10^3 copies of

xenB gene was used for amplification. The liner curve ($R^2>0.99$) listed within the range from 10^3 copies to 10^8 gene copies (Figure VII.2). Therefore, the assay was only able to detect *xenB* gene with over 10^3 copies amplification in samples.

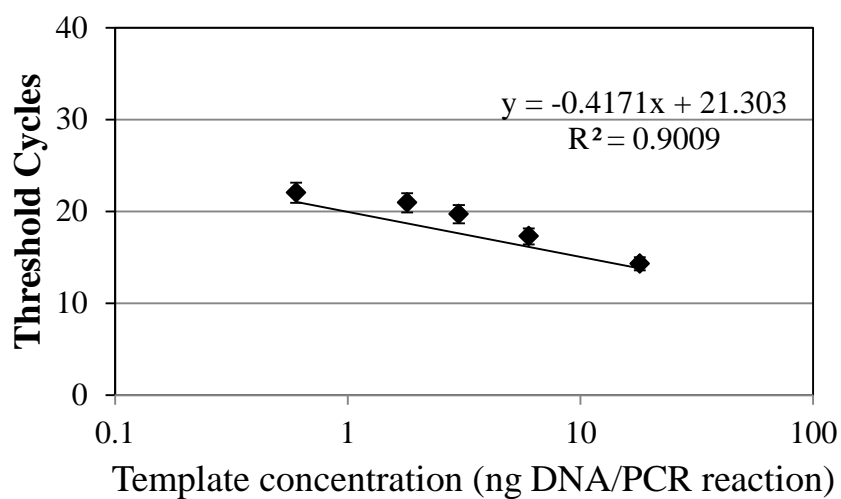


Figure VII.1. Validation the assay with genomic DNA of *P. fluorescens* I-C. Error bar represented the standard deviation of triplication samples

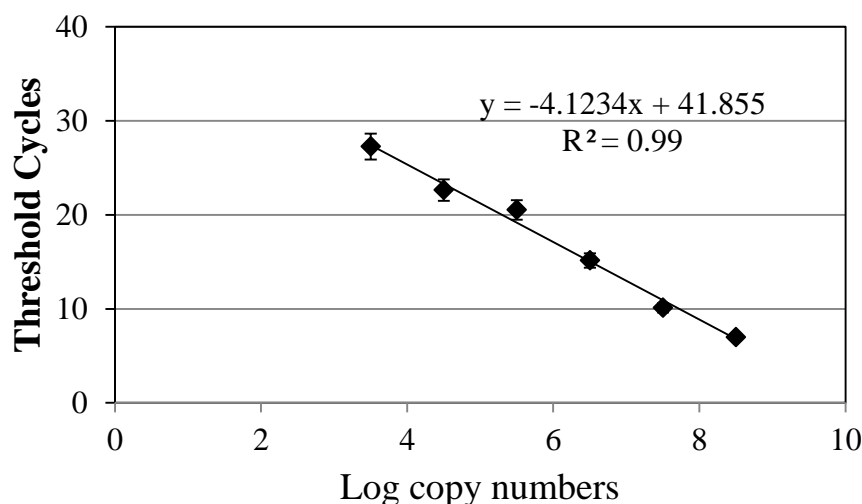


Figure VII.2. Standard curves showing the threshold cycle (Ct) value plotted versus the log number of *xenB* gene copies. Error bar represented the standard deviation of triplication samples.

7.2.2. Application of developed real-time PCR assay for detecting *xenB* genes in groundwater and soil column samples

The developed real-time PCR assays were applied to soil and groundwater samples to detect the presence of *xenB* gene. The RDX-contaminated groundwater was collected and soil column studies were constructed as described in Chapter III. The background groundwater at the sites was aerobic and the site was contaminated with low concentration of RDX over decades. As shown in Table VII.1, *xenB* genes were detected in on sample B of four background groundwater samples and in the influent groundwater samples (sample E) used for the column studies. The average *xenB* gene concentration was 1.1×10^4 gene copies/ml and 5.4×10^3 gene copies/ml in Sample B

(D-04) and Sample E, respectively. The absence of *xenB* gene in the other three background samples might be due to the difference of geochemical conditions within the sites, the low abundance of *xenB* gene copies (i.e. below the detection limit), or the lack of *xenB*-genes carrying bacteria in the surveyed groundwater samples. *xenB* genes were detected in the soil samples collected from the three RDX- degrading columns: Columns 1-3. Each column was made from a 7 cm ID aluminum tubing cut to a length of 30 cm. These three columns were packed with site sediments. Groundwater was collected from well C-02 at the field site and used as the column mobile phase (approximately 0.2 m/day). When the columns were assessed to have equilibrated, the amendment with emulsified vegetable oil substrate (EOS) and/or buffer solution (AquaBupH) were assigned to each column. The concentrations of RDX in effluent were monitored. RDX degradation was observed in all three soil columns, which the steady degradation rate was similar ($3.1 \pm 0.5 \mu\text{g/L/day}$) between Column 1 and Column 3 with EOS and/or buffer solution addition (Table VII.2). The slowest RDX degradation was observed in Column 2 ($2.8 \pm 0.6 \mu\text{g/L/day}$), which is the control without amended EOS (Table VII.2). After the RDX degradation was observed in all three column studies, the soil sediments were collected individually from the bottom column (influent samples K-1, L-1, M-1) to the top column (effluent samples K-3, L-3, M-3). Three sections were collected per column and each section collected within 10 cm of soil. The detection results of *xenB* genes in soil columns samples were varies between the three columns. The *xenB* gene was detected in all of the nine samples, ranging from 1.9×10^5 to 2.6×10^7 gene copies/g soil (Table VII.2). In Column 1, with the amended

Table VII.1. Screening the presence of *xenB* genes in groundwater samples

Sample ID	Source Description	<i>xenB</i> gene* detection	gene copies/ml
Background groundwater	A	C-02	-
	B	D-04	+
	C	IW-8	-
	D	MW-8	-
	E	Influent Groundwater (from C-02)	+

* (+) Detection signal of *xenB* genes in the assay; (-) No detection signal (-) when gene copies less than detection limit. The *xenB* gene was detected in the influent groundwater (from well C-02 with large quantity ~60L) within 5.4×10^3 gene copies/ml. Since the groundwater was aerobic and the site was contaminated low concentration of RDX over decades, the data indicated the potential of indigenous of microbial communities with carrying the *xenB* gene in the selected groundwater monitoring

Table VII.2. Detection of *xenB* genes in soil column samples

Sample ID	Source Description	Treatment	RDX* Degradation rate ($\mu\text{g/L/day}$)	gene copies/ g soil
Column 1	K-1	0-10 cm	EOS-Low Salt	2.61E+07
	K-2	10-20 cm		3.1 ± 0.5
	K-3	20-30 cm		3.86E+05
Column 2	L-1	0-10 cm	Control no amendment	3.33E+06
	L-2	10-20 cm		2.8 ± 0.6
	L-3	20-30 cm		3.03E+05
Column 3	M-1	0-10 cm	EOS-Low Salt and AquaBupH buffer	5.74E+06
	M-2	10-20 cm		3.1 ± 0.6
	M-3	20-30 cm		1.73E+06

* RDX degradation rate was calculated with the observed initiated RDX concentration in the influent and effluent over time during the column studies. An average concentration of RDX in the influent groundwater was reached to approximately 140 $\mu\text{g/L}$. The groundwater feed was set to 0.2 m/day in column studies.

emulsified vegetable oil substrate (EOS) as carbon source/electron donor, the highest of *xenB* gene detection was in the influent of column section (K-1), and then the declined of *xenB* detection was observed in the followed sections (K-2 and K-3). The data indicated the indigenous of microbial population with *xenB* genes were presented in groundwater and soil samples but the numbers of microbial population with *xenB* genes inhibited by the amendment of EOS.

7.2.3. Potential use of *xenB* gene as a biomarker for assessing RDX degradation in engineered systems and/or microbial natural attenuation

Monitoring active RDX degradative microorganisms and/or catabolic genes coding enzymes involved in the RDX degradation in the complex environmental samples will provide valuable information to adequately manage RDX contamination through modification of bioremediation strategies and/or monitored natural attenuation. The presence of *xenB* genes would indicate that indigenous of microbial population with *xenB* genes, which can be used to estimate the potential of RDX natural attenuation. Amendment of nutrient in active bioaugmentation and/or biostimulation site might promote *xenB* gene carrying bacteria. The developed real-time PCR assay will be valuable for assessing the performance of engineered bioremediation for RDX. Future studies are needed to apply this developed assay to various fields for assessing RDX degradation in engineered systems and/or microbial natural attenuation.

CHAPTER VIII

CONCLUSIONS AND RECOMMENDATIONS FOR FUTURE RESEARCH

8.1. Conclusions

RDX is toxic and a possible human carcinogen, therefore detection of RDX in groundwater at many historical mutation sites has raised a public health concern. RDX is biodegradable, however, little is known of the active RDX-degrading microorganisms in the field and their roles of RDX degradation in the natural or engineered systems. The goal of this research is to decipher active RDX-degrading microorganisms in RDX-contaminated groundwater, and to use the obtained information to identify suitable biomarkers for assessing intrinsic and/or engineered biodegradation of RDX. A better understanding of microbiology of RDX biodegradation helps to develop strategies on effectively RDX bioremediation at contaminated sites.

In Chapter IV, this is the first study to apply stable isotope probing (SIP) with ^{13}C -labeled RDX to identify active microorganisms capable of using RDX and/or RDX intermediates as a carbon source and responsible for RDX biodegradation in groundwater microcosms.

- ◆ A total of sixteen different 16S rRNA gene sequences were derived from microcosms receiving ^{13}C -labeled RDX, suggesting the presence of microorganisms able to incorporate carbon from RDX or its metabolites.

- ◆ Derived clones from ^{13}C -fractions, grouped in *Bacteroidia*, Clostridia, α -, β - and δ -*Proteobacteria*, and *Spirochaetes*, were different from previously described RDX degraders.
- ◆ Cheese whey stimulated RDX biotransformation, altered the types of RDX-degrading bacteria, and decreased microbial community diversity. Our findings suggest that RDX-degrading microorganisms in groundwater are more phylogenetically diverse than what has been inferred from studies with RDX-degrading isolates.

In Chapter V, we also applied the ring-, nitro- and fully-labeled ^{15}N -RDX to identify active microorganisms capable of using RDX and/or RDX intermediates as a nitrogen source and responsible for RDX biodegradation in groundwater microcosms.

- ◆ A total of fifteen different 16S rRNA gene sequences were derived from ^{15}N -fractions and grouped in *Clostridia*, β -*Proteobacteria* and *Spirochaetes*., suggesting the presence of microorganisms capable of using RDX and/or RDX intermediates as a nitrogen source.
- ◆ As the same groundwater was used in ^{13}C -RDX study, the common clones in both libraries of ^{13}C -SIP and ^{15}N -SIP studies would indicate that these common clones might be able to use RDX or its metabolites as both nitrogen and carbon source.
- ◆ In comparison to the results between ^{13}C -SIP and ^{15}N -SIP studies when presence of cheese whey, three major groups overlapped were found grouped within β -, γ -*Proteobacteria* and *Bacilli*. Combined these findings from both ^{13}C -SIP and ^{15}N -

SIP studies, the common sequences clustered in γ -*Proteobacteria* (*Pseudomonas*) and *Bacilli* (*Trichococcus*), suggesting these derived *Pseudomonas* sp. and *Trichococcus* sp might play a key role in the transformation of RDX biodegradation in situ with nutrient amendment.

- ◆ In addition, the catabolic genes that code the xenobiotic reductases might be a useful biomarker to assess potential and/or progress of RDX biodegradation under anoxic conditions.

In Chapter VI, we identified the active RDX-degrading microorganisms with ^{13}C -SIP and ^{15}N -SIP under manganese-reducing, iron-reducing, sulfate-reducing, and methanogenic conditions.

- ◆ A total of fifteen sequences were derived and clustered in *Actionbacteria* (*Eggerthella*), α -*Proteobacteria* (unclassified *Rhizobiales*), γ -*Proteobacteria* (*Pseudomonas*), and *Clostridia* (*Desulfosporosinus*) from the ^{13}C -DNA fractions.
- ◆ Similarly, a total of twenty nine sequences were derived from ^{15}N -DNA fractions grouped in α -*Proteobacteria* (unclassified *Rhizobiales*), γ -*Proteobacteria* (*Pseudomonas*), and *Clostridia* (*Desulfosporosinus*). Again, *Pseudomonas* sp. were identified as common sequences in both clone libraries from ^{13}C - and ^{15}N -SIP studies, suggested that *Pseudomonas* sp. are likely play an important role to transform RDX in situ.
- ◆ In addition, a major group of *Desulfosporosinus*, a family of sulfate-reducing bacteria, was identified from both ^{13}C -SIP and ^{15}N -SIP clone libraries from different reducing conditions. The findings suggested the *Desulfosporosinus* sp

is likely to use RDX and its metabolites as a carbon and/or a nitrogen source, and it would be important for degrading RDX at contaminated sites.

In Chapter VII, a real-time PCR assay was developed in this study for targeting catabolic *xenB* gene as a biomarker to monitor the *Pseudomonas fluorescens* I-C population and *xenB* like gene in environmental samples.

- ◆ The real-time PCR assay was validated with a good linear ($R^2 > 0.99$) within the range from 10^3 copies to 10^8 gene copies.
- ◆ The developed real-time PCR assay was applied to soil and groundwater samples to detect the presence of *xenB* gene. The presence of *xenB* genes would indicate that indigenous microbial population with *xenB* genes are present, which can be used to estimate the potential of natural attenuation of RDX.

8.2. Recommendations for future research

- 1) A majority of the clones identified in this study are not closely related to any known RDX degraders. Our findings suggest that RDX-degrading microorganisms in groundwater are phylogenetically diverse. As such, the use of known RDX degraders (like *Rhodococcus* DN22) or a catabolic gene (like *xplA*)— which are associated with aerobic RDX degradation—as biomarkers might not be appropriate to assess RDX biodegradation potential or to monitor the progress of RDX biodegradation in situ, particularly for those under anaerobic conditions. Future research efforts should be placed on the development better biomarkers for assessing RDX biodegradation potential under various geochemical conditions.

- 2) With these identified active RDX-degrading bacteria sequences information from ^{13}C -SIP and ^{15}N -SIP studies, future research efforts can be employed these analysis to develop molecular technique to track the occurrence and abundance of these RDX degraders at contaminated sites.
- 3) The developed real-time PCR assay targeted *xenB* gene will be valuable for assessing the potential of natural attenuation and the performance of engineered bioremediation for RDX under anaerobic condition. Future studies are needed to apply this developed assay to various fields for assessing RDX degradation in engineered systems and/or microbial natural attenuation.

REFERENCES

- (1) Talmage, S. S.; Opresko, D. M.; Maxwell, C. J.; Welsh, C. J. E.; Cretella, F. M.; Reno, P. H.; Daniel, F. B., Nitroaromatic munition compounds: environmental effects and screening values. *Rev. Environ. Contam. Toxicol.* **1999**, *161*, 1-156.
- (2) Crockett A. , C. H., and Jenkins T. Field sampling and selecting on-site analytical methods for explosives in water, EPA/600/S-99/002; U.S. Environmental Protection Agency: Washington, DC, 1999; <http://www.epa.gov/superfund/remedytech/tsp/download/water.pdf>
- (3) Toxicological profile for RDX; U.S. Department of Health and Human Services, Public Health Service, Agency for Toxic Substances and Disease Registry: Atlanta, GA, 2012; <http://www.atsdr.cdc.gov/toxprofiles/tp78.pdf>
- (4) Wujcik, W. J.; Lowe, W. L.; Marks, P. J.; Sisk, W. E., Granular activated carbon pilot treatment studies for explosives removal from contaminated groundwater. *Environ. Prog.* **1992**, *11*, (3), 178-189.
- (5) Oh, S.-Y.; Chiu, P. C., Graphite- and soot-mediated reduction of 2,4-dinitrotoluene and hexahydro-1,3,5-trinitro-1,3,5-triazine. *Environ. Sci. Technol.* **2009**, *43*, (18), 6983-6988.
- (6) Balakrishnan, V. K.; Halasz, A.; Hawari, J., Alkaline hydrolysis of the cyclic nitramine explosives RDX, HMX, and CL-20: new insights into degradation pathways obtained by the observation of novel intermediates. *Environ. Sci. Technol.* **2003**, *37*, 1838-1843.
- (7) Croce, M.; Okamoto, Y., Cationic micellar catalysis of the aqueous alkaline hydrolyses of 1,3,5-triaza-1,3,5-trinitrocyclohexane and 1,3,5,7-tetraaza-1,3,5,7-tetranitrocyclooctane. *J. Org. Chem.* **1979**, *44*, 2100-2103.
- (8) Heilmann, H. M.; Wiesmann, U.; Stenstrom, M. K., Kinetics of the alkaline hydrolysis of high explosives RDX and HMX in aqueous solution and adsorbed to activated carbon. *Environ. Sci. Technol.* **1996**, *30*, 1485-92.

- (9) Singh, J.; Comfort, S. D.; Shea, P. J., Iron-mediated remediation of RDX-contaminated water and soil under controlled Eh/pH. *Environ. Sci. Technol.* **1999**, *33*, 1488-1494.
- (10) Wanaratna, P.; Christodoulatos, C.; Sidhoum, M., Kinetics of RDX degradation by zero-valent iron (ZVI). *J. Hazard. Mater.* **2006**, *136*, 68-74.
- (11) Wildman, M. J.; Alvarez, P. J., RDX degradation using an integrated Fe(0)-microbial treatment approach. *Water Sci. Technol.* **2001**, *43*, 25-33.
- (12) Bonin, P. M. L.; Bejan, D.; Schutt, L.; Hawari, J.; Bunce, N. J., Electrochemical reduction of hexahydro-1,3,5-trinitro-1,3,5-triazine in aqueous solutions. *Environ. Sci. Technol.* **2004**, *38*, 1595-1599.
- (13) Bunce, N. J.; Merica, S. G.; Lipkowski, J., Prospects for the use of electrochemical methods for the destruction of aromatic organochlorine wastes. *Chemosphere* **1997**, *35*, 2719-2726.
- (14) Rodgers, J. D.; Bunce, N. J., Electrochemical treatment of 2,4,6-trinitrotoluene and related compounds. *Environ. Sci. Technol.* **2001**, *35*, 406-410.
- (15) Seth-Smith, H. M. B.; Rosser, S. J.; Basran, A.; Travis, E. R.; Dabbs, E. R.; Nicklin, S.; Bruce, N. C., Cloning, sequencing, and characterization of the hexahydro-1,3,5-trinitro-1,3,5-triazine degradation gene cluster from *Rhodococcus rhodochrous*. *Appl. Environ. Microbiol.* **2002**, *68*, 4764-4771.
- (16) Coleman, N. V.; Nelson, D. R.; Duxbury, T., Aerobic biodegradation of hexahydro-1,3,5-trinitro-1,3,5-triazine (RDX) as a nitrogen source by a *Rhodococcus* sp., strain DN22. *Soil Biol. Biochem.* **1998**, *30*, (9), 1159-1167.
- (17) Thompson, K. T.; Crocker, F. H.; Fredrickson, H. L., Mineralization of the cyclic nitramine explosive hexahydro-1,3,5-trinitro-1,3,5-triazine by *Gordonia* and *Williamsia* spp. *Appl. Environ. Microbiol.* **2005**, *71*, 8265-8272.
- (18) Zhao, J.-S.; Halasz, A.; Paquet, L.; Beaulieu, C.; Hawari, J., Biodegradation of hexahydro-1,3,5-trinitro-1,3,5-triazine and its mononitroso derivative hexahydro-1-nitroso-3,5-dinitro-1,3,5-triazine by *Klebsiella pneumoniae* strain SCZ-1

- isolated from an anaerobic sludge. *Appl. Environ. Microbiol.* **2002**, 68, 5336-5341.
- (19) Zhao, J.-S.; Spain, J.; Hawari, J., Phylogenetic and metabolic diversity of hexahydro-1,3,5-trinitro-1,3,5-triazine (RDX)-transforming bacteria in strictly anaerobic mixed cultures enriched on RDX as nitrogen source. *FEMS Microbiol. Ecol.* **2003**, 46, 189-196.
- (20) Zhao, J.-S.; Paquet, L.; Halasz, A.; Manno, D.; Hawari, J., Metabolism of octahydro-1,3,5,7-tetranitro-1,3,5,7-tetrazocine by *Clostridium bifermentans* strain HAW-1 and several other H₂-producing fermentative anaerobic bacteria. *FEMS Microbiol. Lett.* **2004**, 237, 65-72.
- (21) Freedman, D. L.; Sutherland, K. W., Biodegradation of hexahydro-1,3,5-trinitro-1,3,5-triazine (RDX) under nitrate-reducing conditions. *Water Sci. Technol.* **1998**, 38, 33-40.
- (22) Boopathy, R.; Gurgas, M.; Ullian, J.; Manning, J. F., Metabolism of explosive compounds by sulfate-reducing bacteria. *Curr. Microbiol.* **1998**, 37, 127-131.
- (23) Adrian, N. R.; Arnett, C. M., Anaerobic biodegradation of hexahydro-1,3,5-trinitro-1,3,5-triazine (RDX) by *Acetobacterium malicum* strain HAAP-1 isolated from a methanogenic mixed culture. *Curr. Microbiol.* **2004**, 48, 332-340.
- (24) Kwon, M. J.; Finneran, K. T., Hexahydro-1,3,5-trinitro-1,3,5-triazine (RDX) and Octahydro-1,3,5,7-tetranitro-1,3,5,7-tetrazocine (HMX) Biodegradation Kinetics Amongst Several Fe(III)-Reducing Genera. *Soil Sediment Contam.* **2008**, 17, 189-203.
- (25) Kwon, M. J.; Finneran, K. T., Microbially mediated biodegradation of hexahydro-1,3,5-trinitro-1,3,5-triazine by extracellular electron shuttling compounds. *Appl. Microbiol. Biotechnol.* **2006**, 72, (9), 5933-5941.
- (26) Kwon, M. J.; O'Loughlin, E. J.; Antonopoulos, D. A.; Finneran, K. T., Geochemical and microbiological processes contributing to the transformation of hexahydro-1,3,5-trinitro-1,3,5-triazine (RDX) in contaminated aquifer material. *Chemosphere* **2011**, 84, (9), 1223-1230.

- (27) Bhushan, B.; Halasz, A.; Hawari, J., Effect of iron(III), humic acids and anthraquinone-2,6-disulfonate on biodegradation of cyclic nitramines by *Clostridium* sp. EDB2. *J. Appl. Microbiol.* **2006**, *100*, 555-563.
- (28) Crocker, F. H.; Indest, K. J.; Fredrickson, H. L., Biodegradation of the cyclic nitramine explosives RDX, HMX, and CL-20. *Appl. Microbiol. Biotechnol.* **2006**, *73*, 274-290.
- (29) Torsvik, V.; Øvreås, L., Microbial diversity and function in soil: from genes to ecosystems. *Curr. Opin. Microbiol.* **2002**, *5*, (3), 240-245.
- (30) Cho, K.-C.; Lee, D. G.; Roh, H.; Fuller, M. E.; Hatzinger, P. B.; Chu, K.-H., Application of ¹³C-stable isotope probing to identify RDX-degrading microorganisms in groundwater. *Environ. Pollut.* **2013**, *178*, 350-360.
- (31) Pichtel, J., Distribution and fate of military explosives and propellants in soil: a review. *Appl. Environ. Soil Sci.* **2012**, *2012*, 33.
- (32) Juhasz, A. L.; Naidu, R., Explosives: fate, dynamics, and ecological impact in terrestrial and marine environments reviews of environmental contamination and toxicology. *Rev. Environ. Contam. Toxicol.* **2007**, *191*, 163-215.
- (33) Bhadra, R.; Wayment, D. G.; Williams, R. K.; Barman, S. N.; Stone, M. B.; Hughes, J. B.; Shanks, J. V., Studies on plant-mediated fate of the explosives RDX and HMX. *Chemosphere* **2001**, *44*, (5), 1259-1264.
- (34) Parker, G. A.; Reddy, G.; Major, M. A., Reevaluation of a twenty-four-month chronic toxicity/carcinogenicity study of hexahydro-1,3,5-trinitro-1,3,5-triazine (RDX) in the B6C3F1 hybrid mouse. *Int. J. Toxicol.* **2006**, *25*, (5), 373-378.
- (35) Singh, B.; Kaur, J.; Singh, K., Microbial remediation of explosive waste. *Crit. Rev. Microbiol.* **2012**, *38*, (2), 152-167.
- (36) Liou, M.-J.; Lu, M.-C.; Chen, J.-N., Oxidation of explosives by Fenton and photo-Fenton processes. *Water Res.* **2003**, *37*, (13), 3172-3179.

- (37) Zoh, K.-D.; Stenstrom, M. K., Fenton oxidation of hexahydro-1,3,5-trinitro-1,3,5-triazine (RDX) and octahydro-1,3,5,7-tetranitro-1,3,5,7-tetrazocine (HMX). *Water Res.* **2002**, *36*, 1331-1341.
- (38) Adam, M. L.; Comfort, S. D.; Morley, M. C.; Snow, D. D., Remediating RDX-contaminated ground water with permanganate: laboratory investigations for the Pantex perched aquifer. *J. Environ. Qual.* **2004**, *33*, 2165-2173.
- (39) Adam, M.; Comfort, S.; Snow, D.; Cassada, D.; Morley, M.; Clayton, W., Evaluating ozone as a remedial treatment for removing RDX from unsaturated soils. *J. Environ. Eng.* **2006**, *132*, 1580-1588.
- (40) Boparai, H. K.; Comfort, S. D.; Satapanajaru, T.; Szecsody, J. E.; Grossl, P. R.; Shea, P. J., Abiotic transformation of high explosives by freshly precipitated iron minerals in aqueous Fe(II) solutions. *Chemosphere* **2010**, *79*, 865-872.
- (41) Naja, G.; Halasz, A.; Thiboutot, S.; Ampleman, G.; Hawari, J., Degradation of hexahydro-1,3,5-trinitro-1,3,5-triazine (RDX) using zerovalent iron nanoparticles. *Environ. Sci. Technol.* **2008**, *42*, 4364-4370.
- (42) Comfort, S. D.; Shea, P. J.; Machacek, T. A.; Satapanajaru, T., Pilot-scale treatment of RDX-contaminated soil with zerovalent iron. *J. Environ. Qual.* **2003**, *32*, 1717-25.
- (43) Gent, D. B.; Wani, A. H.; Davis, J. L.; Alshwabkeh, A., Electrolytic redox and electrochemical generated alkaline hydrolysis of hexahydro-1,3,5-trinitro-1,3,5-triazine (RDX) in sand columns. *Environ. Sci. Technol.* **2009**, *43*, (16), 6301-6307.
- (44) Hwang, S.; Felt, D. R.; Bouwer, E. J.; Brooks, M. C.; Larson, S. L.; Davis, J. L., Remediation of RDX-contaminated water using alkaline hydrolysis. *J. Environ. Eng.* **2006**, *132*, (2), 256-262.
- (45) Binks, P. R.; Nicklin, S.; Bruce, N. C., Degradation of hexahydro-1,3,5-trinitro-1,3,5-triazine (RDX) by *Stenotrophomonas maltophilia* PB1. *Appl. Environ. Microbiol.* **1995**, *61*, 1318-22.

- (46) Van, A. B.; Yoon, J. M.; Schnoor, J. L., Biodegradation of nitro-substituted explosives 2,4,6-trinitrotoluene, hexahydro-1,3,5-trinitro-1,3,5-triazine, and octahydro-1,3,5,7-tetranitro-1,3,5-tetrazocine by a phytosymbiotic *Methylobacterium* sp. associated with poplar tissues (*Populus deltoides* × *nigra* DN34). *Appl. Environ. Microbiol.* **2004**, *70*, 508-517.
- (47) Coleman, N. V.; Spain, J. C.; Duxbury, T., Evidence that RDX biodegradation by *Rhodococcus* strain DN22 is plasmid-borne and involves a cytochrome P450. *J. Appl. Microbiol.* **2002**, *93*, 463-472.
- (48) Seth-Smith, H. M. B.; Edwards, J.; Rosser, S. J.; Rathbone, D. A.; Bruce, N. C., The explosive-degrading cytochrome P450 system is highly conserved among strains of *Rhodococcus* spp. *Appl. Environ. Microbiol.* **2008**, *74*, 4550-4552.
- (49) Rylott, E. L.; Jackson, R. G.; Edwards, J.; Womack, G. L.; Seth-Smith, H. M. B.; Rathbone, D. A.; Strand, S. E.; Bruce, N. C., An explosive-degrading cytochrome P450 activity and its targeted application for the phytoremediation of RDX. *Nat. Biotechnol.* **2006**, *24*, 216-219.
- (50) Annamaria, H.; Manno, D.; Strand, S. E.; Bruce, N. C.; Hawari, J., Biodegradation of RDX and MNX with *Rhodococcus* sp. strain DN22: new insights into the degradation pathway. *Environ. Sci. Technol.* **2010**, *44*, (24), 9330-9336.
- (51) Fournier, D.; Halasz, A.; Spain, J.; Fiurasek, P.; Hawari, J., Determination of key metabolites during biodegradation of hexahydro-1,3,5-trinitro-1,3,5-triazine with *Rhodococcus* sp. strain DN22. *Appl. Environ. Microbiol.* **2002**, *68*, 166-172.
- (52) Young, D. M.; Unkefer, P. J.; Ogden, K. L., Biotransformation of hexahydro-1,3,5-trinitro-1,3,5-triazine (RDX) by a prospective consortium and its most effective isolate *Serratia marcescens*. *Biotechnol. Bioeng.* **1997**, *53*, 515-522.
- (53) Fournier, D.; Monteil-Rivera, F.; Halasz, A.; Bhatt, M.; Hawari, J., Degradation of CL-20 by white-rot fungi. *Chemosphere* **2006**, *63*, 175-181.
- (54) Nejdat, A.; Kafka, L.; Tekoah, Y.; Ronen, Z., Effect of organic and inorganic nitrogenous compounds on RDX degradation and cytochrome P-450 expression in *Rhodococcus* strain YH1. *Biodegradation* **2008**, *19*, 313-320.

- (55) Bernstein, A.; Adar, E.; Nejidat, A.; Ronen, Z., Isolation and characterization of RDX-degrading *Rhodococcus* species from a contaminated aquifer. *Biodegradation* **2011**, *22*, (5), 997-1005.
- (56) Hawari, J.; Halasz, A.; Sheremata, T.; Beaudet, S.; Groom, C.; Paquet, L.; Rhofir, C.; Ampleman, G.; Thiboutot, S., Characterization of metabolites during biodegradation of hexahydro-1,3,5-trinitro-1,3,5-triazine (RDX) with municipal anaerobic sludge. *Appl. Environ. Microbiol.* **2000**, *66*, (6), 2652-2657.
- (57) Bradley, P. M.; Dinicola, R. S., Hexahydro-1,3,5-trinitro-1,3,5-triazine (RDX) biodegradation in aquifer sediments under manganese-reducing conditions. *Biorem. J.* **2005**, *9*, 1-8.
- (58) Beller, H. R., Anaerobic biotransformation of RDX (hexahydro-1,3,5-trinitro-1,3,5-triazine) by aquifer bacteria using hydrogen as the sole electron donor. *Water Res.* **2002**, *36*, 2533-2540.
- (59) Sherburne, L. A.; Shrout, J. D.; Alvarez, P. J. J., Hexahydro-1,3,5-trinitro-1,3,5-triazine (RDX) degradation by *Acetobacterium paludosum*. *Biodegradation* **2005**, *16*, 539-547.
- (60) Adrian, N. R.; Arnett, C. M.; Hickey, R. F., Stimulating the anaerobic biodegradation of explosives by the addition of hydrogen or electron donors that produce hydrogen. *Water Res.* **2003**, *37*, 3499-3507.
- (61) Zhang, C.; Hughes, J. B., Biodegradation pathways of hexahydro-1,3,5-trinitro-1,3,5-triazine (RDX) by *Clostridium acetobutylicum* cell-free extract. *Chemosphere* **2002**, *50*, 665-671.
- (62) Bhushan, B.; Halasz, A.; Spain, J. C.; Hawari, J., Diaphorase catalyzed biotransformation of RDX via N-denitration mechanism. *Biochem. Biophys. Res. Commun.* **2002**, *296*, 779-784.
- (63) Zhao, J. S.; Paquet, L.; Halasz, A.; Hawari, J., Metabolism of hexahydro-1,3,5-trinitro-1,3,5-triazine through initial reduction to hexahydro-1-nitroso-3,5-dinitro-1,3,5-triazine followed by denitration in *Clostridium bifermentans* HAW-1. *Appl. Microbiol. Biotechnol.* **2003**, *63*, 187-193.

- (64) Kitts, C. L.; Cunningham, D. P.; Unkefer, P. J., Isolation of three hexahydro-1,3,5-trinitro-1,3,5-triazine-degrading species of the family *Enterobacteriaceae* from nitramine explosive-contaminated soil. *Appl. Environ. Microbiol.* **1994**, *60*, 4608-11.
- (65) Arnett, C.; Adrian, N., Cosubstrate independent mineralization of hexahydro-1,3,5-trinitro-1,3,5-triazine (RDX) by a *Desulfovibrio* species under anaerobic conditions. *Biodegradation* **2009**, *20*, (1), 15-26.
- (66) Pudge, I. B.; Daugulis, A. J.; Dubois, C., The use of *Enterobacter cloacae* ATCC 43560 in the development of a two-phase partitioning bioreactor for the destruction of hexahydro-1,3,5-trinitro-1,3,5-s-triazine (RDX). *J. Biotechnol.* **2003**, *100*, 65-75.
- (67) Zhao, J.-S.; Manno, D.; Hawari, J., Regulation of hexahydro-1,3,5-trinitro-1,3,5-triazine (RDX) metabolism in *Shewanella halifaxensis* HAW-EB4 by terminal electron acceptor and involvement of c-type cytochrome. *Microbiology* **2008**, *154*, (4), 1026-1037.
- (68) Kitts, C. L.; Green, C. E.; Otley, R. A.; Alvarez, M. A.; Unkefer, P. J., Type I nitroreductases in soil enterobacteria reduce TNT (2,4,6-trinitrotoluene) and RDX (hexahydro-1,3,5-trinitro-1,3,5-triazine). *Can. J. Microbiol.* **2000**, *46*, 278-282.
- (69) Fuller, M. E.; McClay, K.; Hawari, J.; Paquet, L.; Malone, T. E.; Fox, B. G.; Steffan, R. J., Transformation of RDX and other energetic compounds by xenobiotic reductases XenA and XenB. *Appl. Microbiol. Biotechnol.* **2009**, *84*, 535-544.
- (70) Bhushan, B.; Halasz, A.; Spain, J.; Thiboutot, S.; Ampleman, G.; Hawari, J., Biotransformation of hexahydro-1,3,5-trinitro-1,3,5-triazine catalyzed by a NAD(P)H: nitrate oxidoreductase from *Aspergillus niger*. *Environ. Sci. Technol.* **2002**, *36*, 3104-3108.
- (71) Kutty, R.; Bennett, G., Biochemical characterization of trinitrotoluene transforming oxygen-insensitive nitroreductases from *Clostridium acetobutylicum* ATCC 824. *Arch. Microbiol.* **2005**, *184*, (3), 158-167.

- (72) Bryant, C.; Hubbard, L.; McElroy, W. D., Cloning, nucleotide sequence, and expression of the nitroreductase gene from *Enterobacter cloacae*. *J. Biol. Chem.* **1991**, *266*, 4126-30.
- (73) Blehert, D. S.; Fox, B. G.; Chambliss, G. H., Cloning and sequence analysis of two *Pseudomonas flavoprotein* xenobiotic reductases. *J. Bacteriol.* **1999**, *181*, 6254-6263.
- (74) Halasz, A.; Hawari, J., Degradation routes of RDX in various redox systems. *Aquatic Redox Chemistry*; Tratnyek, P. G.; Grundl, T. J.; Haderlein, S. B., Eds. American Chemical Society: 2011; pp 441.
- (75) Zhao, J.-S.; Spain, J.; Thiboutot, S.; Ampleman, G.; Greer, C.; Hawari, J., Phylogeny of cyclic nitramine-degrading psychrophilic bacteria in marine sediment and their potential role in the natural attenuation of explosives. *FEMS Microbiol. Ecol.* **2004**, *49*, (3), 349-357.
- (76) Bhushan, B.; Halasz, A.; Thiboutot, S.; Ampleman, G.; Hawari, J., Chemotaxis-mediated biodegradation of cyclic nitramine explosives RDX, HMX, and CL-20 by *Clostridium* sp. EDB2. *Biochem. Biophys. Res. Commun.* **2004**, *316*, 816-821.
- (77) Eaton, H. L.; Durringer, J. M.; Murty, L. D.; Craig, A. M., Anaerobic bioremediation of RDX by ovine whole rumen fluid and pure culture isolates. *Appl. Microbiol. Biotechnol.* **2013**, *97*, (8), 3699-710.
- (78) Yu, C.-P.; Chu, K.-H., A quantitative assay for linking microbial community function and structure of a naphthalene-degrading microbial consortium. *Environ. Sci. Technol.* **2005**, *39*, 9611-9619.
- (79) Radajewski, S.; Ineson, P.; Parekh, N. R.; Murrell, J. C., Stable-isotope probing as a tool in microbial ecology. *Nature* **2000**, *403*, 646-649.
- (80) Radajewski, S.; Webster, G.; Reay, D. S.; Morris, S. A.; Ineson, P.; Nedwell, D. B.; Prosser, J. I.; Murrell, J. C., Identification of active methylotroph populations in an acidic forest soil by stable-isotope probing. *Microbiology* **2002**, *148*, 2331-2342.

- (81) Dumont, M. G.; Murrell, J. C., Stable isotope probing - linking microbial identity to function. *Nat. Rev. Microbiol.* **2005**, *3*, 499-504.
- (82) Friedrich, M. W., Stable-isotope probing of DNA: insights into the function of uncultivated microorganisms from isotopically labeled metagenomes. *Curr. Opin. Biotechnol.* **2006**, *17*, 59-66.
- (83) Kitts, C. L., Terminal restriction fragment patterns: a tool for comparing microbial communities and assessing community dynamics. *Curr. Issues Intest. Microbiol.* **2001**, *2*, 17-25.
- (84) Liu, W. T.; Marsh, T. L.; Cheng, H.; Forney, L. J., Characterization of microbial diversity by determining terminal restriction fragment length polymorphisms of genes encoding 16S rRNA. *Appl. Environ. Microbiol.* **1997**, *63*, (11), 4516-4522.
- (85) Hristova, K. R.; Lutenecker, C. M.; Scow, K. M., Detection and quantification of methyl tert-butyl ether-degrading strain PM1 by real-time TaqMan PCR. *Appl. Environ. Microbiol.* **2001**, *67*, 5154-5160.
- (86) Beller, H. R.; Kane, S. R.; Legler, T. C.; Alvarez, P. J. J., A Real-time polymerase chain reaction method for monitoring anaerobic, hydrocarbon-degrading bacteria based on a catabolic gene. *Environ. Sci. Technol.* **2002**, *36*, 3977-3984.
- (87) Hosoda, A.; Kasai, Y.; Hamamura, N.; Takahata, Y.; Watanabe, K., Development of a PCR method for the detection and quantification of benzoyl-CoA reductase genes and its application to monitored natural attenuation. *Biodegradation* **2005**, *16*, 591-601.
- (88) Chu, K.-H.; Alvarez-Cohen, L., Trichloroethylene degradation by methane-oxidizing cultures grown with various nitrogen sources. *Water Environ. Res.* **1996**, *68*, (1), 76-82.
- (89) Roh, H.; Yu, C.-P.; Fuller, M. E.; Chu, K.-H., Identification of hexahydro-1,3,5-trinitro-1,3,5-triazine-degrading microorganisms via ¹⁵N-stable isotope probing. *Environ. Sci. Technol.* **2009**, *43*, 2505-2511.

- (90) Yu, C.-P.; Ahuja, R.; Sayler, G.; Chu, K.-H., Quantitative molecular assay for fingerprinting microbial communities of wastewater and estrogen-degrading consortia. *Appl. Environ. Microbiol.* **2005**, *71*, 1433-1444.
- (91) Roh, H.; Chu, K.-H., Effects of solids retention time on the performance of bioreactors bioaugmented with a 17 β -estradiol-utilizing bacterium, *Sphingomonas* strain KC8. *Chemosphere* **2011**, *84*, (2), 227-233.
- (92) Schloss, P. D.; Westcott, S. L.; Ryabin, T.; Hall, J. R.; Hartmann, M.; Hollister, E. B.; Lesniewski, R. A.; Oakley, B. B.; Parks, D. H.; Robinson, C. J.; Sahl, J. W.; Stres, B.; Thallinger, G. G.; Van Horn, D. J.; Weber, C. F., Introducing mothur: open-source, platform-independent, community-supported software for describing and comparing microbial communities. *Appl. Environ. Microbiol.* **2009**, *75*, (23), 7537-7541.
- (93) Edgar, R. C.; Haas, B. J.; Clemente, J. C.; Quince, C.; Knight, R., UCHIME improves sensitivity and speed of chimera detection. *Bioinformatics* **2011**, *27*, (16), 2194-2200.
- (94) Wang, Q.; Garrity, G. M.; Tiedje, J. M.; Cole, J. R., Naïve Bayesian classifier for rapid assignment of rRNA sequences into the new bacterial taxonomy. *Appl. Environ. Microbiol.* **2007**, *73*, (16), 5261-5267.
- (95) Tamura, K.; Peterson, D.; Peterson, N.; Stecher, G.; Nei, M.; Kumar, S., MEGA5: molecular evolutionary genetics analysis using maximum likelihood, evolutionary distance, and maximum parsimony methods. *Mol. Biol. Evol.* **2011**, *28*, (10), 2731-2739.
- (96) Junier, P.; Junier, T.; Witzel, K.-P., TRiFLe, a program for *in-silico* terminal restriction fragment length polymorphism analysis with user-defined sequence sets. *Appl. Environ. Microbiol.* **2008**, *74*, (20), 6452-6456.
- (97) Halasz, A.; Manno, D.; Perreault, N. N.; Sabbadin, F.; Bruce, N. C.; Hawari, J., Biodegradation of RDX nitroso products MNX and TNX by cytochrome P450 XplA. *Environ. Sci. Technol.* **2012**, *46*, (13), 7245-7251.
- (98) Paquet, L.; Monteil-Rivera, F.; Hatzinger, P. B.; Fuller, M. E.; Hawari, J., Analysis of the key intermediates of RDX (hexahydro-1,3,5-trinitro-1,3,5-

- triazine) in groundwater: occurrence, stability and preservation. *J. Environ. Monit.* **2011**, *13*, 2304-2311.
- (99) Darrach, M. R.; Chutjian, A.; Plett, G. A., Trace explosives signatures from World War II unexploded undersea ordnance. *Environ. Sci. Technol.* **1998**, *32*, 1354-1358.
- (100) Pennington, J. C.; Brannon, J. M., Environmental fate of explosives. *Thermochim. Acta* **2002**, *384*, 163-172.
- (101) Brannon, J. M.; Price, C. B.; Yost, S. L.; Hayes, C.; Porter, B., Comparison of environmental fate and transport process descriptors of explosives in saline and freshwater systems. *Mar. Pollut. Bull.* **2005**, *50*, 247-251.
- (102) Clausen, J.; Robb, J.; Curry, D.; Korte, N., A case study of contaminants on military ranges: Camp Edwards, Massachusetts, USA. *Environ. Pollut.* **2004**, *129*, 13-21.
- (103) Pennington, J. C.; Brannon, J. M.; Gunnison, D.; Harrelson, D. W.; Zakikhani, M.; Miyares, P.; Jenkins, T. F.; Clarke, J.; Hayes, C.; Ringleberg, D.; Perkins, E.; Fredrickson, H., Monitored natural attenuation of explosives. *Soil Sediment Contam.* **2001**, *10*, 45-70.
- (104) Yamamoto, H.; Morley, M. C.; Speitel, G. E., Jr.; Clausen, J., Fate and transport of high explosives in a sandy soil: adsorption and desorption. *Soil Sediment Contam.* **2004**, *13*, 459-477.
- (105) Hawari, J.; Beaudet, S.; Halasz, A.; Thiboutot, S.; Ampleman, G., Microbial degradation of explosives: biotransformation versus mineralization. *Appl. Microbiol. Biotechnol.* **2000**, *54*, 605-618.
- (106) McCormick, N. G.; Cornell, J. H.; Kaplan, A. M., Biodegradation of hexahydro-1,3,5-trinitro-1,3,5-triazine. *Appl. Environ. Microbiol.* **1981**, *42*, 817-23.
- (107) Sheremata, T. W.; Hawari, J., Mineralization of RDX by the white rot fungus *phanerochaete chrysosporium* to carbon dioxide and nitrous oxide. *Environ. Sci. Technol.* **2000**, *34*, 3384-3388.

- (108) Hawari, J.; Halasz, A.; Beaudet, S.; Paquet, L.; Ampleman, G.; Thiboutot, S., Biotransformation routes of cctahydro-1,3,5,7-tetranitro-1,3,5,7-tetrazocine by municipal anaerobic sludge. *Environ. Sci. Technol.* **2001**, *35*, 70-75.
- (109) Hawari, J.; Halasz, A.; Groom, C.; Deschamps, S.; Paquet, L.; Beaulieu, C.; Corriveau, A., Photodegradation of RDX in aqueous solution: a mechanistic probe for biodegradation with *Rhodococcus* sp. *Environ. Sci. Technol.* **2002**, *36*, 5117-5123.
- (110) Bhatt, M.; Zhao, J.-S.; Monteil-Rivera, F.; Hawari, J., Biodegradation of cyclic nitramines by tropical marine sediment bacteria. *J. Ind. Microbiol. Biotechnol.* **2005**, *32*, 261-267.
- (111) Bhatt, M.; Zhao, J.-S.; Halasz, A.; Hawari, J., Biodegradation of hexahydro-1,3,5-trinitro-1,3,5-triazine by novel fungi isolated from unexploded ordnance contaminated marine sediment. *J. Ind. Microbiol. Biotechnol.* **2006**, *33*, 850-858.
- (112) Fuller, M. E.; Perreault, N.; Hawari, J., Microaerophilic degradation of hexahydro-1,3,5-trinitro-1,3,5-triazine (RDX) by three *Rhodococcus* strains. *Lett. Appl. Microbiol.* **2010**, *51*, (3), 313-318.
- (113) Uhlík, O.; Jecná, K.; Leigh, M. B.; Macková, M.; Macek, T., DNA-based stable isotope probing: a link between community structure and function. *Sci. Total Environ.* **2009**, *407*, (12), 3611-3619.
- (114) Radajewski, S.; McDonald, I. R.; Murrell, J. C., Stable-isotope probing of nucleic acids: a window to the function of uncultured microorganisms. *Curr. Opin. Biotechnol.* **2003**, *14*, 296-302.
- (115) Morris, S. A.; Radajewski, S.; Willison, T. W.; Murrell, J. C., Identification of the functionally active methanotroph population in a peat soil microcosm by stable-isotope probing. *Appl. Environ. Microbiol.* **2002**, *68*, 1446-1453.
- (116) Gallagher, E.; McGuinness, L.; Phelps, C.; Young, L. Y.; Kerkhof, L. J., ¹³C-carrier DNA shortens the incubation time needed to detect benzoate-utilizing denitrifying bacteria by stable-isotope probing. *Appl. Environ. Microbiol.* **2005**, *71*, 5192-5196.

- (117) Gallagher, E. M.; Young, L. Y.; McGuinness, L. M.; Kerkhof, L. J., Detection of 2,4,6-trinitrotoluene-utilizing anaerobic bacteria by ^{15}N and ^{13}C incorporation. *Appl. Environ. Microbiol.* **2010**, *76*, (5), 1695-1698.
- (118) Andeer, P.; Strand, S. E.; Stahl, D. A., High-sensitivity stable-isotope probing by a quantitative terminal restriction fragment length polymorphism protocol. *Appl. Environ. Microbiol.* **2012**, *78*, (1), 163-169.
- (119) Brose, U.; Martinez, N. D.; Williams, R. J., Estimating species richness: sensitivity to sample coverage and insensitivity to spatial patterns. *Ecology* **2003**, *84*, (9), 2364-2377.
- (120) V. Wintzingerode, F.; Göbel, U. B.; Stackebrandt, E., Determination of microbial diversity in environmental samples: pitfalls of PCR-based rRNA analysis. *FEMS Microbiology Reviews* **1997**, *21*, (3), 213-229.
- (121) Fuller, M. E.; McClay, K.; Higham, M.; Hatzinger, P. B.; Steffan, R. J., Hexahydro-1,3,5-trinitro-1,3,5-triazine (RDX) bioremediation in groundwater: Are known RDX-degrading bacteria the dominant players? *Biorem. J.* **2010**, *14*, (3), 121-134.
- (122) Meyer, S. A.; Marchand, A. J.; Hight, J. L.; Roberts, G. H.; Escalon, L. B.; Inouye, L. S.; MacMillan, D. K., Up-and-down procedure (UDP) determinations of acute oral toxicity of nitroso degradation products of hexahydro-1,3,5-trinitro-1,3,5-triazine (RDX). *J. Appl. Toxicol.* **2005**, *25*, 427-434.
- (123) Gregory, K. B.; Larese-Casanova, P.; Parkin, G. F.; Scherer, M. M., Abiotic transformation of hexahydro-1,3,5-trinitro-1,3,5-triazine by Fe(II) bound to magnetite. *Environ. Sci. Technol.* **2004**, *38*, 1408-1414.
- (124) Sheremata, T. W.; Halasz, A.; Paquet, L.; Thiboutot, S.; Ampleman, G.; Hawari, J., The fate of the cyclic nitramine explosive RDX in natural soil. *Environ. Sci. Technol.* **2001**, *35*, (6), 1037-1040.
- (125) Oh, B.-T.; Just, C. L.; Alvarez, P. J. J., Hexahydro-1,3,5-trinitro-1,3,5-triazine mineralization by zerovalent iron and mixed anaerobic cultures. *Environ. Sci. Technol.* **2001**, *35*, 4341-4346.

- (126) Pak, J. W.; Knoke, K. L.; Noguera, D. R.; Fox, B. G.; Chambliss, G. H., Transformation of 2,4,6-trinitrotoluene by purified xenobiotic reductase B from *Pseudomonas fluorescens* I-C. *Appl. Environ. Microbiol.* **2000**, *66*, 4742-4750.
- (127) Motta, A. S.; Brandelli, A., Influence of growth conditions on bacteriocin production by *Brevibacterium linens*. *Appl. Microbiol. Biotechnol.* **2003**, *62*, (2), 163-167.
- (128) Oladimeji, A. T., Kinetics of microbial production of 2, 3-butanediol from cheese whey using *Klebsiella pneumonia*. *Int. J. Biosci. Biochem. Bioinforma.* **2011**, *1*, (3), 177-183.
- (129) Setlow, P., Spore germination. *Curr. Opin. Microbiol.* **2003**, *6*, (6), 550-556.
- (130) Andeer, P.; Stahl, D. A.; Lillis, L.; Strand, S. E., Identification of microbial populations assimilating nitrogen from RDX in munitions contaminated military training range soils by high sensitivity stable isotope probing. *Environ. Sci. Technol.* **2013**.
- (131) Prazeres, A. R.; Carvalho, F.; Rivas, J., Cheese whey management: a review. *J. Environ. Manage.* **2012**, *110*, (0), 48-68.
- (132) Finneran, K. T.; Johnsen, C. V.; Lovley, D. R., *Rhodoferrax ferrireducens* sp. nov., a psychrotolerant, facultatively anaerobic bacterium that oxidizes acetate with the reduction of Fe(III). *Int. J. Syst. Evol. Microbiol.* **2003**, *53*, (3), 669-673.
- (133) Livermore, J. A.; Jin, Y. O.; Arnseth, R. W.; LePuil, M.; Mattes, T. E., Microbial community dynamics during acetate biostimulation of RDX-contaminated groundwater. *Environ. Sci. Technol.* **2013**, *47*, (14), 7672-7678.
- (134) Cummings, D. E.; Caccavo Jr, F.; Spring, S.; Rosenzweig, R. F., *Ferribacterium limneticum*, gen. nov., sp. nov., an Fe(III)-reducing microorganism isolated from mining-impacted freshwater lake sediments. *Arch. Microbiol.* **1999**, *171*, (3), 183-188.
- (135) Pester, M.; Brambilla, E.; Alazard, D.; Rattei, T.; Weinmaier, T.; Han, J.; Lucas, S.; Lapidus, A.; Cheng, J.-F.; Goodwin, L.; Pitluck, S.; Peters, L.; Ovchinnikova,

- G.; Teshima, H.; Detter, J. C.; Han, C. S.; Tapia, R.; Land, M. L.; Hauser, L.; Kyrpides, N. C.; Ivanova, N. N.; Pagani, I.; Huntmann, M.; Wei, C.-L.; Davenport, K. W.; Daligault, H.; Chain, P. S. G.; Chen, A.; Mavromatis, K.; Markowitz, V.; Szeto, E.; Mikhailova, N.; Pati, A.; Wagner, M.; Woyke, T.; Ollivier, B.; Klenk, H.-P.; Spring, S.; Loy, A., Complete genome sequences of *Desulfosporosinus orientis* DSM765T, *Desulfosporosinus youngiae* DSM17734T, *Desulfosporosinus meridiei* DSM13257T, and *Desulfosporosinus acidiphilus* DSM22704T. *J. Bacteriol.* **2012**, *194*, (22), 6300-6301.
- (136) Valverde, A.; Velázquez, E.; Gutiérrez, C.; Cervantes, E.; Ventosa, A.; Igual, J.-M., *Herbaspirillum lusitanum* sp. nov., a novel nitrogen-fixing bacterium associated with root nodules of *Phaseolus vulgaris*. *Int. J. Syst. Evol. Microbiol.* **2003**, *53*, (6), 1979-1983.
- (137) Liu, J.-R.; Tanner, R. S.; Schumann, P.; Weiss, N.; McKenzie, C. A.; Janssen, P. H.; Seviour, E. M.; Lawson, P. A.; Allen, T. D.; Seviour, R. J., Emended description of the genus *Trichococcus*, description of *Trichococcus collinsii* sp. nov., and reclassification of *Lactosphaera pasteurii* as *Trichococcus pasteurii* comb. nov. and of *Ruminococcus palustris* as *Trichococcus palustris* comb. nov. in the low-G+C gram-positive bacteria. *Int. J. Syst. Evol. Microbiol.* **2002**, *52*, (4), 1113-26.
- (138) Kwon, M. J.; Finneran, K. T., Hexahydro-1,3,5-trinitro-1,3,5-triazine (RDX) reduction is concurrently mediated by direct electron transfer from hydroquinones and resulting biogenic Fe(II) formed during electron shuttle-amended biodegradation. *Environ. Eng. Sci.* **2009**, *26*, 961-971.
- (139) Amann, R. I.; Ludwig, W.; Schleifer, K.-H., Phylogenetic identification and in situ detection of individual microbial cells without cultivation. *Microbiol. Rev.* **1995**, *59*, 143-69.
- (140) Kwon, M. J.; Finneran, K. T., Electron shuttle-stimulated RDX mineralization and biological production of 4-nitro-2,4-diazabutanal (NDAB) in RDX-contaminated aquifer material. *Biodegradation* **2010**, *21*, 923-937.
- (141) Boopathy, R.; Kulpa, C. F.; Manning, J., Anaerobic biodegradation of explosives and related compounds by sulfate-reducing and methanogenic bacteria: a review. *Bioresour. Technol.* **1998**, *63*, (1), 81-89.

- (142) Lueders, T.; Manefield, M.; Friedrich, M. W., Enhanced sensitivity of DNA- and rRNA-based stable isotope probing by fractionation and quantitative analysis of isopycnic centrifugation gradients. *Environ. Microbiol.* **2004**, *6*, 73-78.
- (143) Buckley, D. H.; Huangyutitham, V.; Hsu, S.-F.; Nelson, T. A., Stable isotope probing with ¹⁵N achieved by disentangling the effects of genome G+C content and isotope enrichment on DNA density. *Appl. Environ. Microbiol.* **2007**, *73*, 3189-3195.
- (144) Jackson, R. G.; Rylott, E. L.; Fournier, D.; Hawari, J.; Bruce, N. C., Exploring the biochemic properties and remediation applications of the unusual explosive-degrading p450 system XplA/B. *PNAS* **2007**, *104*, 16822-16827.
- (145) Indest, K. J.; Jung, C. M.; Chen, H.-P.; Hancock, D.; Florizone, C.; Eltis, L. D.; Crocker, F. H., Functional characterization of pGKT2, a 182-kilobase plasmid containing the *xplAB* genes, which are involved in the degradation of hexahydro-1,3,5-trinitro-1,3,5-triazine by *Gordonia* sp. strain KTR9. *Appl. Environ. Microbiol.* **2010**, *76*, 6329-6337.
- (146) Indest, K. J.; Crocker, F. H.; Athow, R., A TaqMan polymerase chain reaction method for monitoring RDX-degrading bacteria based on the *xplA* functional gene. *J. Microbiol. Methods* **2007**, *68*, 267-274.

APPENDIX A

APPLICATION OF ^{13}C -STABLE ISOTOPE PROBING TO IDENTIFY RDX-
DEGRADING MICROORGANISMS IN GROUNDWATER

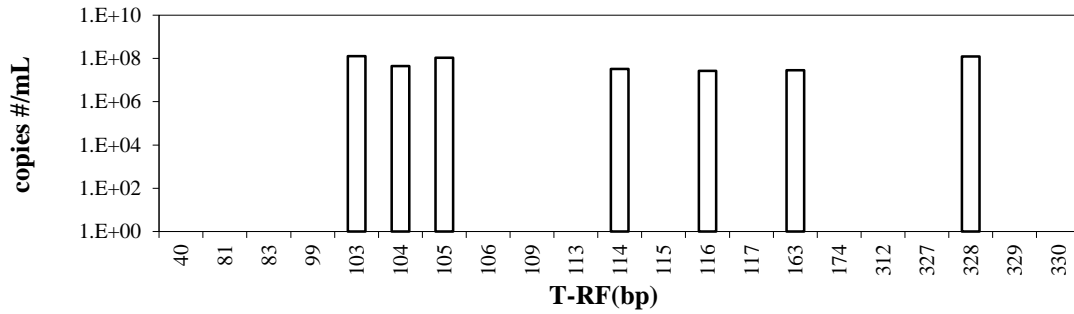


Figure A.1. Real-time T-RFLP profile data for sample 5-0-Ua

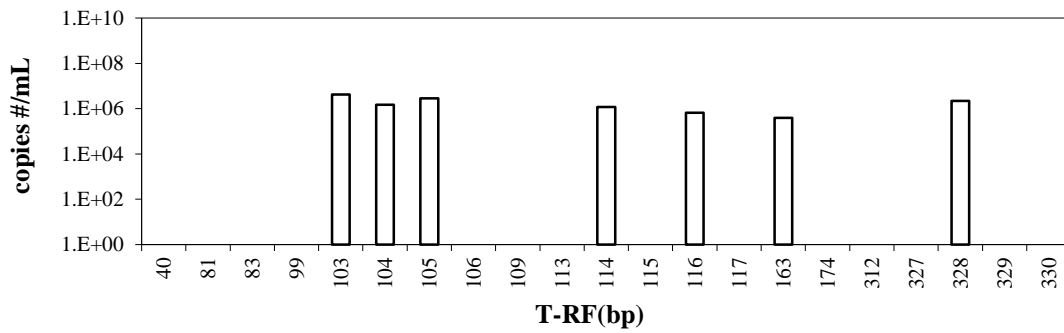


Figure A.2. Real-time T-RFLP profile data for sample 5-0-Ub

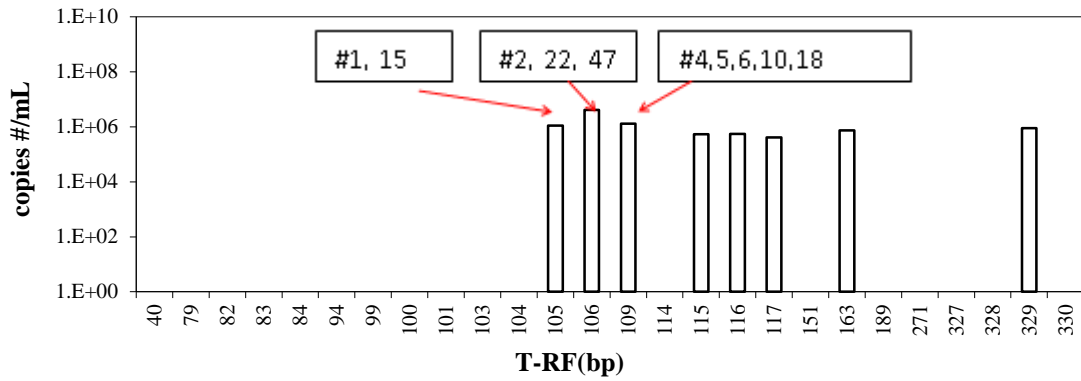


Figure A.3. Real- time T-RFLP profile data for sample 5-0-La

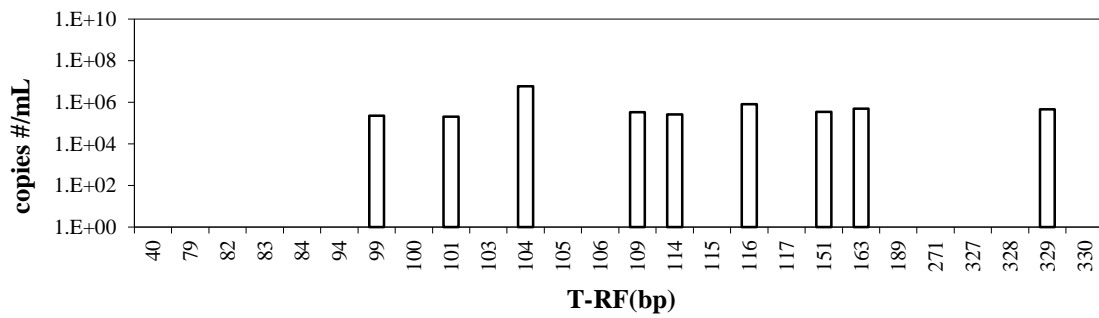


Figure A.4. Real- time T-RFLP profile data for sample 5-C-Ua

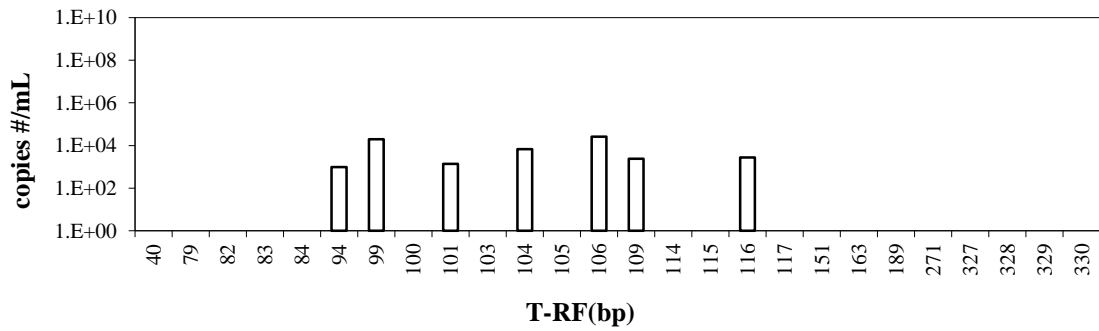


Figure A.5. Real- time T-RFLP profile data for sample 5-C-Ub

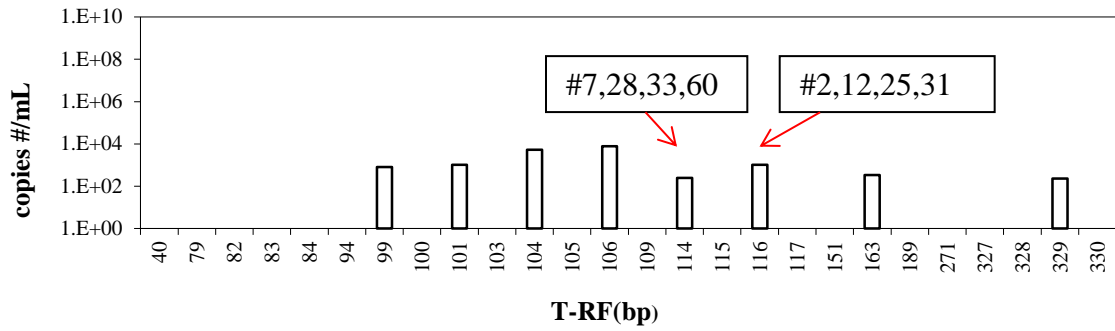


Figure A.6. Real- time T-RFLP profile data for sample 5-C-La

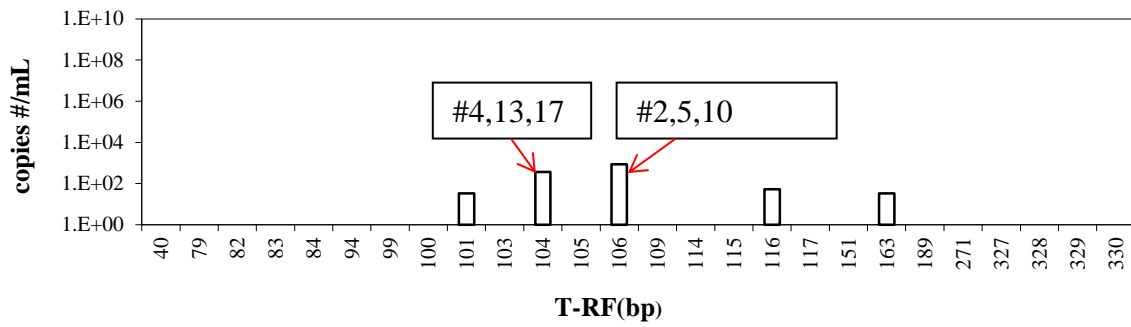


Figure A.7. Real- time T-RFLP profile data for sample 5-C-Lb

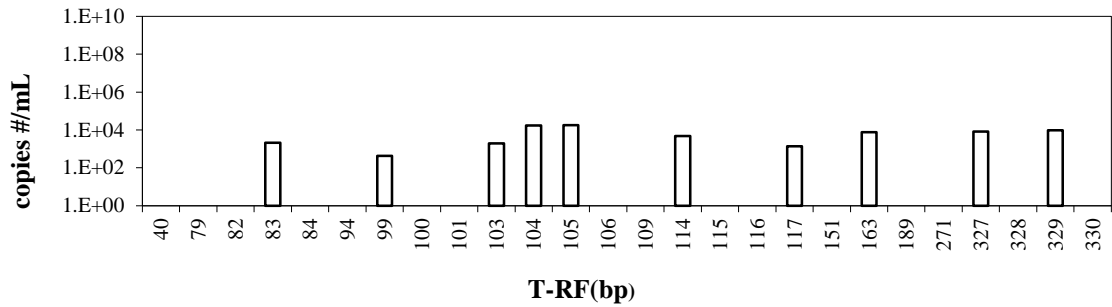


Figure A.8. Real- time T-RFLP profile data for sample 7-0-Ua

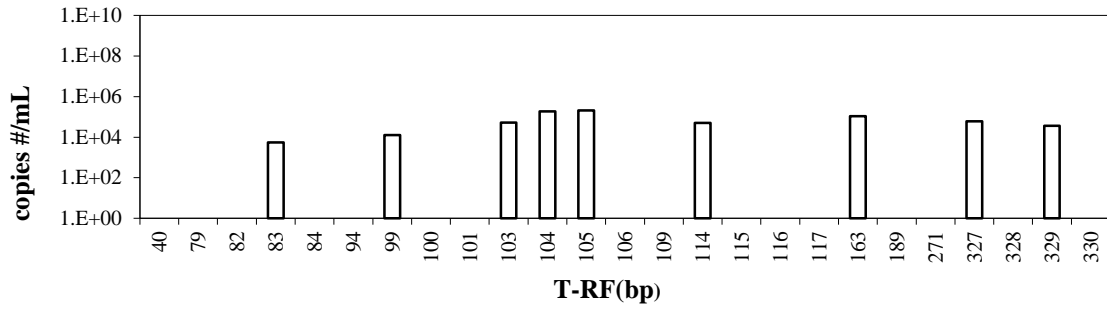


Figure A.9. Real- time T-RFLP profile data for sample 7-0-Ub

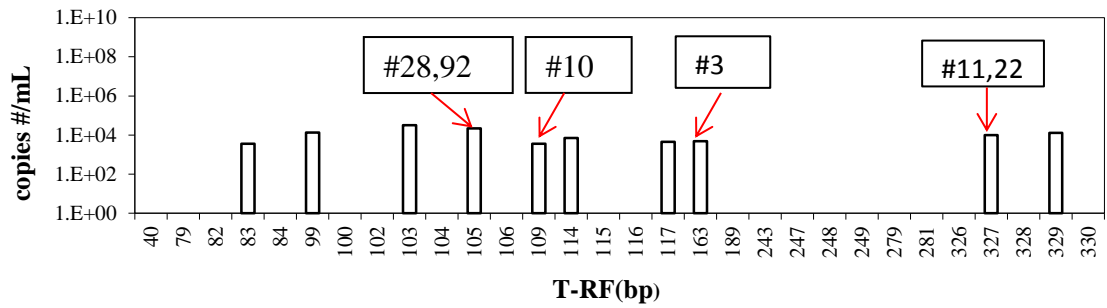


Figure A.10. Real- time T-RFLP profile data for sample 7-0-La

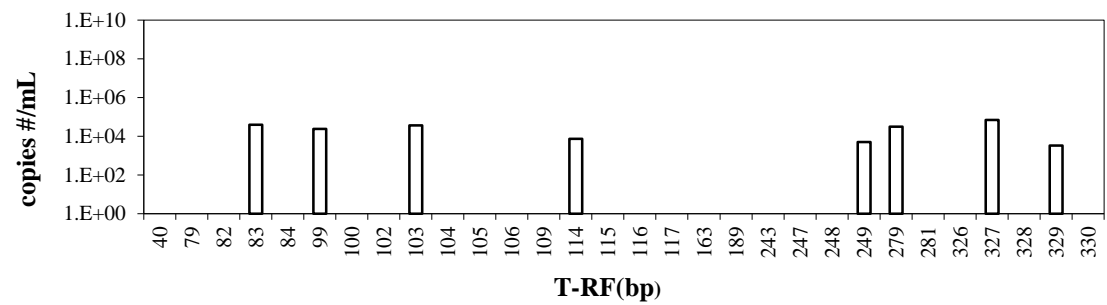


Figure A.11. Real- time T-RFLP profile data for sample 7-0-Lb

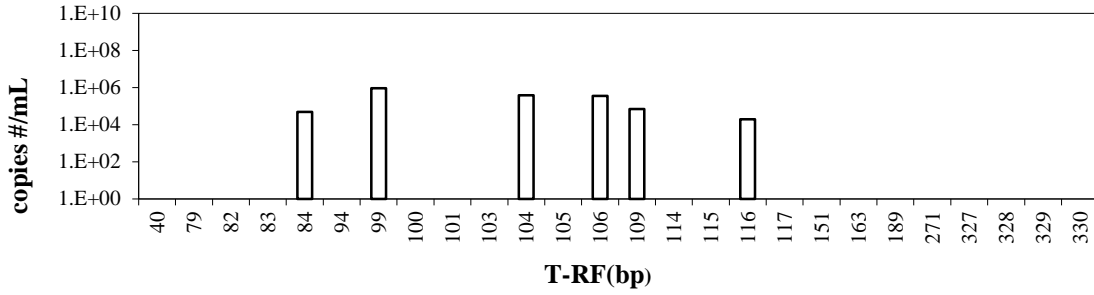


Figure A.12. Real- time T-RFLP profile data for sample 7-C-Ua

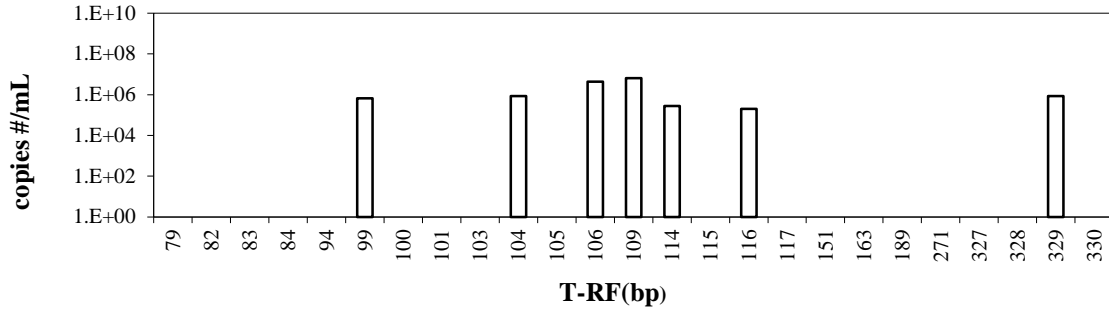


Figure A.13. Real- time T-RFLP profile data for sample 7-C-Ub

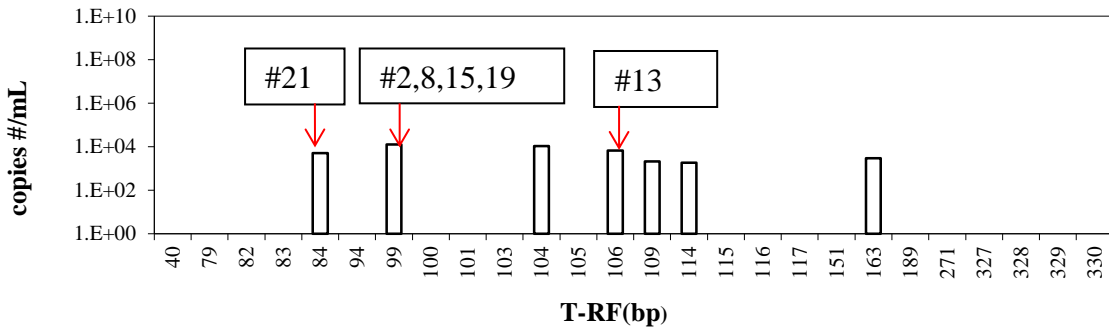


Figure A.14. Real- time T-RFLP profile data for sample 7-C-La

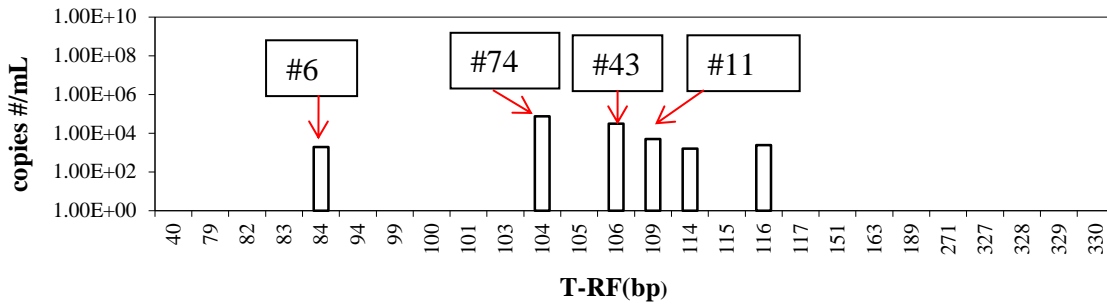


Figure A.15. Real- time T-RFLP profile data for sample 7-C-Lb

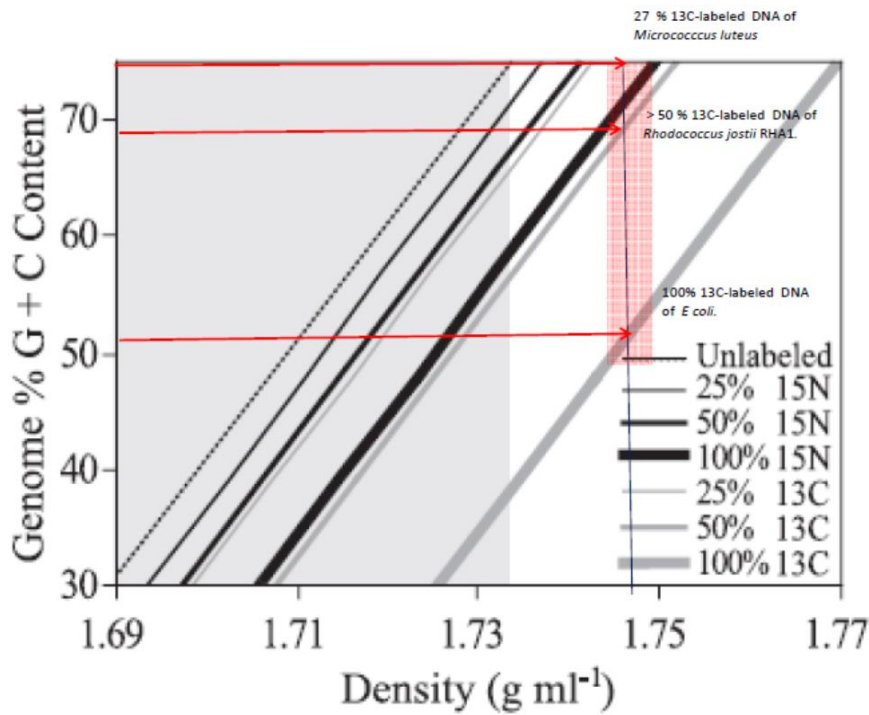


Figure A.16. Predicted relationship between genomic G+C content (ranging from 30-75%) and buoyant density of unlabeled and labeled DNA with ¹³C or ¹⁵N (Buckley et al., 2007.) (143) This figure was marked with three specific cases as shown as three red arrows. Shaded red region in the figure presents the range of densities over which labeled DNA would be captured in this study.

Table A.1. Comparison of 16S rRNA gene sequences derived from the microcosms to the 16S rRNA gene sequences derived from background groundwater

Clones derived from background groundwater* [accession number]	Microcosms ID			
	5-0-L Clone (% Homology**)	7-0-L Clone (% Homology)	5-C-L Clone (% Homology)	7-C-L Clone (% Homology)
GW_Clone_1 [EU907880]	-	-	-	-
GW_Clone_2 [EU907881]	50a4 (87%), 50a5 (87%)	-	-	-
GW_Clone_3 [EU907882]	50a4 (85%), 50a5 (86%)	-	-	-
GW_Clone_4 [EU907883]	50a4 (86%), 50a5 (87%)	-	-	-
GW_Clone_5 [EU907884]	50a4 (86%), 50a5 (87%)	-	-	-
GW_Clone_6 [EU907885]	-	-	-	-
GW_Clone_7 [EU907886]	50a1 (85%), 50a15 (85%)	-	-	-
GW_Clone_8 [EU907887]	50a1 (92%), 50a2 (89%), 50a15 (92%)	70a28 (89%)	-	7Ca2 (90%), 7Ca8 (90%), 7Cb74 (90%)
GW_Clone_9 [EU907888]	50a1 (95%), 50a2 (91%), 50a15 (95%)	70a28 (89%)	-	-
GW_Clone_10 [EU907889]	-	-	5Ca7 (89%), 5Ca33 (89%), 5Ca60 (89%), 5Cb4 (89%), 5Cb17 (89%)	7Ca13 (89%), 7Cb43(89%)
GW_Clone_11 [EU907890]	-	-	-	-
GW_Clone_12 [EU907891]	-	-	5Ca2 (88%), 5Cb2 (88%), 5Cb5 (88%), 5Cb10 (88%)	-
GW_Clone_13 [EU907892]	-	70a28 (85%)	5Ca2 (88%), 5Cb2 (88%), 5Cb5 (88%), 5Cb10 (88%)	-
GW_Clone_14 [EU907893]	-	-	5Ca2 (88%), 5Cb2 (88%), 5Cb5 (88%), 5Cb10 (88%)	-
GW_Clone_15 [EU907894]	50a4 (85%)	-	-	-
GW_Clone_16 [EU907895]	50a1 (95%), 50a2 (90%), 50a15 (96%)	70a28 (88%)	-	7Ca8 (91%), 7Ca2 (91%), 7Cb74 (91%), 7Ca19 (90%)

Table A.1. Continued

Clones derived from background groundwater* [accession number]	Microcosms ID			
	5-0-L Clone (% Homology**)	7-0-L Clone (% Homology)	5-C-L Clone (% Homology)	7-C-L Clone (% Homology)
GW_Clone_19 [EU907898]	-	-	-	-
GW_Clone_20 [EU907899]	-	-	-	-
GW_Clone_21 [EU907900]	-	-	5Ca28 (85%)	-
GW_Clone_22 [EU907901]	50a4 (91%), 50a5 (87%)	-	-	-
GW_Clone_23 [EU907902]	50a1 (95%), 50a2 (90%), 50a15 (95%)	70a28 (89%)	-	7Ca8 (92%), 7Cb74 (92%)
GW_Clone_24 [EU907903]	-	-	5Ca2 (87%), 5Ca12 (87%), 5Ca25 (87%), 5Ca31 (87%), 5Cb2 (88%), 5Cb5 (88%), 5Cb10 (88%),	-
GW_Clone_25 [EU907904]	50a4 (89%), 50a5 (88%)	-	-	-

*Source of GW clones : Roh, H., Yu, C.-P., Fuller, M.E., Chu, K.-H., 2009.

Identification of hexahydro-1,3,5-trinitro-1,3,5-triazine-degrading microorganisms via ¹⁵N-stable isotope probing. Environmental Science and Technology 43, 2505-2511.

** Value in the bracket indicates % homology between the microcosm clone and the GW clone listed on the first column.

Table A.2. Diversity and predicted T-RFs of clones derived from groundwater microcosms receiving ¹³C-labeled RDX

Class	Classification ^a	Percent of recovered sequences assigned to different taxonomic groups				Theoretical T-RF(bp) ^b
		Microcosms ID				
		5-0-L	7-0-L	5-C-L	7-C-L	
<i>Actinobacteria</i>	<i>Unclassified Propionibacteriaceae</i>	-	-	-	20%	84,99
	<i>Cellulomonas</i>	-	-	-	10%	84
	<i>Rhodococcus</i>	-	-	-	10%	109
<i>Bacteroidia</i>	<i>Rikenella</i>	-	17%	-	-	163
<i>Spirochaetes</i>	<i>Treponema</i>	10%	33%	-	-	109
<i>Clostridia</i>	<i>Anaerobacter</i>	-	17%	-	-	327
<i>Bacilli</i>	<i>Trichococcus</i>	-	-	50%	20%	104,106
<i>α-Proteobacteria</i>	<i>Unclassified Rhodzobiales</i>	10%	-	-	-	109
	<i>Unclassified Rhodoferax</i>	10%	-	-	-	109
<i>β-Proteobacteria</i>	<i>Sulfuricella</i>	30%	-	-	-	105
	<i>Sulfuritalea</i>	10%	-	-	-	106
	<i>Ferribacterium</i>	-	33%	-	-	105
	<i>Undibacterium</i>	10%	-	-	-	106
	<i>Undibacterium</i>	-	-	-	40%	99,104
<i>γ-Proteobacteria</i>	<i>Pseudomonas</i>	-	-	50%	-	104
<i>δ-Proteobacteria</i>	<i>Desulfovibrio</i>	20%	-	-	-	109
Total		100%	100%	100%	100%	

- a. Assigned using RDP Classifier with an 80% confidence threshold.
- b. Results of *in-silico* analysis of cloned sequences using TRiFLE with restriction enzyme *MspI* cutting site. The predicted T-RFs are close to measured T-RFs in microbial community profiles (See Appendix A from Figure A.1-A.15).

APPENDIX B

PROBING ACTIVE MICROORGANISMS CAPABLE OF
USING DIFFERENT NITROGEN IN RDX STRUCTURE
AS A NITROGEN SOURCE

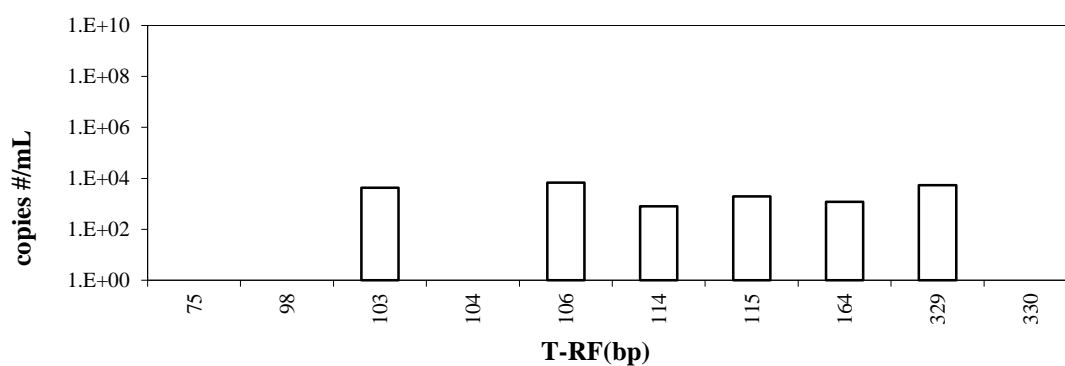


Figure B.1. Real- time T-RFLP profile data for sample 50-Na

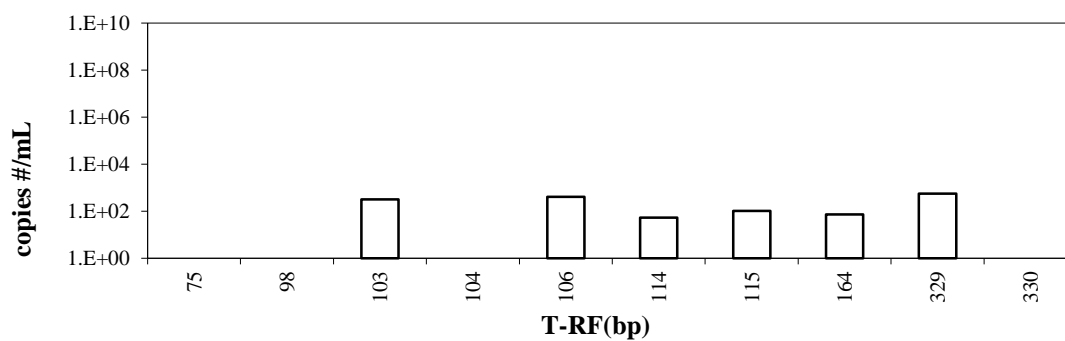


Figure B.2. Real- time T-RFLP profile data for sample 50-Fa

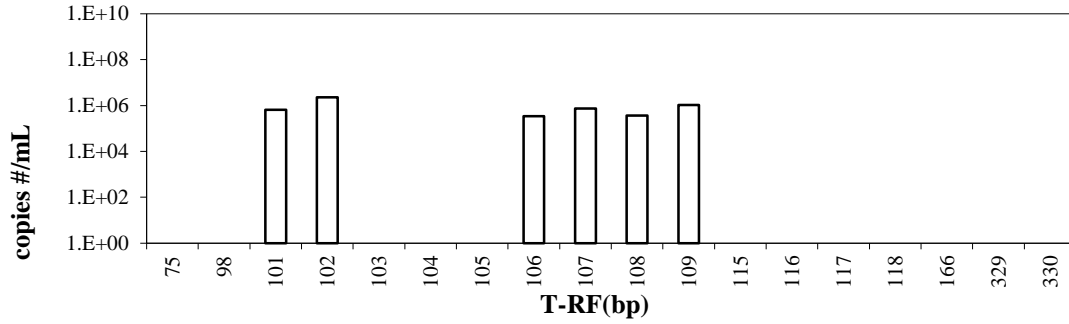


Figure B.3. Real- time T-RFLP profile data for sample 5C-Ra

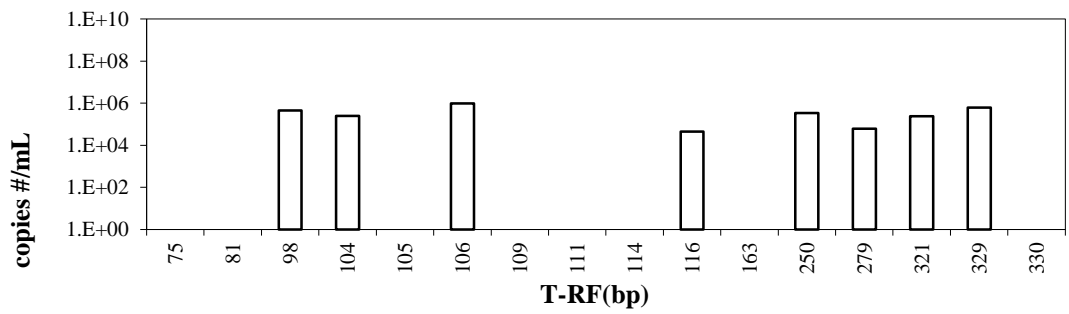


Figure B.4. Real- time T-RFLP profile data for sample 5C-Rb

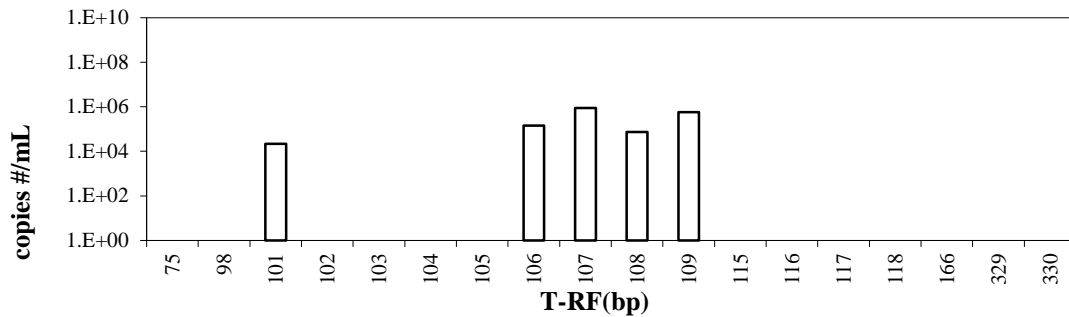


Figure B.5. Real- time T-RFLP profile data for sample 5C-Na

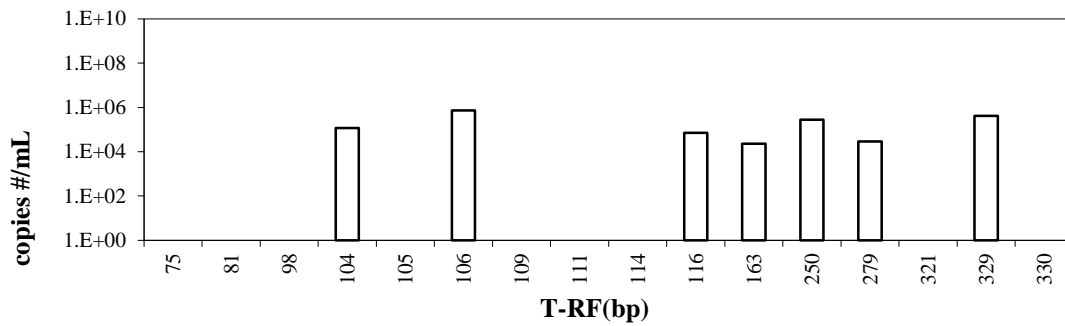


Figure B.6. Real- time T-RFLP profile data for sample 5C-Nb

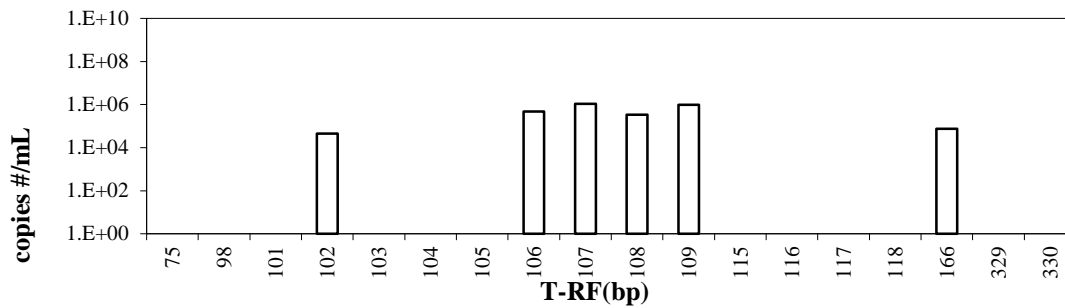


Figure B.7. Real- time T-RFLP profile data for sample 5C-Fa

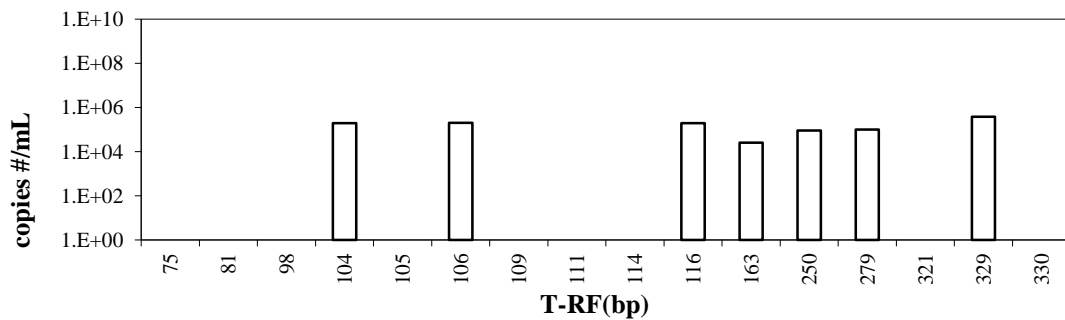


Figure B.8. Real- time T-RFLP profile data for sample 5C-Fb

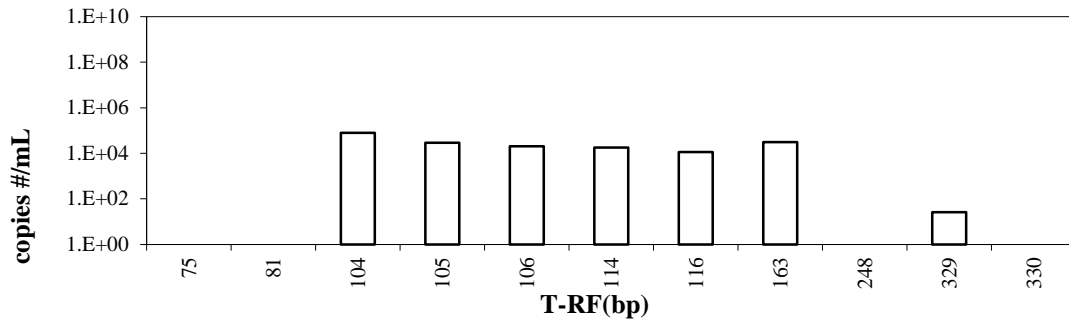


Figure B.9. Real- time T-RFLP profile data for sample 70-Ra

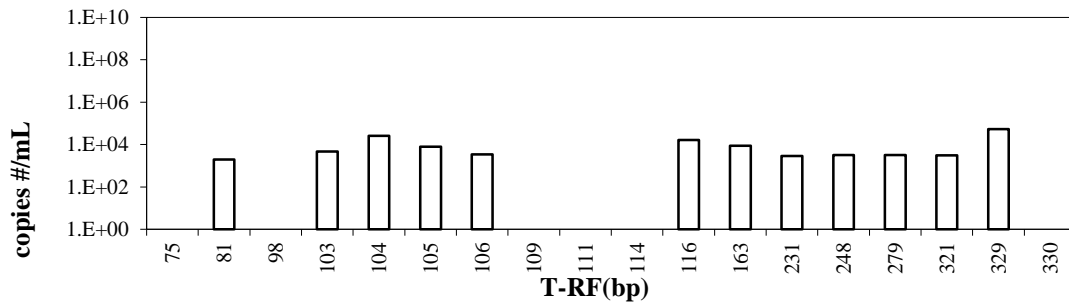


Figure B.10. Real- time T-RFLP profile data for sample 70-Rb

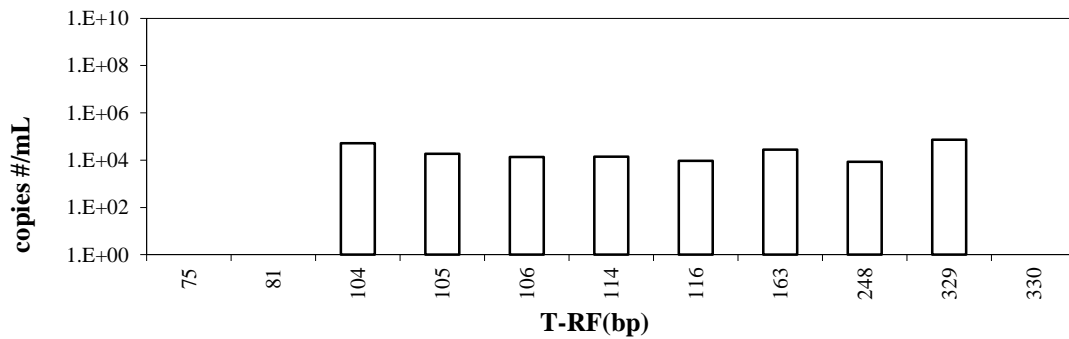


Figure B.11. Real- time T-RFLP profile data for sample 70-Na

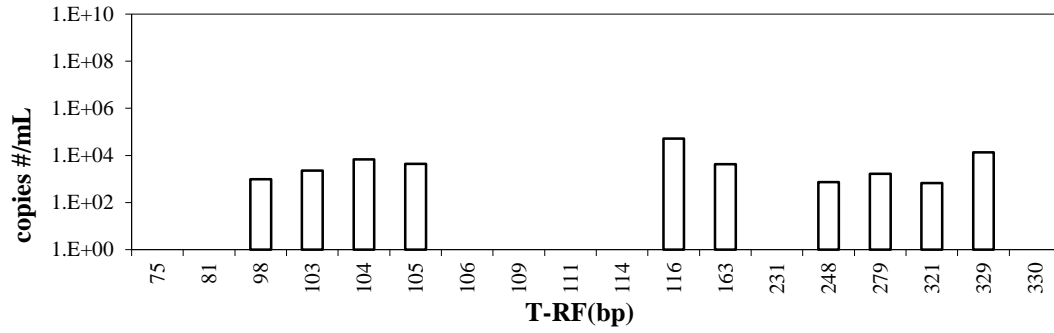


Figure B.12. Real- time T-RFLP profile data for sample 70-Nb

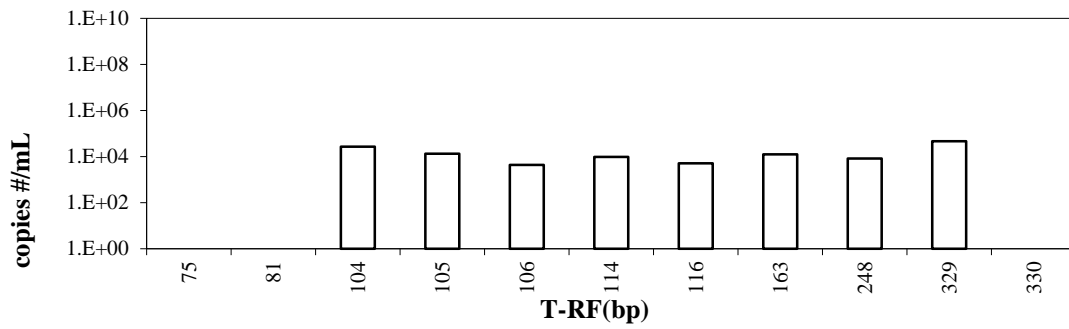


Figure B.13. Real- time T-RFLP profile data for sample 70-Fa

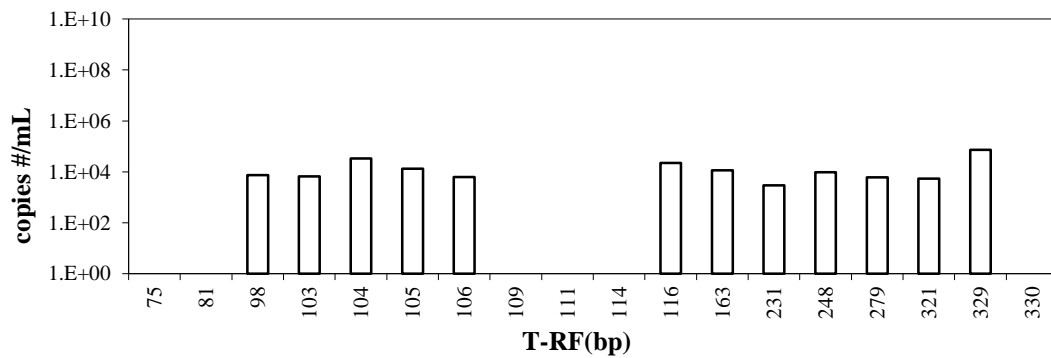


Figure B.14. Real- time T-RFLP profile data for sample 70-Fb

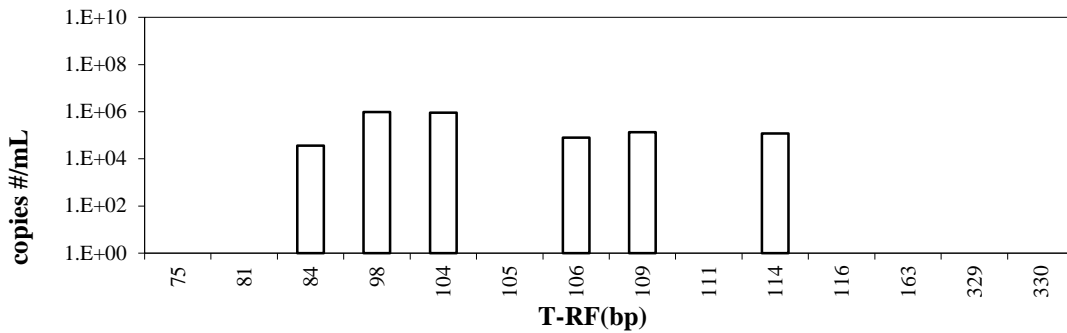


Figure B.15. Real- time T-RFLP profile data for sample 7C-Ra

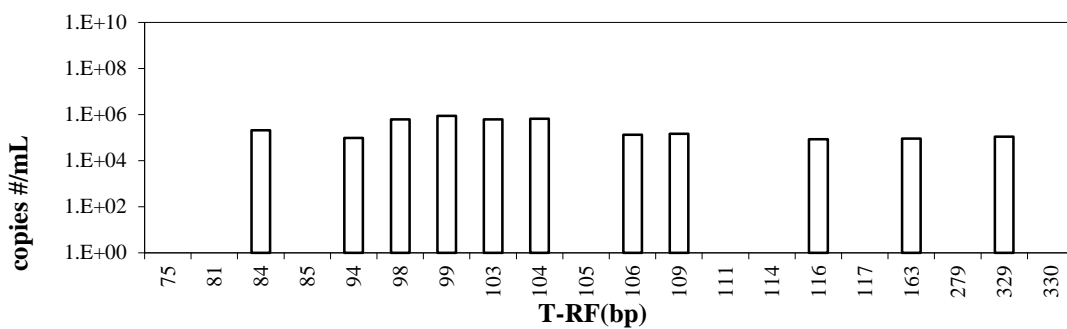


Figure B.16. Real- time T-RFLP profile data for sample 7C-Rb

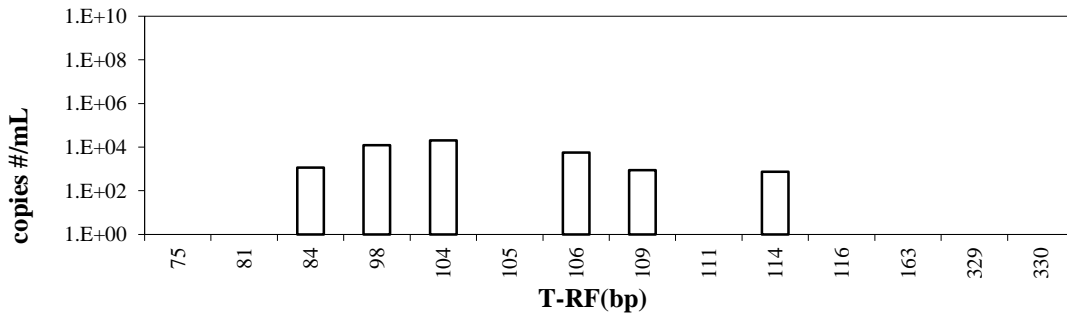


Figure B.17. Real- time T-RFLP profile data for sample 7C-Na

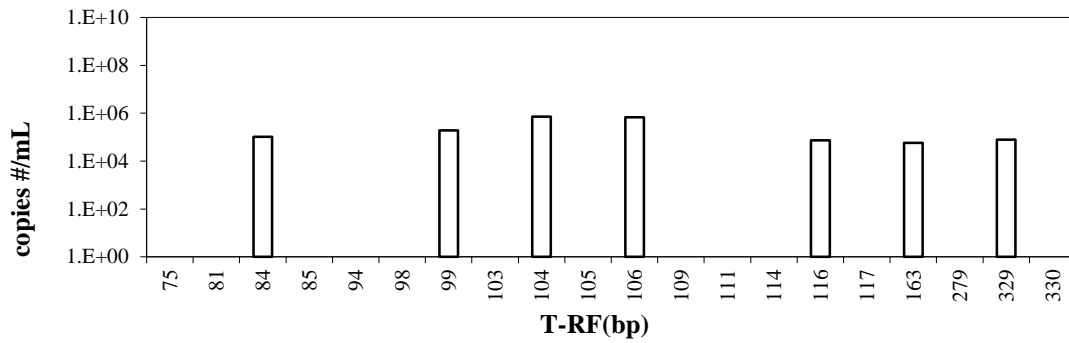


Figure B.18. Real-time T-RFLP profile data for sample 7C-Nb

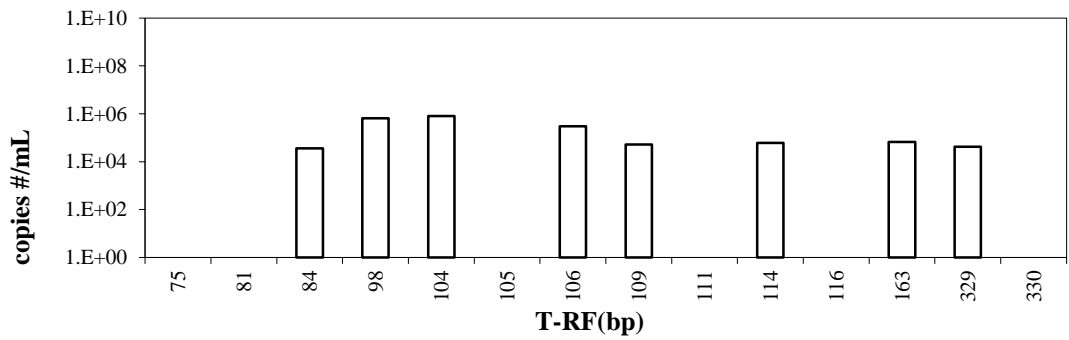


Figure B.19. Real-time T-RFLP profile data for sample 7C-Fa

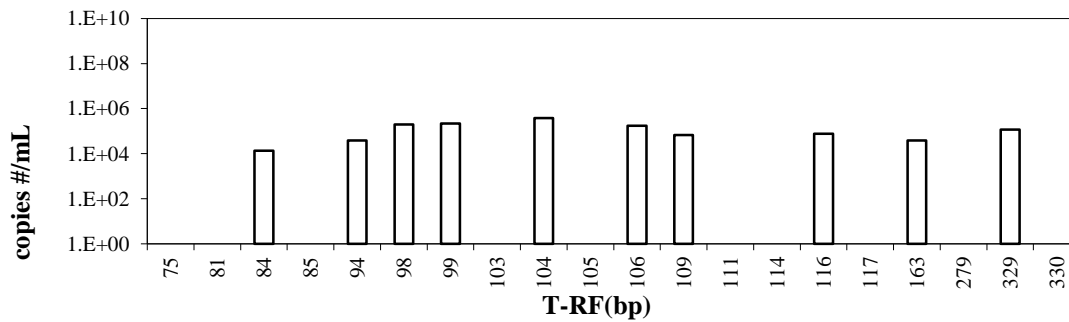


Figure B.20. Real-time T-RFLP profile data for sample 7C-Fb